# CHARACTERIZATION OF THE NADPH OXIDASE COMPLEX IN HUMAN LEIOMYOMA AND NORMAL MYOMETRIAL SMOOTH MUSCLE CELLS AND ITS ROLE IN PDGF AND EGF SIGNALING PATHWAYS

BY

FERNANDO SILVEIRA MESQUITA

DISSERTATION

Submitted in partial fulfillment of the requirements
for the degree of Doctor of Philosophy in Animal Sciences
in the Graduate College of the
University of Illinois at Urbana-Champaign, 2010

Urbana, Illinois

Doctoral Committee:

Professor Romana Nowak, Chair and Director of Research
Associate Professor David Bunick
Associate Professor David Miller
Professor Indrani Bagchi
Professor Janice Bahr

## ABSTRACT

Reactive oxygen species have received an increasing amount of attention over the past decade, not only due to their role in oxidative damage, but also because of their participation as second messengers on the relay of many signaling pathways and their role in the development of numeours fibrotic diseases. This Ph.D. dissertation focused on testing the hypothesis that ROS are necessary components of the EGF and PDGF pathways in leiomyoma and normal myometrial SMCs. The main findings of this work were: 1) leiomyoma smooth muscle cells (LSMCs) and myometrial smooth muscle cells (MSMCs) produce ROS in response to EGF and PDGF; 2) ROS are necessary for EGF- and PDGF-induced LSMCs and MSMCs proliferation, and sufficient to induce LSMCs proliferation; 3) ROS are necessary and sufficient to induce a fraction of Erk1/2 activation in LSMCs and MSMCs; 4) NADPH oxidase components are expressed in leiomyoma and normal myometrial tissue; 5) PDGF induces translocation of $p47^{phox}$ into lipid rafts in LSMCs; 6) PKC mediates Erk1/2 activation by PDGF in MSMCs and LSMCs; 7) PKC activation alone is sufficient to induce ROS production in MSMCs and LSMCs; 8) hydrogen peroxide inhibits the activity of PTPases in LSMCs; 9) regulation of PTPase activity is important for myometrial and leiomyoma SMC proliferation. The findings suggest that ROS are necessary components of the EGF and PDGF pathways. There is also evidence that NADPH oxidase complex is the source of EGF and PDGF-induced ROS production, and that the mechanism of activation of this complex involves translocation of the subunit $p47^{phox}$ into lipid rafts as well as PKC activity. Furthermore, ROS might be acting by regulating protein tyrosine phosphatase enzymes, which in turn affect the proliferation of leiomyoma and myometrial SMCs. Based on the results obtained from my work I speculate that a subset of leiomyoma

tumors may originate from a growth advantage acquired by myometrial SMCs that overexpress NADPH oxidase components leading to tumor development.

## DEDICATION

To my father Renato Antonio da Rocha Mesquita and mother Elsa da Silveira Mesquita, who have overcome numerous very difficult times without ever lo sing focus of my sister and I, our education, and making sure I kept our dignity and honesty. I am proud to be your son.

To my sister Renata Silveira Mesquita for her support and dedication to our family. I am proud of her conduct as a person and her professional success.

To my wife Sibele, who has left the comfort of her family to join me during the mentally and physically challenging journey of graduate school. I oI her much respect for her support and love. Whether through good or bad times, this experience has made us stronger as a family. I am proud to be your husband.

To the sweetest little boy, who now makes our lives complete and full of joy and it is certainly and by far the most important blessing in our lives, our son Luis Antonio. I am proud to be your father.

## ACKNOWLEDGMENTS

First and foremost I want to thank my adviser and mentor Dr. Romana Nowak, who accepted me as her graduate student, back in August of 2003. Dr. Nowak has extended her support and consideration to my family, and has been very understanding of some of the struggles one may go through in life. In science, Dr. Nowak has given me the freedom to think and work. More importantly, I have had her constant support, even during some difficult moments. I feel that she trusts me and that support is priceless. Dr. Nowak chose to emphasize the good aspects of my personality and skills, point out what was/is wrong, and give me the opportunity to complete my degree and pursue my career. For that I am forever grateful.

I want to thank the many colleagues/friends I have made during my stay in the Nowak lab. Jen Wubben, Juli Rowlett, Dr. Andrea Braundmeier, Dr. Li Chen, Summer Dyer, Meagan Grudzien, Amy Ditewig, Cat Dayger, Angela Dirks, Dr. Li-Jung Lin, Sergio Machado, Jiajia Bi, Pavni Mehrotra, Farzaneh Masoud, Faezeh Koohestani, Victorya Ermilova, and all undergraduate students that were part of our group during this process. I praise their friendship and support throughout this journey. I specially want to thank Dr. Robert Belton who has given me technical and intellectual support and with whom I worked and interacted closely, having significant impact on my development as a graduate student.

I want to thank my committee members Dr. David Bunick, Dr. David Miller, Dr. Indrani Bagchi and Dr. Janice Bahr for their contribution to this work. Regardless of how often I interacted with each of you individually, you were always available and willing to help when I needed. Your feedback has been extremely valuable.

Dr. Philip Dziuk, thank you very much for all the Phree advice! You opened up your house for my family. You offered the great opportunity of getting some extra cash as well as exercising and having fun in exchange of chopping and carrying some wood around. The best deal ever. Furthermore, I got to meet Mrs. Dziuk to whom I own my very first tradional American breakfast! It has been great to have you share many of your wonderful experiences and extensive knowledge.

I also would like to thank Dr. Alvaro Hernandez, Alvaro's wife, Gloria, and their children, Nico and Iza. Alvaro made a great effort to find a lab for me. Alvaro and Gloria have treated us like family and provided support at different levels. I hope to be able to reciprocate at least some of what you have done for my family and me.

Last, but definitely not least, I want to thank Dr. João Francisco Coelho de Oliveira and Dr. Paulo Bayard Dias Gonçalves, my Master's adviser and co-adviser, respectively. You gave me the opportunity to get started on research. My positive experience under your supervision and your constant support has stimulated me to pursue a carreer in science.

## TABLE OF CONTENTS

# CHAPTER 1

# INTRODUCTION

Uterine leiomyomas or fibroids are benign tumors of the reproductive tract that represent a significant public health and economic problem in the United States as well as worldwide. These tumors are characterized by abnormal growth of uterine smooth muscle cells and excessive production and deposition of extracellular matrix proteins, namely collagens type I and type III [1, 2]. Symptomatology include mainly pelvic pressure and/or pain, menorrhagia or hypermenorrhea, and infertility in some cases. Economical and social impacts come from the fact that it is estimated that approximately 70-80% of women will develop leiomyomas, with around 25% of symptomatic cases [3, 4].

A hypothesis formulated by our research group suggests that uterine leiomyomas may originate from a local injury to the uterine smooth muscle cells due to hypoxia or ischemia that occur during menstruation, as the spiral arteries of the myometrium constrict prior to the loss of the endometrium. This hypothesis is in agreement with some other well-established models such as the development of atherosclerosis plaques upon angioplasty/restenosis injury, and the development of liver fibrosis. These conditions share in common the mesenchymal origin of the normally quiescent cells and the phenotype switch into a more proliferative, myofibroblast-like cell type [5-8].

Recent studies have revealed that high levels of reactive oxygen species (ROS) is a common feature among several chronic disorders, some of which are fibrotic (Refer to APPENDIX A for a list of abbreviations). Pulmonary, hepatic, and cardiac fibrosis, atherosclerosis, type I diabetes, renal disorders, and a number of cancers are some of the illnesses

that have been associated with altered ROS production [9]. Although some studies have focused on the role of increased ROS levels in the context of oxidative stress and cell damage, I am interested in the role of ROS as a signaling molecule. Whether studies focus on oxidative stress or intracellular signaling, a significant portion of the literature supports the NADPH oxidase complex as the main source of ROS. For instance, this enzymatic complex is responsible for the release of ROS leading to cell growth and transformation [10, 11]. ROS production can affect the redox intracellular environment and ultimately influence the cell cycle [12, 13]. ROS can also regulate protein tyrosine phosphatases (PTPases) by oxidizing specific cysteine residues and rendering enzymes inactive [14-16]. In addition, NADPH oxidase-derived ROS is necessary for a variety of cellular events such as proliferation, migration, and transformation, in response to a variety of factors, e.g EGF, PDGF, insulin, angiotensin II [10, 11, 17-22].

The overall goal of this work was to investigate the involvement of ROS in the EGF and PDGF proliferative pathways in myometrial and leiomyoma SMCs. My overall hypothesis is that ROS are necessary for the proliferative pathways of the tested growth factors, and the scientific model I propose can be observed on Figure 1. Chapter 2 has an overview of the origin and regulation of SMC-specific gene expression, characteristics of leiomyoma tumors, description of the NADPH oxidase complex, and PTPases as targets of oxidation. Chapter 3 shows experiments performed to accomplish specific aim 1 by determining the involvement of ROS as an intermediate in the PDGF proliferative pathway. Chapter 4 reports the characterization of the NADPH oxidase complex and its mechanism of activation in myometrial and leiomyoma SMCs, which is part of specific aim 2. Chapter 5 focuses on specific aim 3 in which ROS regulation of PTPases and the role of PTPases in proliferation of myometrial and leiomyoma SMCs were examined.

# CHAPTER 2

# LITERATURE REVIEW

## 2.1 MYOMETRIAL SMOOTH MUSCLE CELLS

### *2.1.1 Origin*

Embryologically, smooth muscle cells (SMCs) originate from mesodermal or neural-crest mesenchymal cells. Smooth muscle cells from visceral organs, such as the uterus, derive from mesenchymal cells of splanchnic mesoderm origin, whereas smooth muscle in the head and neck region and vascular smooth muscle cells are derived mainly from neural-crest cells [23]. The development of the human uterus is due to proliferation of the mesenchymal cells present around the fused Mullerian ducts [24]. In a 16-day-old mouse, one can observe mesenchymal cells surrounding the Mullerian ducts [25] (figure 2). The adult uterus is composed of several layers of specific cell types. The innermost layer lining the uterine cavity is the epithelium, which along with the underlying stroma form the endometrium. A circular and a longitudinal layer of smooth muscle cells follow the endometrium respectively. Last, a single layer of cells, called the serosa, lines the outer side of the organ. Konishi (1984) observed by light microscopy that the uterus of a 12-week gestation human fetus has sparse mesenchymal cells with no smooth muscle cells present. At 14 weeks the mesenchymal layer is divided into an inner and outer layer, whereas at 18 weeks the first cells with some smooth muscle characteristics are observed. These are considered immature smooth muscle cells. At 40 weeks the outer layer is classified as the myometrium as the cells composing it express marked smooth muscle cell characteristics, whereas the inner layer corresponds to the uterine stroma [24]. Electron microscopy has confirmed the mesenchymal origin of uterine smooth muscle cells. Mesenchymal cells at 12

weeks contain few mitochondria, rough endoplasmic reticulum and free ribosomes with no evidence of cytoplasmic filaments or intracellular junctions, and only sparse collagen fibrils, indicative of an undifferentiated cell state. With progression of gestation, cells in the outer layer (prospective myometrium) acquire the morphological ultrastructure of smooth muscle cells such as abundant filaments with dense areas, numerous surface vesicles and external lamina [24]. Furthermore, at the junction between the myometrial layer and the endometrial stromal cells there are cells characterized as immature smooth muscle cells, suggestive of an area where cells are in a transitional state [24]. Brody et al. (1989) showed that in rats and mice there are 3 layers of mesenchymal cells: inner (adjacent to the epithelium), middle (prospective inner/circular myometrium) and outer. They also observed that early in myometrial development the outer and middle layers coexpress actin and vimentin, the latter being a marker for mesenchymal and fibroblastic cells [25]. Vimentin expression is repressed as smooth muscle cells differentiate, but remains present in cells that will compose the endometrial stromal [25]. These authors also reported that the cellular differentiation observed is accompanied by a change in cell orientation as stromal cells go from a radial to a random orientation whereas the inner myometrial layer becomes circular [25]. The interaction between epithelial and mesenchymal cells seems to be important for smooth muscle cell morphological differentiation as well as orientation as cells immediately adjacent to the epithelium become the endometrial stroma and cells further away become the circular and longitudinal myometrial cells. Furthermore, stromal cells immediately surrounding endometrial glands also acquire a circular orientation around the glandular epithelial cells [25]. Cunha et al. (1989) demonstrated that the endometrial epithelium is necessary and sufficient to induce differentiation of mesenchymal cells into smooth muscle cells [26]. By grafting uterine tissue under the kidney capsule of mice the authors observed that in grafts

containing both epithelium and mesenchyme, whether from intact uteri, digested uteri or tissue recombinants, mesenchymal cells formed bundles of actin-positive smooth muscle cells. There was no effect of the age of the epithelial cells on their ability to induce differentiation of mesenchymal cells [26]. On the other hand, grafts of mesenchymal cells alone were composed mainly of fibroblast cells, forming small amounts of smooth muscle cells mostly associated with blood vessels. More recently, Ono et al. (2007) identified a local source of uterine smooth muscle cells with stem cell-like characteristics [27]. These authors isolated a side population of the uterine myometrial cells, which were classified as immature smooth muscle cells due to low expression of several SMC markers. These cells were arrested in G0 phase with poor proliferation, however upon exposure to hypoxic conditions the cells proliferated efficiently and begun expressing smooth muscle cell markers such as α-smooth muscle actin and calponin. Furthermore, this human side population of myometrial cells was incorporated into mouse uteri following intra-uterine transplantation and underwent differentiation into smooth muscle cells. These cells also became activated during pregnancy as evidenced by oxytocin receptor expression.

*2.1.2 Molecular Control of Smooth Muscle Cell Gene Expression and Plasticity*

The majority of the data regarding the molecular control of smooth muscle-specific gene expression has been generated using vascular smooth muscle cells as a model. Vascular smooth muscle cells have high plasticity and can reversibly switch phenotype according to environmental cues (e.g. conversion from a quiescent to a highly proliferative phenotype upon local injury). From what is known about uterine smooth muscle cells, mature, fully differentiated cells in the adult uterus are quiescent with very low proliferation rates. However, the highly

proliferative characteristic of uterine smooth muscle cells in leiomyoma tumors and their increased secretion of collagen, as well as the uterine growth in early pregnancy due to hyperplasia are suggestive of an ability of these cells to modulate their phenotype according to specific local conditions.

Although there are a number of smooth muscle cell markers such as smooth muscle (SM) α-actin, SM myosin heavy chain (SM-MHC), calponin, SM 22α, h-caldesmon, and smoothelin, most of them, with the exception of SM-MHC, are expressed at least transiently in other tissues in vivo [28]. Upon a phenotypic change these SM markers become downregulated. This differentiation pathway is regulated mainly at the transcriptional level. Some of the transcription factors involved are MADS box proteins (e.g. serum response factor-SRF), homeodomain proteins (e.g. HoxB7), kruppel-like zinc finger proteins (e.g. Sp1/3), GATA family (GATA4/5/6), helix-loop-helix (e.g. Twist), myocardin, Egr-1, AP-1, c-myb and others [28].

Serum response factor (SRF) is a transcription factor that was discovered as the factor activating transcription of c-fos in response to serum. It binds to the serum response element, called CArG box ($CC[A/T]_6GG$), as a dimer and regulates the expression of many muscle-specific genes. SRF is ubiquitously expressed, which suggests the necessity of other SM-specific regulatory mechanisms. There is evidence indicating that cofactors, posttranscriptional modifications of SRF, and altered SRF binding affinity to DNA are some of the mechanisms used to regulate SM-specific expression. A major finding in the field was the identification of a potent transcriptional cofactor, exclusively expressed in SMCs and cardiomyocytes, called myocardin [29]. Myocardin was first identified as a regulator of cardiac-specific gene expression and cardiac development, and has also been shown to activate SM-specific genes, without activating the SRF-responsive gene c-fos.

More recently chromatin modifications have also been reported as an important regulator of SM-specific gene expression. For instance, SRF binds preferentially to SM α-actin and SM-MHC promoters in differentiated rather than undifferentiated cells, which coincides with higher acetylation levels in differentiated cells [30]. Moreover, the chromatin in promoters of SMC-specific genes is more available for nuclease digestion in SMCs than in non-SMC [30]. These findings were strengthened by data showing the interaction of SRF with acetyltransferases such as CREB binding protein (CBP) and p300 and the synergistic activation of the SM MHC promoter by GATA6 and p300 interaction [30]. Furthermore, myocardin itself has a SAP domain with chromatin remodeling function [30]. In addition, platelet-derived growth factor BB (PDGF-BB) is abundant at site of vascular injury as well as in leiomyoma tumors. It can reversibly repress SMC-specific genes inducing a switch in cell phenotype [30]. Interestingly, PDGF-BB treatment leads to competition for SRF between the transcription factors Elk and myocardin, by inducing nuclear translocation of Elk. It also induces expression of the histone deacetylase KLF4 leading to deacetylation of histone H4 and reduction in SRF binding to SM-specific genes [30]. However growth-responsive genes retain high acetylation and have their transcription induced. McDonald and Owens (2007) created a model in which physiological chromatin of differentiated SMCs undergoes reorganization in response to events triggered by PDGF-BB and becomes transcriptionally repressive creating a pathological chromatin environment and leading to inhibition of SRF/myocardin complexes binding. The effects of PDGF-BB are reversible. In summary, PDGF-BB can inhibit the expression of SMC-specific genes in favor of the expression of growth responsive genes inducing a phenotypic switch from a contractile phenotype into a more proliferative one [30].

## 2.2 UTERINE LEIOMYOMAS

### *2.2.1 Classification, Epidemiology and Genetics*

Uterine leiomyomas, also called myomas, leiomyomata or fibroids, are benign tumors that arise from smooth muscle cells of the human myometrium. Leiomyomas are characterized by an increase in SMC proliferation and excessive deposition of extracellular matrix proteins primarily collagens type I and type III [1, 2, 31-33]. They can be classified as intramural (within the myometrium), submucosal (lying just beneath or within the endometrium), or subserosal (located just beneath the outer serosa) according to the spatial localization of these tumors in the uterine wall (Figure 3) [34]. Figures 4A and B show images of a normal size uterus with an intramural leiomyoma tumor and a uterus with two large subserosal leiomyoma tumors as well as some smaller intramural tumors, respectively. Epidemiological studies have shown that seven out of every ten Caucasian women and eight out of every ten African-American women will eventually develop uterine leiomyomas [3]. Whereas the estimated incidence indicates that the majority of women will be affected by this disorder, only 1 in every 4 women present with symptoms. These include pelvic pressure, abnormal uterine bleeding, and reproductive dysfunction. Figure 5A shows the distended abdomen of a woman carrying multiple leiomyoma tumors, which can be present at a variety of sizes and shapes (Figure 5B). Of women with employer-sponsored health insurance, age groups 35-44 and 45-54 represented 43.29% and 45.65% of the clinically relevant leiomyoma cases, respectively, and of the 59.2% of women who had leiomyoma surgical treatment, more than 75% were hysterectomies [35]. Recent survey studies have reported that over 600,000 hysterectomies are performed in the United States every year, and that uterine leiomyomas represent 29.4% and 41.4% of the hysterectomies carried out in women ages 18-44 and 45-64, respectively [4]. The bleeding pattern in women with

leiomyomas is characterized by menorrhagia or hypermenorrhoea, and can cause anemia as well as loss of work productivity and a sense of social stigmatization [32]. Alternative treatments for symptomatic leiomyoma tumors include less invasive surgeries such as myomectomy, uterine artery embolization, and endometrial ablation which preserve the uterus but may lead to reoccurrence. Non-surgical treatment involves the use of gonadotropin-releasing hormone (GnRH) agonists which effectively reduce tumor size but lead to bone density loss and resumption of tumor growth once treatment is terminated. This approach is a good option as a temporary treatment used prior to surgical removal of tumors to reduce tumor size. Recent studies by Hassan et al. (2009) using the Eker rat, which spontaneously develops leiomyoma tumors, tested the effectiveness of gene therapy as treatment for these tumors. The authors used adenovirus to deliver the herpes simplex virus 1 thymidine kinase gene to leiomyoma cells through intra-tumor injections. This procedure was followed by administration of ganciclovir, which is a target of simplex virus 1 thymidine kinase and upon phosphorylation becomes a toxic compound that leads to cellular apoptosis [36]. In a similar, study Hassan et al. (2008) delivered a dominant-negative estrogen receptor gene into leiomyoma tumors of Eker rats [37]. Both studies observed significant reductions in tumor size due to reduced proliferation and expression of proliferation-related genes as well as induction of apoptosis with no noticeable toxic effects, indicating that this technique may be a promising therapy for treatment of uterine leiomyomas.

Ethnicity is a significant factor in the epidemiology of uterine leiomyomas. African American women having a 9.4 odds ratio having a tumor in the population analyzed by Faerstein et al. (2001), indicating that African American are more likely to develop these benign tumors than Caucasian women [38]. African Americans also are average 5.3 years younger at the time of uterine leiomyoma diagnosis and have more severe symptoms than Caucasian women [39].

Other factors such as early menarche (<10 years old), high body mass index (BMI), diabetes, hypertension, and chlamydial infection are also positively correlated with higher risk of uterine leiomyomas, whereas use of oral contraceptive has been shown to have a negative influence on this condition [38, 40]. Pregnancy is a protective factor, with nulliparous women being an average 3 years younger at the age of diagnosis [39]. Other evidence for genetic predisposition comes from twin studies showing a strong correlation with women undergoing hysterectomy for leiomyomas [41], and studies showing that first-degree relatives of an affected woman were more likely to develop leiomyomas. However, these results may be biased, as a relative of a patient with leiomyomas might be more likely to seek diagnosis [42]. Studies using the X-linked glucose 6-phosphate dehydrogenase isozyme to determine clonality of leiomyomas have confirmed that these tumors are monoclonal in origin, meaning that a single SMC carrying a mutation that confers a growth advantage will give rise to the entire tumor cell population [43]. The monoclonal origin hypothesis was also confirmed by experiments testing the inactivation of X-linked phosphoglycerate-kinase [44]. Mutations in the fumarate hydratase gene, coding for a Kreb's cycle enzyme, are associated with hereditary leiomyomatosis and renal cell cacinoma syndrome as well as Reed's syndrome (Multiple Cutaneous and Uterine Leiomyomata). Both syndromes include cutaneous and uterine leiomyomas as well as a higher incidence of renal cell carcinoma and leiomyosarcoma, and they are now considered the same disease [45, 46]. Chromosomal abnormalities are present in 40-50% of leiomyoma tumors removed at surgery, with the most common ones being a translocation between chromosomes 12 and 14, deletion of chromosome 7, trisomy of chromosome 12, and rearrangements of 6p10q and 13q. Translocations between chromosomes 12 and 14 also occur in other mesenchymal solid tumors and involve HMGA2, a gene encoding a DNA binding protein that induces conformational

changes in DNA and may regulate transcription. Hodge et al. (2009) have reported a single TC repeat allele with 27 TC repeats located upstream of the transcription starting site in the 5'UTR of the HMGA2 gene to be associated with the presence of leiomyoma tumors, and tumors positive for the allele had slightly higher HMGA2 expression [47]. Moreover, rearrangement of chromosome 6 disrupts *HMGA1* [48-50]. The diversity of genetic mechanisms potentially affecting leiomyoma development suggests that these benign tumors are composed of various, distinct subtypes of neoplasms, just as cancers are divided into numerous specific subsets of disorders [51]. Polymorphisms in genes like CYP17, cathechol-O-methyltransferase, and estrogen receptor, have all been associated with a higher risk of developing leiomyomas. The genotypes for the latter two genes, which were associated with higher risk of developing the tumors, show a higher frequency in African American women [52, 53].

*2.2.2 Sex Steroid Hormones*

Although the mechanisms leading to the development of uterine leiomyomas remain to be determined, sex steroid hormones have been shown to play important roles in controlling tumor growth. The identification of steroid receptor expression in leiomyoma cells indicates a possible direct effect of these hormones on tumor growth. The cell proliferation rate is higher in leiomyoma than in normal myometrium regardless of the phase of the cycle but, when looking at the two different phases of the cycle, leiomyomas show a higher proliferative rate during the secretory phase during which progesterone is the dominant hormone [54, 55]. Estrogen receptors (ER) α and β and progesterone receptors (PR) A and B are upregulated at the mRNA and protein level in leiomyoma tissue compared to adjacent myometrium [55-58]. Treatment of leiomyoma SMCs with estrogen or progesterone increases cell proliferation [54, 59, 60], whereas use of

respective antagonists blocks this effect [59, 60]. Leiomyomas have also been found to express the aromatase P450 enzyme suggesting the presence of an autocrine/paracrine system within leiomyomas by which the SMCs produce their own estradiol which stimulates growth independently of systemic sex steroid hormones [61, 62]. GnRH treatment causes suppression of the hypophyseal-gonadal axis, decreasing ovarian steroid levels and leading to tumor regression [63, 64]. Based upon the steroid-dependent characteristics of leiomyoma growth, therapy with either GnRH agonists or antagonists has been a successful alternative for treatment of uterine leiomyomas. A recent study by Hermon et al. (2008) showed the upregulation of ERα in leiomyoma compared to normal myometrium both in the secretory and proliferative phases [65]. Furthermore, this study also reported higher protein levels of phosphorylated ERα (phospho-Ser118) in tumors versus normal tissue, with significantly higher levels in tumors at the proliferative phase in comparison to the secretory phase, suggesting higher responsiveness of tumor cells to estrogen. In addition, the above authors found higher levels of phospho-p44/42 MAPK in leiomyoma tumors in the proliferative phase, with higher PCNA labeling in tumors in both phases of the menstrual cycle [65].

*2.2.3 Growth Factors, Extracellular Matrix and MicroRNAs*

In addition to a direct effect on cell cycle and apoptosis regulation, sex steroid hormones also exert mitogenic effects through stimulation of growth factor production by their target cells. These in turn can act in an autocrine/paracrine fashion to modulate cell growth. After detecting estrogen-stimulated increases in leiomyoma SMC proliferation, Barbarisi et al. (2001) observed that platelet-derived growth factor (PDGF) levels were increased in the conditioned medium from these cells and that this growth factor was responsible for the estrogen-induced mitogenic

effect on leiomyoma SMCs [60]. Furthermore, GnRH agonist therapy downregulates PDGF expression in women with leiomyomas and causes a reduction in tumor volume [66].

The expression of other growth factors such as epidermal growth factor (EGF), insulin-like growth factor I (IGF-I), transforming growth factor beta 1 (TGF β1), basic fibroblast growth factor (bFGF) and heparin-binding EGF-like growth factor (HB-EGF), their respective receptors, and their regulation by estrogen and/or progesterone has been reported in leiomyomas [54, 59, 67-71]. EGF is upregulated by progesterone during the luteal phase of the menstrual cycle in leiomyomas and EGF-R is upregulated by estrogen, whereas treatment of women with GnRH agonist reduced the binding of EGF to leiomyoma tissues versus leiomyomas from untreated patients [54, 72, 73]. Both EGF and PDGF stimulate proliferation of myometrial cells [74, 75]. HB-EGF, a member of the EGF family, has been shown to stimulate leiomyoma and myometrial cell proliferation and to inhibit apoptosis [68], however, these effects were more pronounced in myometrial cells, probably due to a higher expression of HB-EGF receptor (HER1) observed in those cells.

The FGF receptor/ligand system, important for angiogenesis and induction of extracellular matrix (ECM) remodeling enzymes, also appears to play a role in the pathogenesis of leiomyomas as bFGF induces proliferation of both myometrial and leiomyoma SMCs. Expression of bFGF is stronger in leiomyoma tumors than in normal myometrium regardless of the phase of the cycle [70] and its expression is reduced during GnRH agonist treatment [76].

IGF-I is another growth factor implicated in the pathogenesis of leiomyomas. Both the expression of IGF-1 and its binding are increased by exposure to estrogen, and IGF-I seems to preferentially induce mitogenic activity in leiomyoma SMCs [67, 77]. The increase in cell number upon IGF-I treatment seems to be a result of its ability to promote proliferative activity

through upregulation of PCNA expression, and upregulation of Bcl-2, which inhibits apoptosis [78]. Recently, Yu et al. (2008) reported higher protein expression for EGF-R, ErbB4, FGFR1, FGFR2α, FGFR3, FGFR4, IR, IGF-IR, HGF-R, MSP-R, PDGF-Rα, PDGF-Rβ, SCF-R, Fit3, and M-CSF-R in leiomyoma tumors versus normal myometrium tissue [79]. These authors went further to study the IGF-I pathway and observed higher protein expression for IGF-I as well as higher levels of phosphorylation of downstream effectors of the IGF-I pathway such as IGF-IRβ, p44/42 MAPK and Shc in tumors compared to patient matched myometrium [79].

TGFβ is an important family of growth factors that play a significant role in the development of fibrotic conditions such as renal and hepatic fibrosis. Expression of TGF-β and TGF-β receptors has been confirmed in leiomyoma and myometrial SMCs, being more abundant in leiomyomas than in myometrium [80-82]. TGF-β 3 mRNA levels were increased during the luteal phase of the menstrual cycle, and treatment with the GnRH agonist leuprolide acetate caused a decrease in expression of TGF-β family members [83, 84]. Lee & Nowak (2001) also found that TGF-β3 inhibited DNA synthesis in myometrial SMCs, but stimulated it in leiomyoma cells [82]. Furthermore, inhibition of TGF-β caused a decrease in collagen I and III mRNAs in both myometrial and leiomyoma SMCs. Higher expression of TGF-β in leiomyomas and its role in stimulating increased synthesis of collagen correlates with the findings of Stewart et al. (1994), who observed a more intense immunostaining for collagen I and III in leiomyoma tissues [1]. This characteristic increase in collagen deposition in leiomyoma tumors was also observed by Leppert et al. (2004), who determined by electron microscopy that collagen fibrils in leiomyomas are very abundant and distributed in a disorganized fashion, as compared to fewer and well-aligned parallel fibrils in normal myometrium [33]. In addition to ECM protein production, processes associated with matrix turnover and remodeling are equally important,

being tightly regulated by matrix metalloproteinases (MMPs) and tissue inhibitor of MMPs (TIMPs). Dou et al. (1997) reported very low levels of MMP-1, -2 and -3 mRNA in leiomyomas compared to myometrium [85]. Another aspect related to the influence of the matrix composition to tumor growth is the level of glycosaminoglycans (GAGs). GAGs are present in the cellular and extracellular environment of tumors and can facilitate tumor cell migration, movement of molecules, and serve as a reservoir for growth factors and affect secretion of enzymes that degrade ECM. Wolanska et al. (1998) reported an increase in leiomyoma tissue content of sulphated GAGs during tumor growth [86].

Vasoactive agents (angiotensin II, serotonin), cytokines (tumor necrosis factor alpha - TNFα, interleukin 1 - IL-1), oleic acid, and thrombin also have been shown to play important roles in proliferation, migration and/or differentiation of cells of mesenchymal origin, either from the vascular system, rat leiomyoma cells (ELT-3), liver or in the kidney during development of fibrotic disorders [87-95].

More recently some studies have focused on the expression of microRNAs in leiomyoma tumors. Pan et al. (2008) identified a significant reduction in the number of microRNAs expressed in leiomyoma tissues compared to normal myometrial tissues. In addition, when comparing microRNA expression in myometrial tissue to leiomyoma tissue, myometrial SMCs, leiomyoma SMCs, immortalized leiomyoma SMCs and a leiomyosarcoma cell line there was a progressive decline in the number of microRNAs [96]. These findings suggest that microRNAs may play an important role in regulating the development of leiomyoma tumors. These authors also observed that the expression of miR-20a, miR-21 and miR-26a is responsive to ovarian steroids as tested in leiomyoma and myometrial SMCs by treatment with estradiol, medroxy progesterone acetate (MPA), estrogen receptor antagonist ICI-182780 and progesterone receptor

antagonist RU-486 [96]. Interestingly, qRT-PCR confirmed the expression pattern of numerous of microRNAs, several of which have as predicted targets a number of known important players in the pathogenesis of leiomyomas, such as TGFβ family members, EGR1 and 3, FGF familiy members, EGF, Bcl2, ESR1 and 2, PDGFA, IGF-I, VEGFB, PCNA, and enzymes related to steroid metabolism [96].

*2.2.4 Atherosclerosis Model*

Atherosclerosis is a chronic consequence of obesity and diabetes, and results in thickening and hardening of the blood vessel walls (sclerosis), as well as loss of elasticity. The African American population has a high prevalence of hypertension (52% - >45 years old), and diabetes (12-15%), with 60% being over weight or obese [97]. African American women also have a higher prevalence of uterine leiomyomas and as the mechanism of atherosclerosis development is somewhat similar to the changes occurring during the formation of uterine leiomyomas. I will next review the results generated from research in vascular biology to try to gain insight in the mechanisms leading to the development of uterine leiomyomas.

Hypertension, a symptom of cardiovascular disorders associated with atherosclerosis, is positively correlated with risk for uterine leiomyoma in premenopausal women [87]. Furthermore, angiotensin II, oleic acid, glucose and serotonin are found at elevated concentrations in hypertensive patients, and because these factors can also induce SMC proliferation and migration [90-92, 98-100], they have become targets of studies looking at their possible role in the pathology of cardiovascular disorders.

Whereas the pathophysiology of uterine leiomyoma is unclear, these tumors are well characterized by increased growth of uterine SMCs and remodeling of the extracellular matrix

(ECM), particularly the abundant deposition of collagens I and III [1, 32, 33]. These processes are also present during the formation of atherosclerotic lesions, as described by Ross (1995) [101]. Both vascular smooth muscle cells (VSMCs) and UtSMCs undergo a phenotype change during the development of atherosclerosis and leiomyoma, respectively, mostly determined by matrix remodeling. Differentiated, non-proliferating cells are classified as the "contractile phenotype". These cells express a series of proteins associated with contraction and are present in normal vasculature and myometrium. In atherosclerotic lesions, upon disruption of the basal membrane of blood vessels, some of these contractile proteins are downregulated, whereas ECM proteins, especially collagen I – III and fibronectin are upregulated. Under such conditions cells appear to dedifferentiate, assuming a "proliferative phenotype", which also allows for cell migration. Shanahan & Weissberg (1998) identified several genes that are associated with the contractile (α-SM actin, γ-SM actin, calponin, SM myosin heavy chain, elastin, etc) versus proliferative (osteopontin and matrix gla protein) phenotypes [102]. Such phenotypic changes induced by different ECM proteins affect cell proliferation in vitro, as shown by Hirst et al. (2000), who observed that VSMC expressed lower levels of contractile markers (SM-MHC, calponin, SM-α-actin) when grown in fibronectin or collagen I, and had higher mitogen-induced proliferation rates than cells grown on laminin and Matrigel [5]. In addition, porcine VSMC showed a higher rate of proliferation in response to PDGF and bFGF when grown on fibronectin versus cells grown on laminin [103]. Given the influence of ECM on SMC phenotype, Blindt et al. (2002) decided to determine which integrins are important for cell-matrix interactions [104]. The authors found that SMCs grown on fibronectin expressed more integrin α5β1, and that inhibition of α5β1 was sufficient to inhibit migration, invasiveness, and attachment of SMCs to fibronectin.

Extrapolation of findings from development of vascular disorders to the development of leiomyomas gains further support when the pathophysiology of other fibrotic conditions is observed. Activation of stellate cells, mesenchymal cells present in the perivascular space in the liver, leads to the transformation of these cells from a quiescent cell into a myofibroblastic, proliferative and fibrogenic phenotype. This process is triggered by liver injury and results in changes in ECM composition. Fully activated stellate cells cause further ECM remodeling leading to scarring of the liver [6]. Interestingly, smooth muscle α-actin, a marker for smooth muscle cells, is also a marker for activated stellate cells [6]. Zeisberg et al. (2001) showed that inhibition of the basolateral assembly of collagen IV, an important component of basement membranes, caused epithelial-to-mesenchymal transdifferentiation of proximal tubular epithelial cells in renal fibrosis [7]. Such results reinforce the notion that this cell type is important in the developmental mechanisms of renal interstitial fibrosis, which include accumulation of fibroblasts and increased deposition of ECM components [7]. According to studies mentioned earlier in this chapter discussing the development of smooth muscle cells, they share some similarities with another important mesenchymal cell type with an important role in fibrosis, the stellate cells discussed above. Whether the SMCs present in leiomyoma tumors are dedifferentiated SMCs, recruited stem cells or originated from fully differentiated endothelial cells it is still unclear, because that can certainly depend on the kind of stimulus and the local microenvironment. However, the hypothesis of injury-induced phenotypic switch and abnormal proliferation has been proven in other fibrotic conditions and may be relevant for the pathogenesis of leiomyomas [8].

In addition to the significant changes in ECM composition another acknowledged feature of these fibrotic disorders is a local increase in production of growth factors and expression of

their receptors, accounting for an autocrine/paracrine regulation of further ECM deposition, cell proliferation and cell migration. Of particular interest to us is the mechanism by which growth factors, specifically EGF and PDGF lead to intracellular signal transduction ultimately causing these changes in gene expression.

*2.2.5 ROS and Signaling Pathways*

Regardless of the downstream molecules involved in the signaling pathway of EGF, PDGF, vasoactive factors and cytokines, most of them share a common feature upon binding to the respective receptor. An NADPH oxidase complex is activated to generate reactive oxygen species (ROS), mainly $H_2O_2$. Furthermore, ROS generation is necessary for downstream signaling leading to protein modifications, changes in gene expression, cell proliferation, migration, differentiation and tissue remodeling in a variety of cell types [10, 89, 91, 94, 99, 105-120].

ROS production through stimulation of NADPH oxidase is important for the proliferative and migratory response of SMCs to many factors. Nox1, a necessary component for NADPH oxidase activity in non-immune cells, shows increased mRNA and protein expression in vascular SMCs in response to PDGF [11], EGF [121], angiotensin II [109-111, 122], PGF2 α [123], and high glucose levels in diabetic mice [124]. Furthermore, treatment with angiotensin II [109-111], EGF [115], PDGF [91], glucose [124], thrombin [105], and oleic acid [89] induces ROS production in vascular SMCs as well as in other cell types such as endothelial cells [106] and renal mesangial cells [107]. As upregulation of Nox1 gene expression and protein is associated with increased ROS production, and because Nox1 gene expression is also regulated by the above factors, it was postulated that ROS production could be an important step on the signaling

pathway of these factors. The use of ROS scavengers (catalase, superoxide dismutase, N-acetyl cysteine) and NADPH oxidase inhibitors (DPI) blocks the growth factor-induced increase in endothelial and SMCs proliferation and migration, indicating that these effects are indeed mediated by ROS production. Further studies on the mechanisms of action of ROS have confirmed their role as signaling molecules. $H_2O_2$, a more stable ROS and product of growth factor-induced NADPH oxidase activation, specifically reacts with thiolate anion ($-S^-$), found only in cysteines located at a positively charged electrostatic field, allowing dissociation of the $S^-$ and stabilization of the structure. This reaction forms sulfenic acid as an intermediate, which is easily reduced, allowing for reversibility of the process. Both specificity and reversibility of the reaction are important characteristics of molecules involved in regulation of signaling pathways [125].

Much work has been done looking at the redox regulation of cell signaling, namely the influence of reducing or oxidizing agents on proteins involved in cell signaling. ROS generation has been primarily associated with increased phosphorylation and activity of ERK 1/2, p38 MAPK, and/or JNK [89, 90, 93, 94, 98, 99, 108, 112, 114, 116, 120]. Antioxidants or NADPH oxidase inhibitors can block these effects and treatment with $H_2O_2$ can mimic them, although there is no evidence for direct interaction between ROS and these kinases.

Many fibrotic conditions such as pulmonary, hepatic and pancreatic fibrosis are associated with overproduction of ROS [9], therefore compounds that can inhibit specific NOX/DUOX family members represent potential therapeutic approaches for treatment of these chronic diseases [126]. ROS are strong candidates to be important in leiomyoma tumor development. Some work has been done on the characterization of the ROS generating system, ligand-dependent ROS generation, downstream targets of ROS action and cells' responses to

increased and/or decreased ROS levels in other cell types. From these studies it appears that the parameters affected vary according to the specific cell type being studied. Thus there is no clear evidence as to the determining factors for ROS generation in leiomyoma SMCs and which molecules and pathways are activated by ROS in these cells.

*2.2.6 NADPH Oxidase: ROS-Generating System in Immune Cells*

NADPH oxidase is a membrane-associated enzyme complex that catalyzes the one-electron reduction of oxygen to superoxide anion ($O^2$-) using NADPH as a substrate. Superoxide is then further dismuted to hydrogen peroxide ($H_2O_2$), as well as other reactive oxygen species (ROS) that are used as microbicidals for host defense [127]. The NADPH oxidase complex was first characterized in immune cells where it can be activated by antigens and inflammatory mediators. The complex is composed of five subunits: $gp91^{phox}$, $p22^{phox}$, $p47^{phox}$, $p67^{phox}$, and $p40^{phox}$, where phox stands for **ph**agocytic **ox**idase. $Gp91^{phox}$ is a transmembrane protein, and its C-terminal region can interact with cytosolic components during enzyme activation [127]. $P22^{phox}$ is another transmembrane protein, with intra and extracellular portions. It interacts with $gp91^{phox}$ to form cytochrome b558 (cytb). Dissociation of the cytb complex causes enzyme inactivity. $P47^{phox}$ and $p67^{phox}$ are cytosolic proteins containing two SH3 domains important for interaction with other proteins. These proteins can be found in a free form or in a complex. NADPH oxidase can be activated in a receptor-mediated or receptor independent manner. In immune cells receptor mediated stimuli are chemotactic tripeptide N-formyl-Met-Ley-Phe (FMLP) and immune complexes, and receptor independent stimuli are long-chain unsaturated fatty acids and phorbol 12-myristate 13-acetate (PMA). These stimuli ultimately lead to phosphorylation of $p47^{phox}$, which binds to $p67^{phox}$ and the complex is then translocated to the

cell membrane, where these two interact with cytb to form activated NADPH oxidase. $P40^{phox}$ is 40kDa protein and the last member of the NADPH oxidase complex identified in bone marrow cells such as neutrophils, mast cells, B and T cells, monocytes and basophils. It is found associated with $p47^{phox}$ and $p67^{phox}$ in a complex [128].

*2.2.7 NADPH Enzyme Complex Activation*

As inhibitors of phosphorylation prevented NADPH oxidase activation in cell free systems, it was hypothesized that at least one of the enzyme complex components has to be phosphorylated to allow for enzyme activity. Ago et al. (1999) showed in a cell-free as well as whole-cell system that $p47^{phox}$ has 3 amino acids that undergo conformational changes upon phosphorylation, thus becoming exposed and allowing for interaction with $p22^{phox}$ on the cell membrane (Figure 6) [129]. $p47^{phox}$ is thought to act only as a link between $p67^{phox}$ and the cytochrome b558, because in a free cell system $p47^{phox}$ is not necessary for enzyme activity, while $p67^{phox}$ is important for the transfer of electrons from NADPH to the flavincytochrome b558 [127, 130]. In some cell types phospholipase C (PLC), phosphoinositide-3 kinase (PI3K) and protein kinase C (PKC) are upstream mediators of NADPH oxidase complex activation [89, 113, 118, 119, 131].

Guanine nucleotide-binding proteins (GTPase) are necessary components for NADPH oxidase activation and ROS production. Rac2 is important for NADPH oxidase activation in phagocytes [130, 132], while in non-phagocytic cells Rac1 seems to be important instead [133]. Rac GTPase exchanges GTP for GDP and becomes active, being targeted to the cell membrane. Quinn et al. (1993) have shown that Rac is translocated to the cell membrane in response to both receptor and non-receptor stimulation of NADPH oxidase and its translocation kinetics was

parallel to $p47^{phox}$/$p67^{phox}$ translocation and superoxide production, indicating a possible participation of Rac during complex activation [132]. Further evidence for the role of Rac during NADPH oxidase activation comes from studies showing that GTP-bound Rac contains a domain, called Switch I, which undergoes conformational changes that are important for Rac interaction with $p67^{phox}$ and consequently, for NADPH oxidase activity [130] Chanock [127].

Although in endothelial cells the NADPH oxidase complex exists as a preassembled intracellular complex [134], in VSMCs the complex seems to function more similarly to the way it does in phagocytes, with membrane subunits and cytosolic subunits that need to be translocated to the cell membrane making the complex active upon stimulation [110]. Cheng & Lambeth (2004) indicated that cells co-transfected with Nox1, Noxo1 and Noxa1 display constitutive ROS production regardless of the presence of a stimulus, as Noxo1 co-localizes with Nox1 on the membrane of resting cells bound to phosphatidylinositol lipids [135]. Mutations in the PX domain of Noxo1, which mediates its interaction with the cell membrane, lead to a decrease in its lipid binding and Nox1 activation with consequent lower ROS production. Such results indicate that the mechanism by which ROS are produced might depend on the NADPH oxidase subunit homologues being expressed in specific cell types and their combination to form the active complex as well as their own specific characteristics. For example, in cells in which $p47^{phox}$ is among the subunits responsible for the NADPH oxidase complex activity, $p47^{phox}$ needs to be phosphorylated in order to be targeted to the membrane. However, if Noxo1 is required instead, the NADPH oxidase complex is usually found preassembled and constantly active. Furthermore, c-Src kinase has been shown to be necessary for NADPH oxidase activation in one study [110], but only a downstream target of ROS in another [91]. Even the MAP kinases that are affected by ROS generation vary according to the cell type studied.

*2.2.8 NADPH Oxidase in Non-Immune Cells*

In addition to the generation of ROS as a defense mechanism by immune cells, ROS are also thought to be an undesirable product of oxygen metabolism that, by being highly reactive, can cause uncontrolled protein and DNA modifications. Studies showing that non-immune cells are able to generate ROS in response to growth factors, hormones, and lipids raised the question whether ROS, released in a controlled manner, could be signaling molecules necessary for the intracellular relay of extracellular signals. The ability of NADPH oxidase inhibitors to block ROS generation in non-immune cells suggests the presence of a NADPH oxidase-like ROS generating system in these cells. When looking for the components of the NADPH oxidase complex, non-phagocytic cells were still able to generate similar amounts of ROS compared to normal cells even though they lacked the $gp91^{phox}$ subunit, a necessary component for ROS production in phagocytic cells. Such results are indicative that homologues of this subunit could be present in non-phagocytic cells [136, 137]. In fact, the laboratory of Dr David Lambeth was the first group to identify a homolog of human $gp91^{phox}$, initially called Mox1, and now officially termed Nox1 (**N**ADPH **ox**idase) [11]. Subsequently, his lab also cloned and sequenced three new homologues of $gp91^{phox}$, called Nox3, Nox4 and Nox5 and assessed their expression in different cell types [137] (Figure 7).

$Gp91^{phox}$ homologues in non-immune cells (Figure 8) are classified in three subgroups. The first is the $gp91^{phox}$ sub-family, consists of $gp91^{phox}$ (neutrophils, macrophages), nox1 (colon, VSMCs, prostate), nox3 (fetal kidney, fetal liver, fetal lung, fetal spleen) and nox4 (kidney, osteoclasts, pancreas, placenta, skeletal muscle, ovary, astrocytes), all approximately 65kD in size and very similar in conformation to $gp91^{phox}$. Duox1 (thyroid, lung) and duox2 (thyroid, colon) are approximately three times larger than $gp91^{phox}$ (≈ 180kD) and form the Duox

sub-family, which contains two extra domains, an N-terminal peroxidase homology domain and a central domain with two EF-hand calcium-binding motifs. The Nox5 subgroup has a short splice variant (fetal kidney) similar to gp91$^{phox}$ in size, or a long variant (spleen, testis) containing a calcium-binding domain [136-140].

The cytosolic subunits p47$^{phox}$ and p67$^{phox}$ have also been found to have homologues in non-phagocytic cells. The p47$^{phox}$ homolog is a 41kD protein called Nox organizer 1 (Noxo1), and the p67phox homolog is a 51kD protein called Nox activator 1 (Noxa1). Both novel subunits support ROS production and respond more efficiently in cells containing the non-phagocytic catalytic subunit of the NADPH oxidase complex, Nox1 [141, 142] (Figure 9). Noxo1 has a 27% sequence identity (percentage of identical amino acid residues), a 46% sequence similarity (percentage of amino acid residues with similar properties) and a high structural similarity (similarities in size and conserved domain structure) to p47$^{phox}$. Despite these similarities Noxo1 lacks serine residues on the C-terminal region. These serine residues are present on p47$^{phox}$ and account for an auto-inhibitory domain. When phosphorylated, C-terminal serine residues allow interaction of p47$^{phox}$ with the NADPH complex. A PXXP motif, also present in the PX domain of p47$^{phox}$ and important for intra-molecular interaction with the protein C-terminal SH3 domains, is also lacking in Noxo1. Noxa1 is also very similar to its phox homolog, p67$^{phox}$, with 38% sequence identity and 56% sequence similarity. The only structural difference between the two is the lack of a central SH3 domain in Noxa1 [141].

### *2.2.9 Protein Tyrosine Phosphatases (PTPases)*

Inhibition of phosphatase activity is an important process for the tight regulation of signaling pathways, as control over the sequential steps during the signal relay is obtained

mainly through phosphorylation and dephosphorylation of proteins by kinases and phosphatases, respectively. Protein tyrosine phosphatases (PTPases) are known targets of ROS action and could account for the effects of ROS generation on MAPK phosphorylation and activation. This specific family of phosphatases is characterized by a motif containing a cysteine residue that resides in a unique environment providing the cysteine with a very low pKa. This feature enhances its nucleophilic properties but also makes it susceptible to oxidation [15]. Very detailed work on $H_2O_2$ inhibition of PTPase was done by Denu & Tanner (1998), who showed that $H_2O_2$ action is specific to PTPase, not inhibiting serine/threonine phosphatases (PP) [143]. The authors also showed that PTPase inactivation was reversed by thiols (DTT, β-ME, reduced glutathione, and cysteine) and that PTPase inactivation was reversible. However, others have shown that $H_2O_2$ is able to inhibit the activity of the serine/threonine phosphatases, PP1 and PP2A, and thiol-specific reducing agents (DTT, β-ME, and NAC) blocked this effect. Well documented evidence for the role of $H_2O_2$ in the signaling pathways of hormones and growth factors can be found in papers by Meng et al. [144, 145], who showed that different PTPases are inactivated in response to insulin and PDGF stimulation, and that this inactivation was dependent on ROS production. Moreover, in both cases, PTPase activity was associated with a decrease in the activation of downstream effectors of the respective pathways. Lee et al. (1998) suggested that inactivation of PTPases by $H_2O_2$ following EGF binding to its receptor is required for optimum tyrosine phosphorylation levels [18]. It is speculated that NADPH oxidase-derived ROS oxidizes and inactivates MAP kinase phosphatases and maintains oncogenic Ras MEK-induced activation of ERK [146].

$H_2O_2$ is produced upon growth factor stimulation of vascular SMCs and treatment with $H_2O_2$ causes cell growth. Since $H_2O_2$ is also involved in the regulation of PTP activity, it has

been proposed that $H_2O_2$ might be a necessary component of the intracellular signaling relay of molecules such as PDGF, EGF, angiotensin II, serotonin, and oleic acid that control ROS production [89, 91, 98, 99, 120].

## 2.3 FIGURES

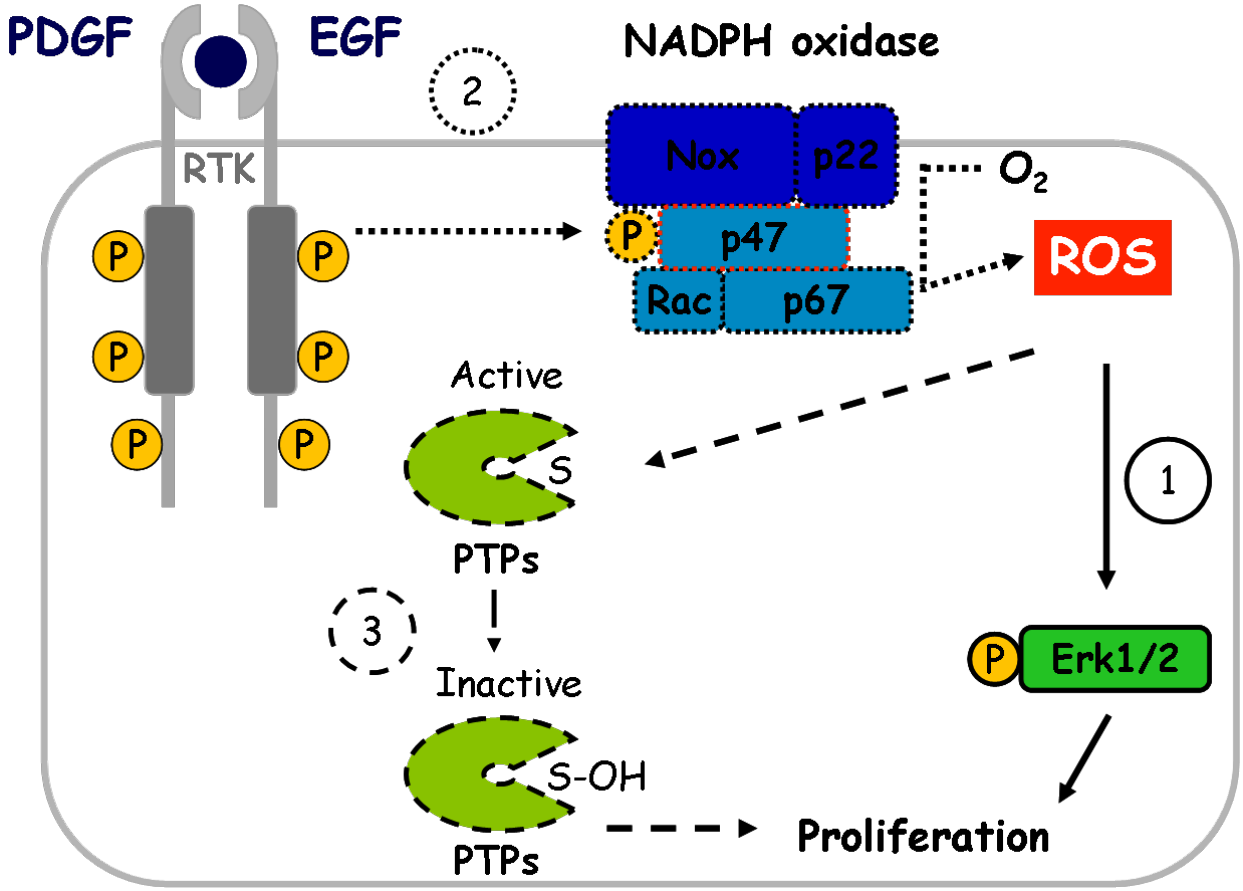


Figure 1. Scientific model to illustrate my proposed working hypotheses relative to each specific aim proposed for this work. Number 1 and solid lines indicate work related to specific aim 1; Number 2 and dotted lines indicate work related to specific aim; Number 3 and dashed lines indicate work related to specific aim 3.

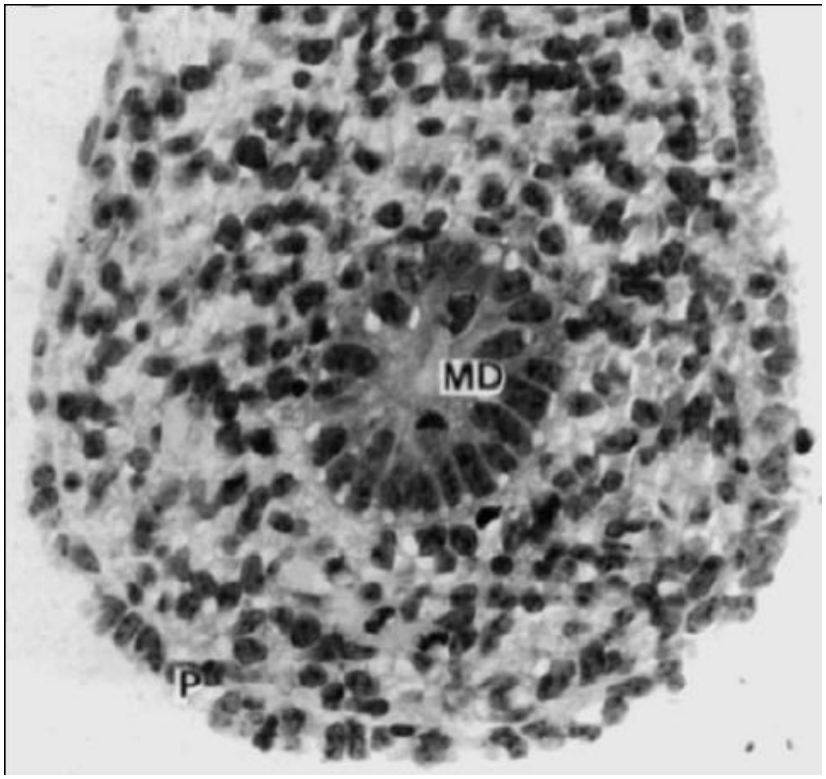


Figure 2. Localization of uterine mesenchymal cells in the developing mouse uterus. Mullerian duct (MD)

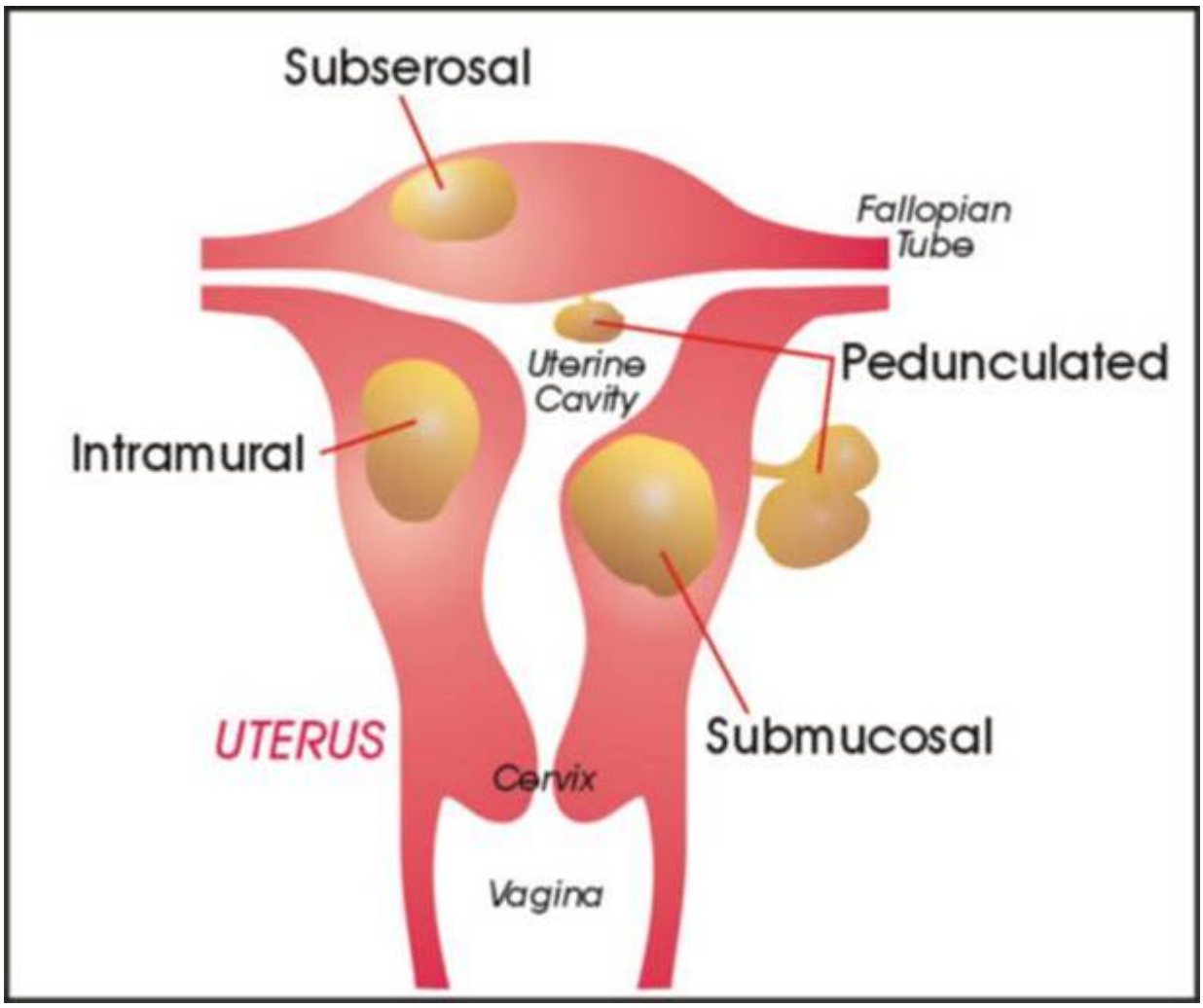


Figure 3. Classification of leiomyoma tumors according to their localization in the uterus.

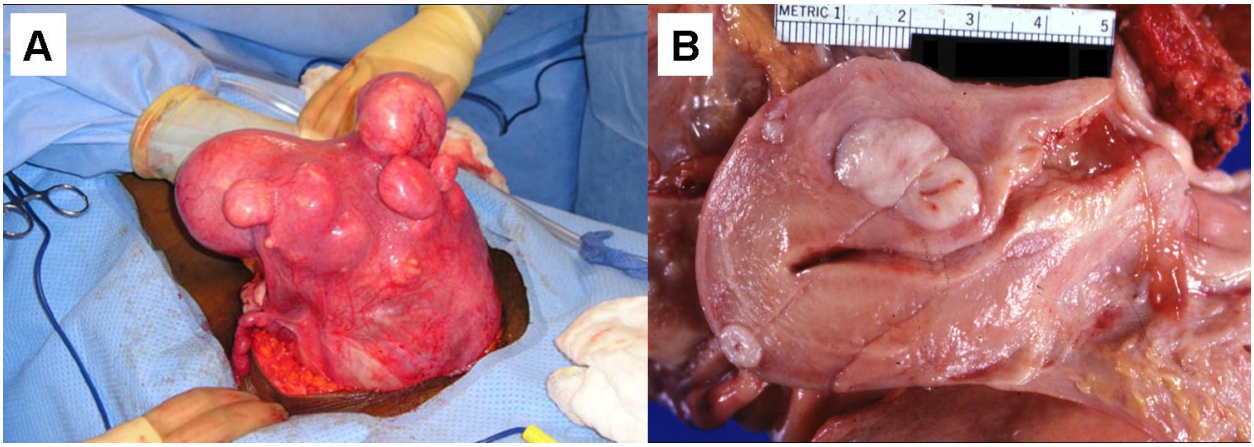


Figure 4. Leiomyoma tumors. A) Uterus with similar size to a 28-week pregnancy prior to myomectomy. B) Normal size uterus with 3 intramural leiomyoma tumors. Images courtesy of Dr Jay Goldberg, MD, MSCO, of Jefferson Medical College, Philadelphia, and Dr Peter Anderson, DVM, PhD, PEIR Digital Library, UAB Department of Pathology.

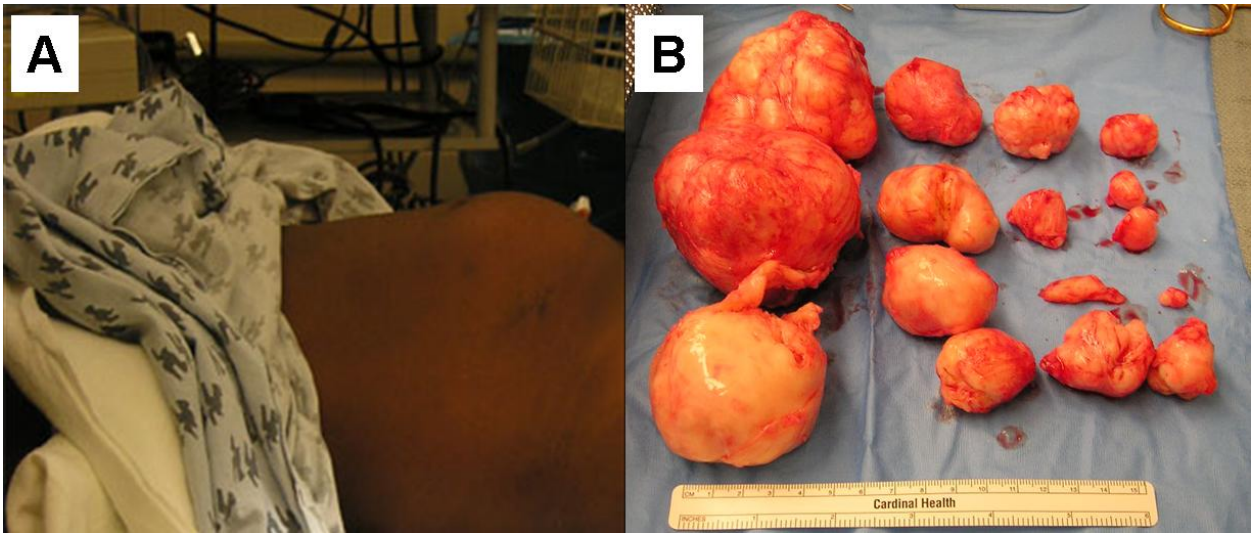


Figure 5. Leiomyoma tumors. A) Abdomen of a woman the size of a 28-week pregnancy prior to myomectomy. B) 16 leiomyomas removed at myomectomy in patient wishing to avoid hysterectomy. Images courtesy of Dr Jay Goldberg, MD, MSCO, of Jefferson Medical College, Philadelphia.

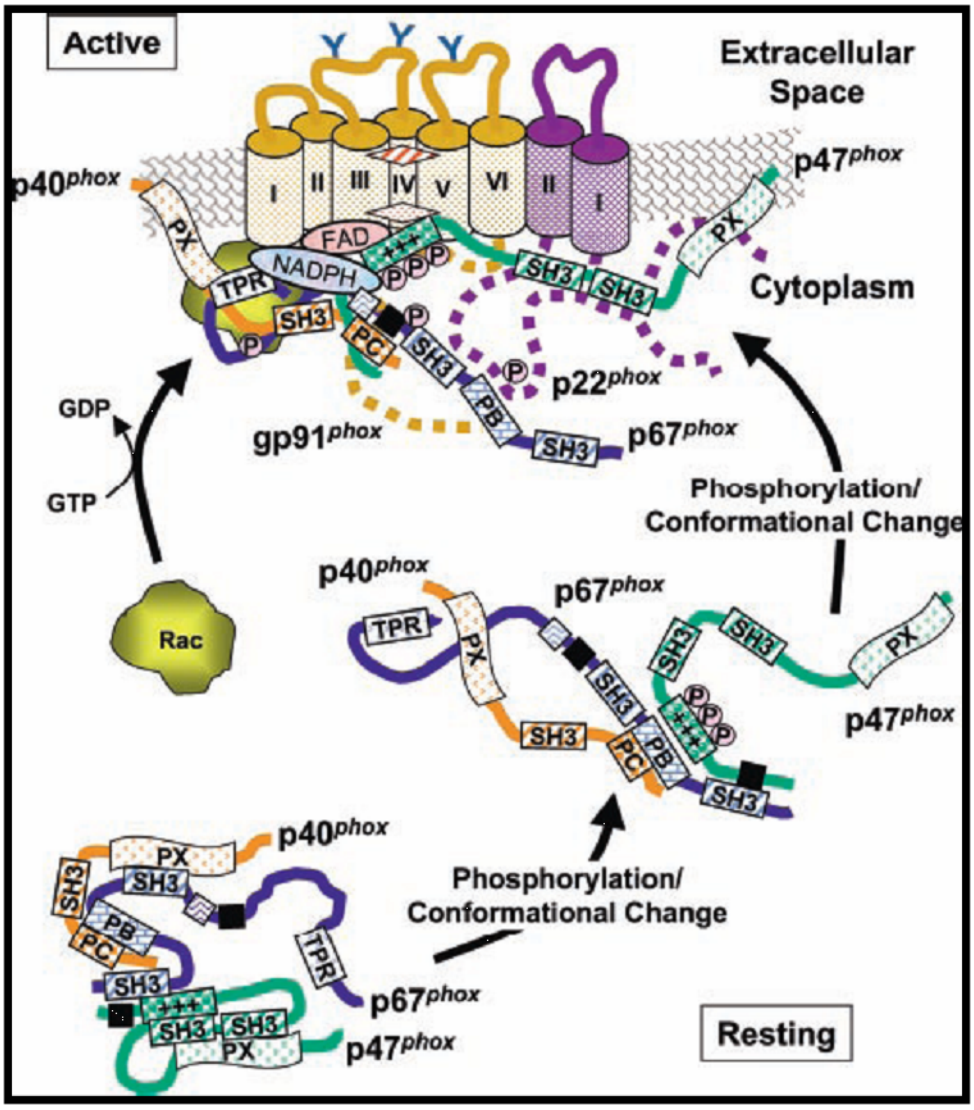


Figure 6. Activation of the NADPH oxidase complex in phagocytic cells.

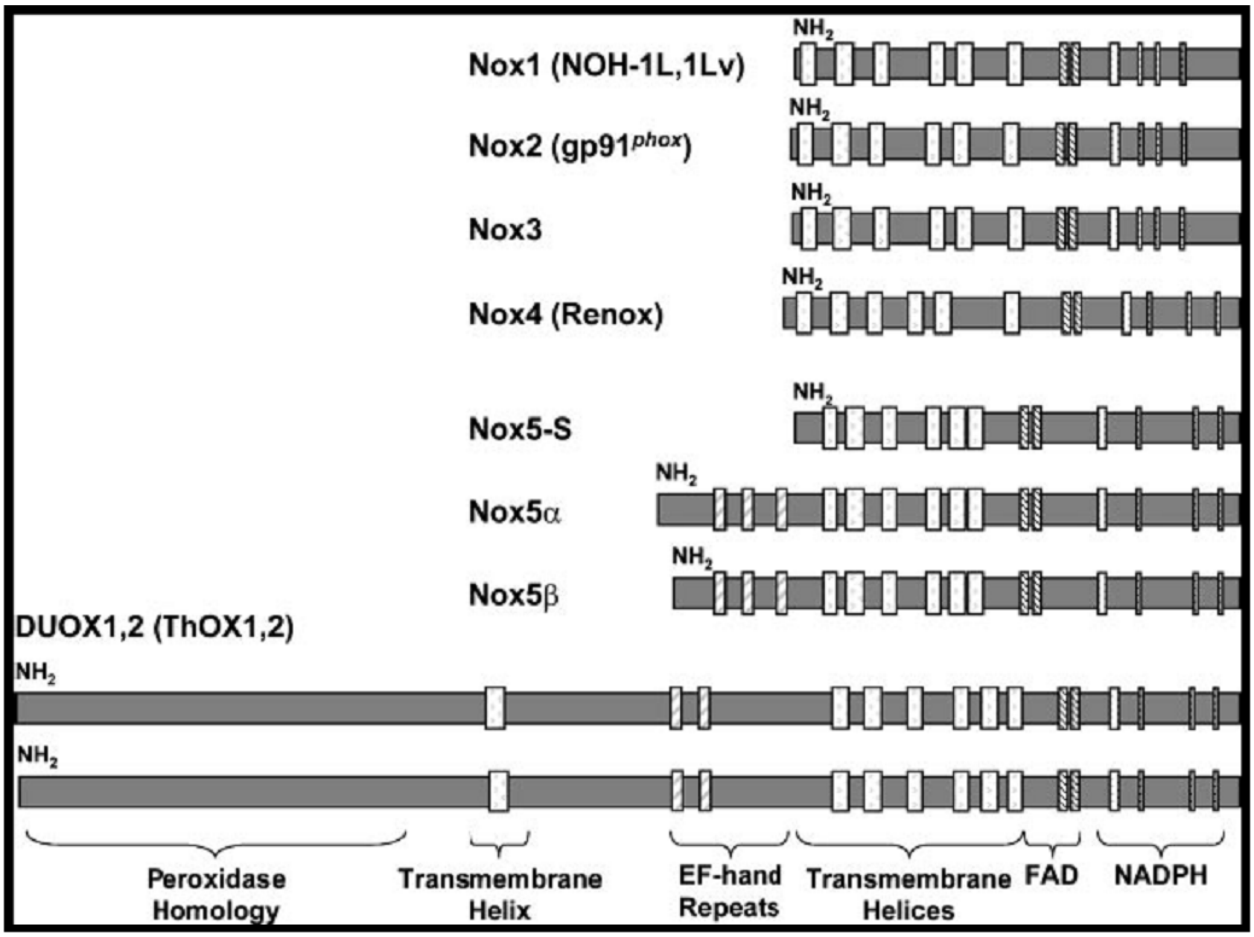


Figure 7. Homologues of gp91$^{phox}$ (Nox2) in non-phagocytic cells.

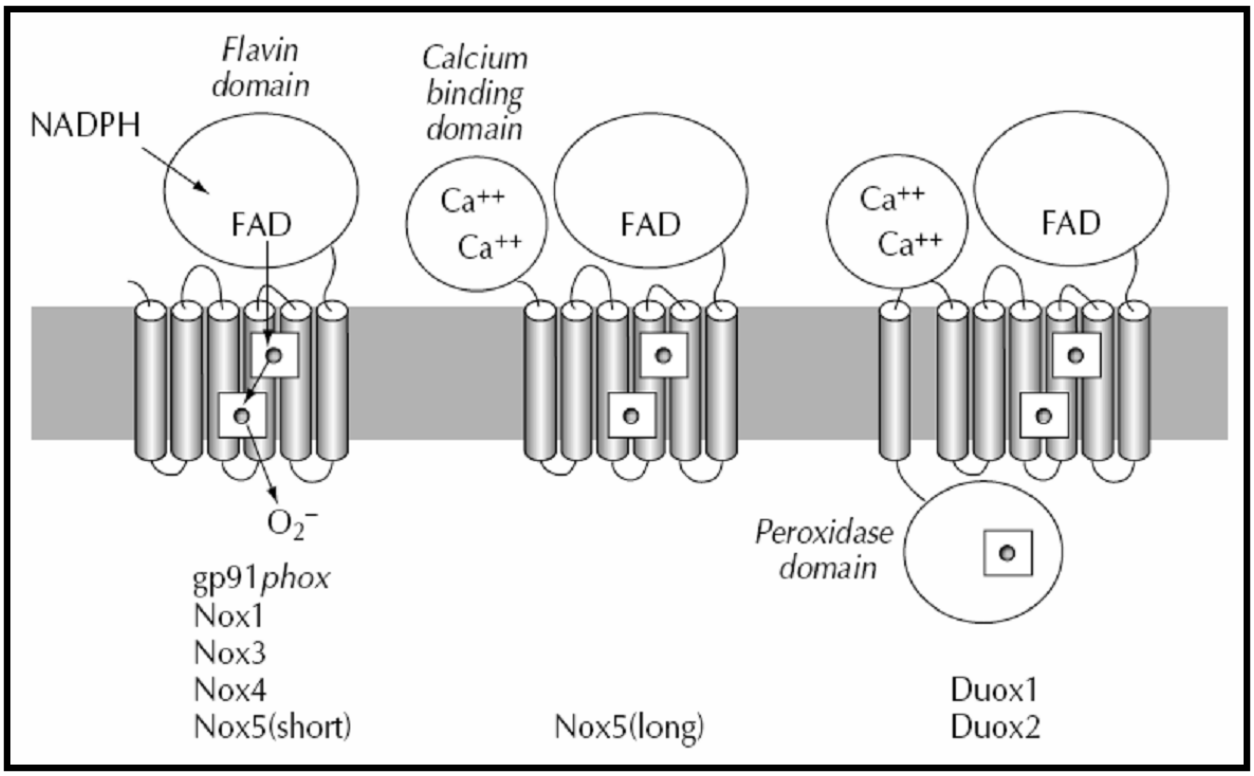


Figure 8. Sub-families of NADPH oxidase core protein.

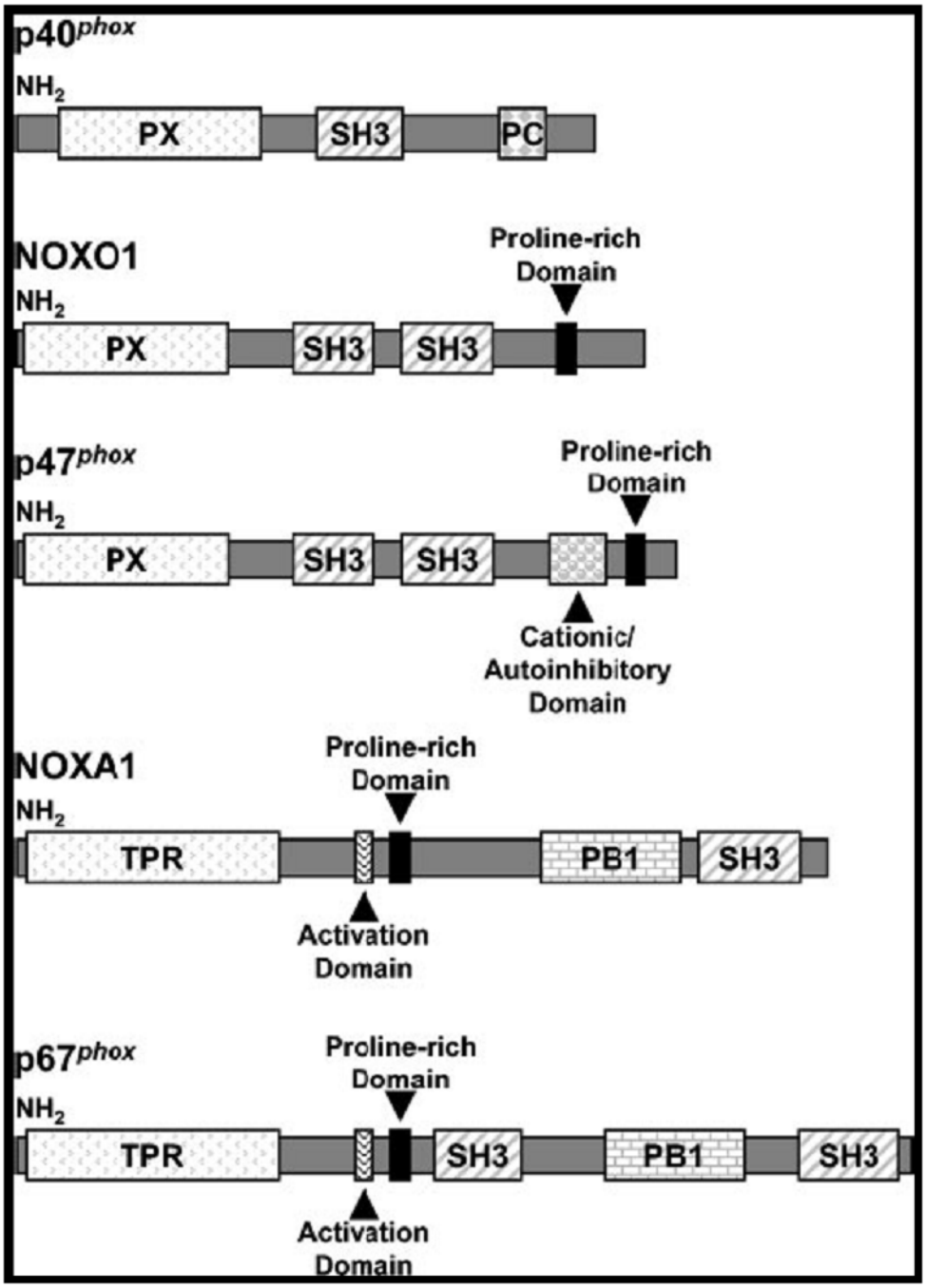


Figure 9. Homologues of the NADPH oxidase complex cytosolic subunits.

# CHAPTER 3

# REACTIVE OXYGEN SPECIES MEDIATE MITOGENIC GROWTH FACTOR SIGNALING PATHWAYS IN HUMAN LEIOMYOMA SMOOTH MUSCLE CELLS

## 3.1 ABSTRACT

Uterine leiomyomas are benign uterine tumors characterized by extracellular matrix remodeling, increased collagen deposition and increased smooth muscle cell (SMC) proliferation. The reactive oxygen species (ROS) producing NADPH oxidase complex is involved in the signaling pathways of several growth factors, cytokines, and vasoactive agents that stimulate proliferation of a variety of cell types. My objective was to test the hypothesis that ROS derived from NADPH oxidase are necessary components of the MAP kinase mitogenic pathway activated by platelet derived growth factor (PDGF) and epidermal growth factor (EGF) in leiomyoma SMCs (LSMCs). Primary cell cultures of LSMCs were used as the experimental model. Results showed that stimulation of these cells with PDGF or EGF caused a marked increase in intracellular ROS production and that the NADPH oxidase inhibitor, DPI, blocks ROS production. In addition, inhibition of ROS production by NADPH oxidase inhibitors blocked, in a dose-dependent manner, the EGF- and PDGF-induced increase in [$^3$H]thymidine incorporation by LSMCs. Furthermore, an exogenous source of ROS, hydrogen peroxide, was sufficient to stimulate [$^3$H]thymidine incorporation in LSMCs but did not affect *COL1A2* and *COL3A1* mRNA levels. Inhibition of the NADPH oxidase complex decreased PDGF-induced ERK1/2 activation whereas exogenous hydrogen peroxide induced ERK1/2 activation. This manuscript is the first report suggesting the presence of the NADPH oxidase system and its importance in mitogenic signaling pathways in LSMCs. The necessity of NADPH oxidase-

derived ROS for EGF and PDGF signaling pathways leading to cell proliferation points to another potential therapeutic target for treatment and/or prevention of uterine leiomyomas.

## 3.2 INTRODUCTION

Uterine leiomyomas, or fibroids, are characterized by an increase in SMC proliferation and excessive deposition of extracellular matrix proteins, primarily collagens type I and III [1, 2, 33]. Recent survey studies have reported that over 600,000 hysterectomies are performed in the USA, and that uterine leiomyomas represent 29.4% and 41.4% of the hysterectomies in women ages 18-44 and 45-64, respectively [4]. Epidemiological studies have shown that seven out of every ten Caucasian women and eight out of every ten African-American women will eventually develop uterine leiomyomas [3].

Ovarian steroid hormones are known to play a central role in the regulation of uterine leiomyoma growth because leiomyomas develop only in post pubertal and pre-menopausal women. A significant reduction in tumor size is observed after the onset of menopause and in response to treatment with gonadotropin-releasing hormone or progesterone antagonists [59, 60]. Steroid hormones induce mitogenic effects directly through their receptors or by regulating expression of growth factors such as EGF and PDGF and their respective receptors [54, 60]. Both EGF and PDGF receptors have previously been identified in LSMCs [70, 74]. Furthermore, EGF and PDGF have been shown by numerous investigators to stimulate the proliferation of LSMCs [74, 75]. Vascular SMCs show similar mitogenic responses to these same growth factors [147, 148].

The pathophysiology of uterine leiomyomas is similar to that of other fibrotic conditions such as atherosclerosis, vascular restenosis, liver, pancreatic and renal interstitial fibrosis, in

which an injury triggers normally quiescent cells to dedifferentiate into a myofibroblast-like, more proliferative phenotype [5-8]. It is likely that the development of leiomyomas may parallel these pathological conditions, occurring in response to some type of injury to the myometrium such as hypoxia.

Reactive oxygen species (ROS), which were once regarded as purely cytotoxic, are now recognized as effective second-messenger molecules regulating protein modifications, gene expression, cell proliferation, migration, and differentiation as well as tissue remodeling in a variety of cell types [10, 91, 94, 108, 112, 113, 115-117, 119]. ROS activation is biphasic [149], and the signaling effects can be both immediate and long-lasting. NADPH oxidase serves as the primary source of intracellular ROS, specifically hydrogen peroxide, in a variety of cell types [150, 151]. Sundaresan and colleagues were the first to uncover the importance of increasing intracellular ROS levels in response to specific growth factor ligands [17]. This group showed that upon treatment with PDGF, ROS levels in vascular SMCs rose rapidly and returned to baseline within approximately thirty minutes. Furthermore, after blocking the PDGF-stimulated generation of intracellular ROS, they noted a marked inhibition of MAPK activation and proliferation. More recent studies have shown that growth factors (including EGF and PDGF), chemokines, cytokines, and vasoactive agents such as angiotensin can induce NADPH oxidase-dependent ROS production, which in tunr activates various MAPKs that regulate downstream cell proliferation or matrix production [94, 112, 116].

The focus of my research is to gain a better understanding of the signaling pathways involved in regulation of uterine leiomyoma growth. My goals in this study were to determine 1) whether ROS are necessary components of the signaling pathways for PDGF and EGF in LSMCs and 2) the potential involvement of ERK1/2 as intermediate molecules mediating the

effects of ROS on leiomyoma SMC proliferation. Results show that NADPH oxidase-derived ROS are indeed an important component of these signaling pathways.

## 3.3 MATERIALS AND METHODS

### *3.3.1 Chemicals and Reagents*

PDGF (120-HD) and EGF (236-EG) were purchased from R&D Systems (Minneapolis, MN). Diphenyleneiodonium chloride (DPI; D2926) and DMSO (D2650) were purchased from Sigma (St. Louis, MO). Tritiated thymidine ([$^3$H]thymidine) (NET-027) was purchased from PerkinElmer. Thirty percent hydrogen peroxide (H325-100) and bovine serum albumin (BP1600-100) were purchased from Fisher Scientific. Restore Western Blot Stripping Buffer (21059), BCA protein assay kit, and SuperSignal West Pico Chemiluminescent Substrate (34080) were purchased from Thermo Scientific (Rockford, IL). Anti-ERK1/2 and anti-phosphorylated ERK1/2 antibodies, and anti-mouse and anti-rabbit HRP-linked antibodies were purchased from Cell Signaling (Danvers, MA). Dulbecco modified Eagle medium (DMEM; 12-614F), penicillin-streptomycin (17-602E), phenol-red-free-DMEM (PRF-DMEM, 12-917F), and L-glutamine (17-605E) were purchased from Biowhittaker. Dulbecco's PBS/Modified (SH30264.01), fetal bovine serum (FBS; SH30071.03) and bovine calf serum (BCS; SH30072.03) were purchased from Hyclone. Carboxy-$H_2$DCFDA (5-(and-6)-carboxy-2',7'-dichlorodihydrofluorescein diacetate) (C400), dihydroethidium stabilized in DMSO (D23107), and Trizol Reagent (15-596-018) were purchased from Invitrogen (Carlsbad, CA).

*3.3.2 Cell Culture*

Leiomyomas were obtained from patients undergoing hysterectomy who had given written consent in accordance with the University of Illinois and Northwestern University IRB committees. Tissues were minced, digested in collagenase overnight, and then placed into flasks in DMEM + 5% FBS + 5%BCS which will be referred to as DMEM/10% serum. Cells were characterized for expression of the smooth muscle cell specific markers α-actin and desmin, and for lack of expression of the fibroblast-specific marker vimentin. These primary cells were then cultured in DMEM/10% serum, supplemented with BCS, penicillin-streptomycin (10,000U pen/ml, 10,000 μg strep/ml), and L-glutamine (200 mM) in 75 $cm^2$ cell culture flasks (Midwest Scientific, 90075). Cells were maintained at 37°C in a humidified atmosphere of 95% air and 5% $CO_2$. For all the experiments reported in this dissertation, cells were used between passages 3-8.

*3.3.3 Measurement of Intracellular ROS Production: Dihydroethidium (DHE)*

LSMCs were cultured on 2-well collagen-coated glass slides (Becton Dickinson, 354627) in 2 ml per well of DMEM/10% serum at a density of 50,000 cells per well. Cells were tested once they attained approximately 50% confluence to prevent fluorescent dye from becoming trapped in the extracellular matrix. The generation of intracellular ROS was measured using DHE as a fluorescent probe.

To determine the effects of PDGF or EGF on intracellular ROS production, cells received the following treatments for increasing time increments of 0, 5, 10, or 15 minutes: DMEM + 0.1% BSA, 10 ng/ml PDGF (maximal dose), or 100 ng/ml EGF (maximal dose). All treatments were applied using phenol-red-free-DMEM (PRF-DMEM) containing 0.1% BSA, pen-strep, and L-glutamine. Cells were washed once using phenol red free-DMEM/0.1% BSA. Cells were then

loaded with the fluorescent DHE dye (10 μM) in phenol red free-DMEM/0.1% BSA for 20 minutes. This dye can passively enter cells and produces a red fluorescent signal upon its oxidation by intracellular ROS. The oxidized ethidium bromide then becomes intercalated within the cell's DNA, producing a long-lasting fluorescence. After removal of the dye, cells were washed twice with phenol red free-DMEM. The medium was then removed and cells were visualized using a Zeiss Axiovert 25 fluorescence microscope. Pictures were taken using a Zeiss Axiocam camera to record fluorescent images. An increase in intracellular fluorescence indicated an increase in intracellular ROS production.

*3.3.4 Measurement of Intracellular ROS Production: Carboxy-$H_2$DCFDA*

LSMCs were cultured in 35mm μ-dishes (80136) from Ibidi (Munchen, Germany) in 800 μl of DMEM/10% serum at a density of 2,000 cells per dish. Once cells attained 50% confluence the experiment was performed. Cells were washed three times in warm DPBS and carboxy-$H_2$DCFDA dye was added to the cells in 800 μl of DPBS at a 10 μM concentration. After 15 minutes of incubation, dye was removed and cells were washed two times and treatment was added. Cells were exposed to either DPBS alone (negative control), $H_2O_2$ (10 μM) (positive control), EGF (50 ng/ml) or PDGF (10 ng/ml) in DPBS for 15 minutes. Growth factors were added in absence or presence of 25 μM DPI. After treatment, cells were washed two times and images were immediately captured using a fluorescence microscope (Zeiss Axiovert 200M).

*3.3.5 Densitometric Quantification of Fluorescence Images*

Individual cells were randomly selected from several different microscopic fields, and fluorescence as well as DIC-Nomarski images were captured and saved as TIFF files. Images

were loaded and analyzed on Axiovision software (Zeiss). The intracellular compartment of cells was determined by using DIC images. To be consistent with regards to the areas of fluorescence measurements circles were drawn around the nucleus of every cell. The average of the fluorescence measurements from each cell was taken and used for statistical analysis.

### *3.3.6 [$^3$H]Thymidine Incorporation Assays: Effect of Exogenous ROS*

LSMCs were cultured in 96-well plates in 200 µL of DMEM/10% serum at a density of 4,000 cells per well. Once cells attained 80% confluence, they were growth-arrested in DMEM/0.5% FBS for 48 hours to synchronize the cells.

To examine stimulation of cell proliferation by exogenous ROS, cells were placed in fresh DMEM/0.5% FBS and were pulse-treated once each hour for five hours with hydrogen peroxide (10, 50, 100 or 200 µM). [$^3$H]thymidine (0.4 µCi) was added to the cells at the beginning of the five-hour treatment. Cells were then harvested and counted in a beta-scintillation counter to quantitate [$^3$H]thymidine incorporation. DNA synthesis was recorded as counts per minute (cpm).

### *3.3.7 [$^3$H]Thymidine Incorporation assays: Effect of ROS Inhibitor*

LSMCs were cultured as described in the previous section. To determine whether proliferation observed in response to EGF or PDGF could be inhibited by treatment with a ROS inhibitor, cells were maintained in DMEM/0.5% FBS and pretreated with 200 µl of diphenyleneiodonium chloride (DPI) at increasing concentrations of 0, 5, 25 or 50 µM for 60 minutes. DPI was then removed and cells were washed twice with DMEM/0.5% FBS and then treated with either 50 ng/ml EGF or 10 ng/ml PDGF for 24 hours. Control cells that were not

pretreated with the inhibitor were either treated with EGF (50 ng/ml), PDGF (10 ng/ml), or no growth factor. Cells were labeled during the final 6 hours of treatment with [$^3$H]thymidine (0.4 μCi). Cells were then harvested and counted using a beta-scintillation counter to measure the rate of [$^3$H]thymidine incorporation. DNA synthesis was recorded as counts per minute (cpm).

*3.3.8 Assessment of Proliferation Using Cell Counts*

LSMCs were plated in 6-well plates in 2 ml of DMEM/10% serum at a density of 50,000 cells per well. Upon attaining 80% confluence cells were growth arrested in DMEM/0.5% FBS for 24 hours and experiments were performed. To determine the effects of $H_2O_2$ on cell numbers, cells were given new medium every hour for 8 hours per day, over a 2 day period. Treatments consisted of DMEM/0.5% FBS or $H_2O_2$ (20 μM and 100 μM). To determine the effects of DPI on cell numbers of EGF- and PDGF-stimulated cells, cells were exposed to either DMEM/0.5% FBS, EGF (50 ng/ml), or PDGF (10 ng/ml) for 48 hours. Growth factors were added in the absence or presence of DPI (25 μM). At the end of the treatment period cells were detached with 1 ml of trypsin for 8 minutes, mixed with 1 ml of DMEM/10% serum and counted using a hemocytometer.

*3.3.9 COL1A2 and COL3A1 Gene Expression*

LSMCs were grown in 60 mm culture dishes and allowed to attain 80% confluence. Cells were then washed and switched to DMEM/0.5% FBS. Cells then were given hourly pulses of hydrogen peroxide (20 μM) for 5 hours or were treated with one-200 μM hydrogen peroxide pulse for 24 hrs. Total RNA was isolated from cells using Trizol Reagent. Complementary DNA synthesis was performed and followed by qRT-PCR to determine relative fold differences in

collagen type 1 alpha 2 (*COL1A2*) and collagen type 3 alpha 1 (*COL3A1*) mRNA expression in response to ROS. Applied Biosystems TaqMan Gene Expression Assay for *COL3A1*: Hs00164103_m1; Applied Biosystems TaqMan Gene Expression Assay for *COL1A2*: Hs00164099_m1

*3.3.10 Immunoblotting*

LSMCs were serum-starved for1 hour in 60 mm dishes. Two hundred microliters of concentrated hydrogen peroxide (10 μM final concentration), EGF (50 ng/ml final concentration), or PDGF (10 ng/ml final concentration) were added directly to the cells and treatments continued for the specified time periods. When pretreatment with NADPH oxidase inhibitor was necessary, cells were exposed to DPI for 60 minutes and concentrated growth factors were then added to the cells in the presence of the inhibitor. Cell lysates were harvested by removing medium and adding warm (95ºC) 1X-Laemmli sample buffer (LSB) (2% SDS, 10% glycerol, 62.5 mM Tris, pH 6.8). Cells were scraped off the dishes, added to a 1.5 ml tube, sonicated (10 pulses) and stored at -20ºC. BCA assays were performed on the cell lysates to determine protein concentrations. Either 5 μg (ERK1/2 blots) or 45 μg (EGF-R or PDGF-R blots) of total protein were loaded on SDS-PAGE gels (12%) and run initially at 80 V for 30 minutes, then at 150 V for 90 minutes. Protein transfer was carried out at 60 mA for 16 hours at room temperature. Primary antibody (anti-phosphorylated ERK1/2 1:2000 in 5% milk; anti-ERK1/2 1:1000 in 3% BSA; anti-phoshporylated EGF-R and anti-PDGF-R 1:500 in 5% milk; anti-EGF-R and anti-PDGF-R 1:500 in 3% BSA) incubation was performed for 90 minutes at room temperature. HRP-conjugated secondary antibody was incubated with membranes in 5% milk for 60 minutes at room temperature (1:10,000). The SuperSignal West Pico

Chemiluminescent Substrate kit was used as substrate for HRP. Membranes were first probed with anti-phosphorylated ERK1/2 antibody, and then reprobed with anti-total ERK1/2 as a loading control. Membranes were stripped with Restore Western Blot Stripping buffer from Thermo Scientific (Rockford, IL) before being reprobed.

### *3.3.11 Densitometric Analysis of Western Blots*

Films developed after exposure to chemiluminescence on the membranes were scanned and images saved at high resolution in a TIFF format. Images were analyzed using the ImageJ software from NIH (available at http://rsbweb.nih.gov/ij/download.html). Software was calibrated for optical density measurements using a Kodak no. 3 calibrated step tablet available at http://rsb.info.nih.gov/ij/docs/examples/calibration/. Bands of interest were measured by drawing the smallest rectangle capable of measuring the optical density of all the bands. The same rectangle was used to measure all the bands in one film. Measurements of bands referring to the activated form of the proteins (phosphorylated form) were normalized for loading differences using measurements obtained from the bands obtained using antibodies that recognized all forms of the specific proteins (loading control). Graphs represent LSmeans and SEM.

### *3.3.12 Statistical Analysis*

Quantitative RT-PCR experiments were performed using the relative standard curve method. To show changes in gene expression relative to control level (control set as 1), each biological replicate was normalized to the average of the control group within each experiment. Relative fold difference values from qRT-PCR experiments and cpm values from [$^3$H]thymidine

incorporation experiments in each experiment were checked for normality and common variances, respecting the assumptions for performing analysis of variance. All distributions were normal. Statistical analysis for all experiments followed the same approach. A completely randomized design corresponding to the following linear model was used: $Xik = \mu + \tau i + \varepsilon ik$, where *Xik*: an observation, $\mu$: population mean, $\tau i$: effect of $i^{th}$ treatment, $\varepsilon ik$: error term. The Linear model for densitometry analysis of the western blots used values for total ERK1/2, EGF-R or PDGF-R as a covariate. A priori comparisons determined by contrasts were used to minimize testing the null hypothesis multiple times ($\alpha$=0.05). The contrasts were only performed when ANOVA indicated significant effect due to treatment. The data analyses for this paper were generated using SAS software (SAS Institute Inc.).

## 3.4 RESULTS

### *3.4.1 EGF and PDGF Stimulate Intracellular ROS Generation*

To test the hypothesis that ROS are necessary mediators of EGF and PDGF signaling pathways, I first examined whether EGF or PDGF would induce an increase in intracellular ROS production in LSMCs. Figure 10A indicates an increase in fluorescence after 15 minutes of stimulation with PDGF and the bright field image shows that fluorescence was specifically observed intracellularly. Cells were loaded with DHE fluorescent dye following growth factor treatment and the presence of fluorescence indicated oxidation of DHE and, therefore, the presence of ROS. Intracellular fluorescence was observed in cells following treatment with either 10 ng/ml PDGF or 100 ng/ml EGF, and fluorescence increased over time, with maximum fluorescence occurring after 15 minutes of treatment (Figure 10B). However, the effects of EGF or PDGF treatment on ROS production were evident as early as 5 minutes.

*3.4.2 NADPH Oxidase Inhibitor Blocks EGF- and PDGF-Stimulated ROS Production*

To capture higher power images and get better intracellular resolution with the intracellular ROS detection experiments I used another oxidation sensitive dye, carboxy-$H_2$DCFDA. I first tested whether this dye was sensitive to oxidation by $H_2O_2$. Indeed, upon addition of $H_2O_2$ (10 μM) to the culture medium, the compound entered the cells readily and induced a significant increase in intracellular fluorescence (Figure 11A). In the same experiment I also confirmed the increase in ROS production after LSMC treatment with EGF and PDGF. Similar results were obtained when using DHE dye (Figures 11A and 10A, respectively). After validating the carboxy-$H_2$DCFDA dye, my next goal was to validate the compound diphenyleneiodonium (DPI) as an inhibitor of the enzymatic complex which Ihypothesize is responsible for ROS production (NADPH oxidase). When cells were treated with EGF or PDGF in the presence of DPI (25 μM) for 15 minutes there was a significant drop in the amount of fluorescence observed intracellularly. DIC-Nomarski images indicate the localization of the cells, and when merged with the fluorescence channel, support the intracellular ROS localization. These results show that carboxy-$H_2$DCFDA is a highly sensitive probe that can detect changes in intracellular ROS concentrations; DPI can block growth factor-induced ROS production by LSMCs; and that the NADPH oxidase complex is active and potentially involved with EGF and PDGF signaling pathways. Figure 11B shows the densitometric analysis of the fluorescence images as a means of quantitatively comparing the different treatments.

*3.4.3 NADPH Oxidase Inhibitor Blocks EGF- and PDGF-Stimulated Proliferation of LSMCs*

Based upon the results showing that ROS are produced in response to EGF and PDGF, the next logical step was to test the hypothesis that ROS are a necessary component of the EGF

and PDGF mitogenic pathways and that NADPH oxidase is the enzymatic complex involved in this receptor-mediated ROS production. After validating DPI, Iused this NADPH oxidase inhibitor to block ROS generation in the presence of either EGF or PDGF. Ithen assessed the effect of DPI on EGF- and PDGF-induced LSMC proliferation by measuring changes in DNA synthesis using [$^3$H]thymidine incorporation assays. Pretreatment of cells with increasing concentrations of DPI before adding EGF resulted in significant inhibition of proliferation when compared to those cells treated with EGF alone (Figure 12A). In fact, the levels of DNA synthesis at the two higher concentrations were reduced to levels below those observed in the controls (0.5% FBS only). Similarly, when cells were exposed to DPI prior to treatment with PDGF, a reduction in growth factor-stimulated proliferation was again observed (Figure 12B).

The effects of DPI on EGF- or PDGF-stimulated cell proliferation were significant. This inhibitory effect was dose-dependent, as the highest concentration of DPI blocked DNA synthesis almost completely.

To confirm whether the results obtained with the [$^3$H]thymidine incorporation assays were paralleled by similar changes in cell number Iperformed cell count experiments using a hemocytometer. Cells exposed to either EGF or PDGF in the presence of DPI had a dramatic decrease in cell number in comparison to growth factors alone (Figure 12C). Similar results were observed with myometrial SMCs (APPENDIX B).

### *3.4.4 Exogenous $H_2O_2$ Stimulates LSMC Proliferation*

After demonstrating that inhibition of the ROS-producing NADPH oxidase complex inhibited growth factor-induced cell proliferation, Itested whether an exogenous source of ROS was sufficient to induce LSMC proliferation. ROS are extremely labile and, therefore, difficult to

use as a treatment for cells in vitro. In light of this characteristic of hydrogen peroxide, Iused increasing concentrations of exogenous hydrogen peroxide (10 to 200 μM) as pulse treatments once per hour for five hours and then assessed change in DNA synthesis. Interestingly, hydrogen peroxide at 10 μM increased DNA synthesis, whereas higher concentrations of the compound (50 μM and 100 μM) had no effect compared to control, and 200 μM was inhibitory (Figure 13A). These data indicate that within the range of concentrations used it was possible to separate the specific mitogenic effects of hydrogen peroxide from its inhibitory effects, which may be related to oxidative stress. Cell count experiments confirmed that at relatively low concentrations (20 μM) $H_2O_2$ causes in increase in cell number compared to untreated control, whereas at higher concentrations (100 μM), it inhibited cell proliferation (Figure 13B). Similar experiments did not detect an effect of either hydrogen peroxide concentration tested in myometrial SMCs (APPENDIX B).

*3.4.5 NADPH Oxidase Inhibitor Blocks PDGF-Stimulated ERK1/2 Activation*

To elucidate the inhibitory pathway further Iinvestigated the involvement of the well-known mitogen-activated protein kinase pathway on ROS-dependent proliferative responses of LSMCs, specifically ERK1/2. Both EGF and PDGF induced phosphorylation of ERK1/2 within five minutes of treatment with maximum phosphorylation occurring between 10 and 15 minutes (Figure 14). Similar results were observed with myometrial SMCs (APPENDIX C). I hypothesized that activation of ERK1/2 occurs downstream of the increase in ROS production and that inhibition of ROS production would reduce the level of ERK1/2 phosphorylation in response to EGF or PDGF treatment. No effects of DPI treatment on EGF-induced ERK1/2 activation were observed (Figures 15A and 15B). However, pre-treatment of LSMCs with DPI

reduced PDGF-induced ERK1/2 activation. This result is indicated by the decrease in intensity of the phosphorylated ERK1/2 band from the cells treated with 50 μM of DPI in comparison to that observed for growth factor treatment alone (Figure 15C and 15D). Results showing inhibition of PDGF-induced ERK1/2 activation by DPI and lack of inhibition of EGF-induced ERK1/2 activation suggest a specific regulation of PDGF signaling pathway by ROS. Similar results were observed with myometrial SMCs (APPENDIX D).

To test whether DPI was potentially having toxic effects I decided to focus on the activation of molecules that are not regulated by ROS and would not be affected by DPI unless the inhibitor is having non-specific effects. I measured the ability of EGF-R or PDGF-R to undergo autophosphorylation upon exposure to EGF or PDGF in the presence of DPI in LSMCs. Although there was a trend towards a decrease in PDGF-R autophosphorylation in the presence of increasing concentrations of DPI, there was no statistical significance. Figure 16 provides evidence that LSMCs were able to respond to both growth factors even in the presence of the highest DPI concentration. This result is supported by the lack of a statiscally significant reduction of EGF-R and PDGF-R autophosphorylation (Figures 16B and 16D). Similar results were observed with myometrial SMCs (APPENDIX E).

*3.4.6 Exogenous $H_2O_2$ Stimulates ERK1/2 in LSMCs*

I next tested whether treatment with exogenous hydrogen peroxide was sufficient to induce ERK1/2 phosphorylation. Similarly to the response observed in [$^3$H]thymidine incorporation experiments, exogenous hydrogen peroxide alone induced activation of the ERK1/2 pathway (Figure 17). ERK1/2 reached maximum activation within 10 and 15 minutes after hydrogen peroxide treatment returning to basal levels after 30 minutes. Similar results were observed with myometrial SMCs (APPENDIX F).

*3.4.7 Effects of Exogenous $H_2O_2$ on COL1A2 and COL3A1 Gene Expression in LSMCs*

Based on results showing that $H_2O_2$ had a positive effect on LSMC proliferation and ERK1/2 activation, I tested whether $H_2O_2$ might also be involved in regulating collagen expression. Cells were either untreated, given five hourly pulses of 10 μM $H_2O_2$, or a higher concentration of $H_2O_2$ (100 μM) for 24 hrs. Total RNA was harvested and analyzed for changes in mRNA levels of *COL1A2* and *COL3A1* using qRT-PCR. Exogenous $H_2O_2$ did not alter *COL1A2* and *COL3A1* mRNA expression in LSMCs (data not shown). Treatment with either EGF or PDGF also did not affect levels of collagen mRNAs (data not shown).

**3.5 DISCUSSION**

The goal of this study was to determine whether ROS are necessary components of the PDGF and EGF signaling pathways for LSMC proliferation. These results are the first to demonstrate that ROS generated by the NADPH oxidase system in LSMCs are involved as intermediates in the signaling pathway of these growth factors. The main findings of this study are that 1) LSMCs produce ROS in response to EGF and PDGF; 2) ROS are necessary and

sufficient to induce LSMC proliferation; and 3) ROS are necessary and sufficient to induce a fraction of ERK1/2 activation in LSMCs.

To determine the role of reactive oxygen species in the mitogenic signaling pathways of EGF and PDGF in LSMCs, I first needed to show that these growth factors induced ROS generation in such cells. EGF and PDGF have been shown previously to stimulate intracellular ROS production in other cells types [17, 112, 115, 152]. This study is the first to show that both PDGF and EGF induce intracellular ROS generation in LSMCs. This receptor-mediated ROS production was initially discovered in cells of the immune system and shown to be derived from the plasma membrane flavohemoprotein complex NADPH oxidase [127]. One of the first reports of Matsubara and Ziff [153] focusing on non-immune cells from showed that endothelial cells released superoxide in response to specific cytokines. Since this first evidence linking ROS generation to regulation of inflammatory responses, many other groups have become interested in the role of the NADPH oxidase complex in hyperproliferative disorders [11]. More recently, NADPH oxidase-derived ROS have been implicated as a necessary component of numerous signaling pathways and associated with specialized cell functions [11, 121, 152-154].

If ROS are a necessary component of the PDGF and EGF signaling pathways then the addition of exogenous ROS should mimic the effects of these growth factors. In fact, when treated with exogenous hydrogen peroxide, LSMCs exhibited a notable increase in DNA synthesis and cell number. The pathway by which exogenous ROS produced this effect in LSMCs is still unknown and may not be the same as that of EGF or PDGF. One of the first evidences of the participation of ROS, specifically hydrogen peroxide, in signaling pathways was provided by experiments showing hydrogen peroxide-dependent glucose oxidation in response to insulin [155]. ROS were later shown to be required for cell growth and transformation [10, 11,

121]. Hydrogen peroxide has been recognized as a signaling molecule since investigators determined that its concentration can rapidly and transiently increase in response to receptor-mediated signaling events. Furthermore, hydrogen peroxide undergoes quick enzymatic degradation, is diffusible, and can act in a specific and reversible fashion [14, 15]. Rao and Berk [156] demonstrated that hydrogen peroxide caused an increase in [$^3$H]thymidine incorporation in vascular smooth muscle cells, in agreement with what my results have shown. In addition, other studies have demonstrated that a shift in intracellular ROS levels towards a more oxidizing environment stimulates the G1 to S phase transition in the cell cycle [12, 13].

Experiments focusing on the role of ROS in normal cell function are complicated by the fact that ROS are extremely short-lived molecules. In the present study a low hydrogen peroxide concentration of 10 μM was added as a pulse, every hour for 5 hours, in contrast to 200 μM every 3 hours for 24 hours by Rao and Berk [156]. The replenishment system allowed me to overcome the problem with hydrogen peroxide being labile and degrading rapidly over time, as well as to the use of concentrations which may more closely resemble physiological levels. Although it is difficult to determine what the physiological levels are and how specific hydrogen peroxide action is, I used concentrations that are 20 times lower than several other studies. Furthermore, *COL1A2* and *COL3A1*gene expression was not affected by the same hydrogen peroxide administration regimen suggesting that the higher proliferation rate was not due to increased collagen deposition, or to a general non-specific effect of hydrogen peroxide. I also observed that the use of concentrations above 50 μM abolished even basal levels of proliferation confirming the negative effect of high levels of ROS on cells.

Pretreatment with the NADPH oxidase inhibitor DPI significantly inhibited EGF- and PDGF-induced proliferation of LSMCs. These data support my hypothesis that ROS are critical

intermediates in the mitogenic signaling pathways of EGF and PDGF and also suggests for the first time the presence of the NADPH oxidase complex in the uterus. DPI has been used successfully by numerous other laboratories to prevent hormone/growth factor-induced, ROS-dependent, cell proliferation in vascular smooth muscle cells [157-159]. DPI pretreatment did not appear to have caused cytotoxic effects at the concentrations used, as cells were able to respond to growth factor treatment with receptor autophosphorylation. This finding suggests a tight regulation of ROS production in the cell. When ROS levels are too high, it is believed that ROS function as potent oxidizing agents, potentially causing oxidative damage and cytotoxic effects. However, if intracellular ROS concentrations fall below a critical level crucial cellular signaling events might be disrupted.

Inhibition of PDGF-induced ERK1/2 activation by DPI and induction of ERK1/2 activation by exogenous hydrogen peroxide suggest ROS are necessary and sufficient to trigger the ERK1/2 signaling pathway associated with PDGF. The fact that the responsiveness of LSMCs to EGF with regards to ERK1/2 activation seemed unaffected by the presence of DPI may suggest another level of specificity to the role of ROS in regulating PDGF signaling pathway. Although the present study provides new information regarding the role of ROS in leiomyoma SMCs, ERK1/2 activation in response to hydrogen peroxide has been observed previously in vascular smooth muscle cells, in agreement with my results [99]. Several studies have reported activation of a variety of specific downstream targets including ROS-dependent p38MAPK activation, but not ERK1/2 [94], activation of both ERK1/2 and MAPK14 [114], as well as activation of only MAPK8 [116]. Some of the studies utilized NADPH oxidase inhibitors or ROS scavengers to confirm participation of ROS in these signaling pathways, whereas others tested the effects of exogenous hydrogen peroxide at concentrations ranging from 5 to 100 fold

higher than those used in the current study. The use of different hydrogen peroxide concentrations may explain the discrepancies between results I obtained and those of others. ROS are involved in the activation of several signaling events including regulation of EGF and PDGF receptor activation or transactivation through induction of CSK activity [113, 160], VEGF-dependent HIF1 activation [161], IL1-dependent regulation of MP3K14 [162], TGFB1-dependent activation of EGR1 gene expression [163], and ultimately, the regulation of protein tyrosine phosphatase activity. Hydrogen peroxide cannot directly phosphorylate proteins, but it can specifically oxidize certain cysteine residues within protein tyrosine phosphatases, which become then unavailable to interact with phosphate substrates rendering the enzyme inactive [14, 15]. Redox regulation of protein tyrosine phosphatases such as PTEN, PTPN1, ACP1, and CDC25C has been reported [16, 18-20]. Furthermore, the importance of PTPs in regulating the level of activation of growth factor receptors and the role of reductases in counteracting the effects of oxidants on PTPs during cell signaling have also been confirmed [21, 22, 164]. Whether NADPH oxidase-derived ROS affect proliferation and activation of ERK1/2 pathways in LSMCs by regulating protein tyrosine phosphatase activity remains to be tested.

The involvement of ROS generated through the NADPH oxidase complex in the development of chronic diseases including fibrotic conditions such as pulmonary, hepatic and pancreatic fibrosis has been proposed recently by other investigators [9]. Many of these disorders are associated with overproduction of ROS and are linked to higher expression of the NADPH oxidase subunits [9]. The increased production of ROS may occur as part of an inflammatory response and may contribute to the abnormal cell proliferation that is observed in conditions such as atherosclerosis or diabetic vascular disease. Drugs that can target the NADPH oxidase complex such as specific inhibitors of the NOX/DUOX family members

represent potential therapeutic approaches for treatment of these chronic diseases [126]. Uterine leiomyomas are also an example of a chronic fibrotic disease and thus, the characterization and understanding of the NADPH oxidase complex in LSMCs may be important for future directions in treatment of these tumors.

In summary, the findings of my research suggest that reactive oxygen species are an important component of the EGF and PDGF signaling pathways involved in LSMC proliferation. Specifically regarding the PDGF signaling pathway, these data suggest that the activation of ERK1/2 is an important step following PDGF-induced ROS production, which may be necessary for ROS-induced LSMC proliferation. This mechanism is likely occurring through the stimulation of NADPH oxidase and the subsequent generation of intracellular ROS. My findings provide the first evidence of (1) ROS as a second messenger in LSMCs proliferation, and (2) of a non-phagocytic NADPH oxidase complex in leiomyoma smooth muscle cells. This research presents a novel target for the development of preventive strategies or therapeutic approaches to treat uterine leiomyomas through the targeting of intracellular ROS and, specifically, NADPH oxidase. Although no differences were observed between normal myometrial cells and leiomyoma cells in regards to the influence of NADPH oxidase-derived ROS on the signaling pathways examined, the presence of the complex in myometrial and leiomyoma cells provides the basis to investigate other pathways.

## 3.6 FIGURES

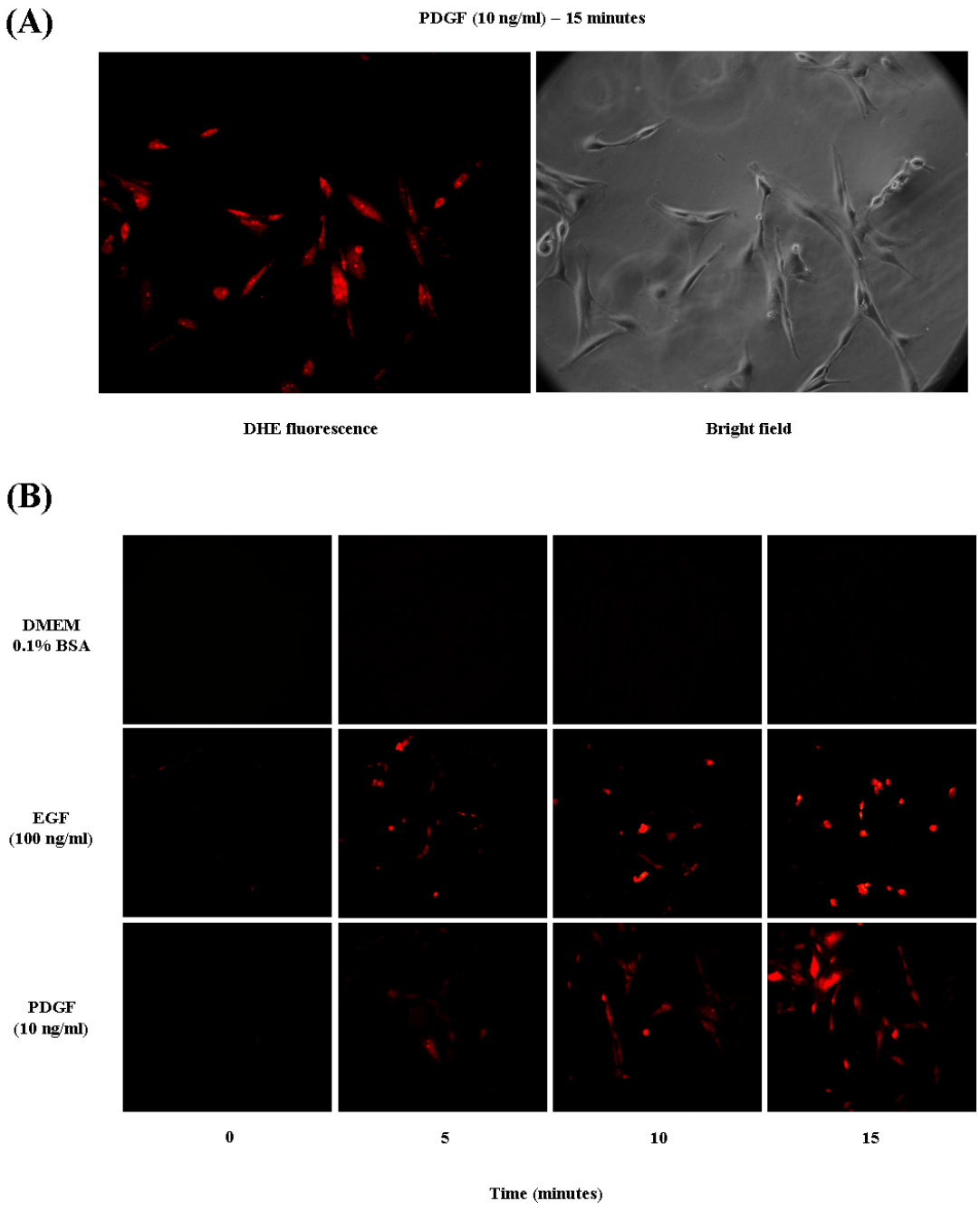


Figure 10. Intracellular ROS production by LSMCs increases in response to treatment with EGF or PDGF. (A) Left panel: Intracellular ROS production is indicated by the presence of red fluorescence in LSMCs in response to PDGF (10 ng/ml) treatment for 15 minutes; Right panel: Bright field image indicating that the fluorescence is located specifically within the LSMCs; (B) LSMCs were exposed to DMEM/0.1% BSA (negative control), EGF (100 ng/ml), or PDGF (10 ng/ml) for increasing time periods up to 15 minutes. An increase in fluorescence indicated an increase in intracellular ROS production. (n=3. Representative image of LSMC response).

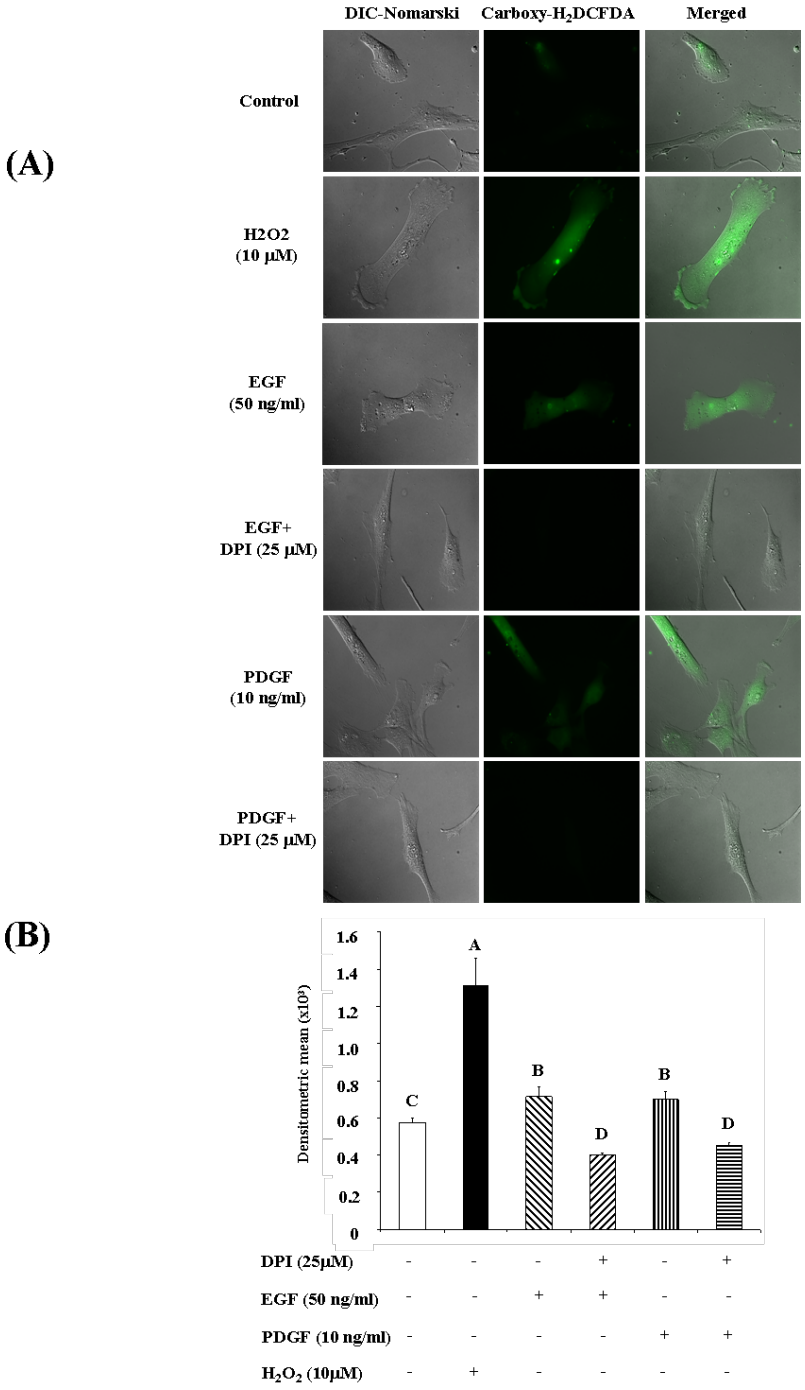


Figure 11. The NADPH oxidase inhibitor DPI blocks PDGF- and EGF-stimulated intracellular ROS production. An increase in fluorescent signal indicates ROS production. (A) Rows indicate different combinations of treatments; the left column shows bright field DIC-Nomarski, the middle column shows the fluorescent signal (Carboxy-$H_2$DCFDA), and the right column is the merged image indicating intracellular ROS production; (B) Graphic representation of the LSmeans ± SEM of fluorescent signal from cells exposed to different treatments. Different capital letters indicate statistical difference ($p<0.05$). [n=3. Representative images of LSMCs response were used for (A)].

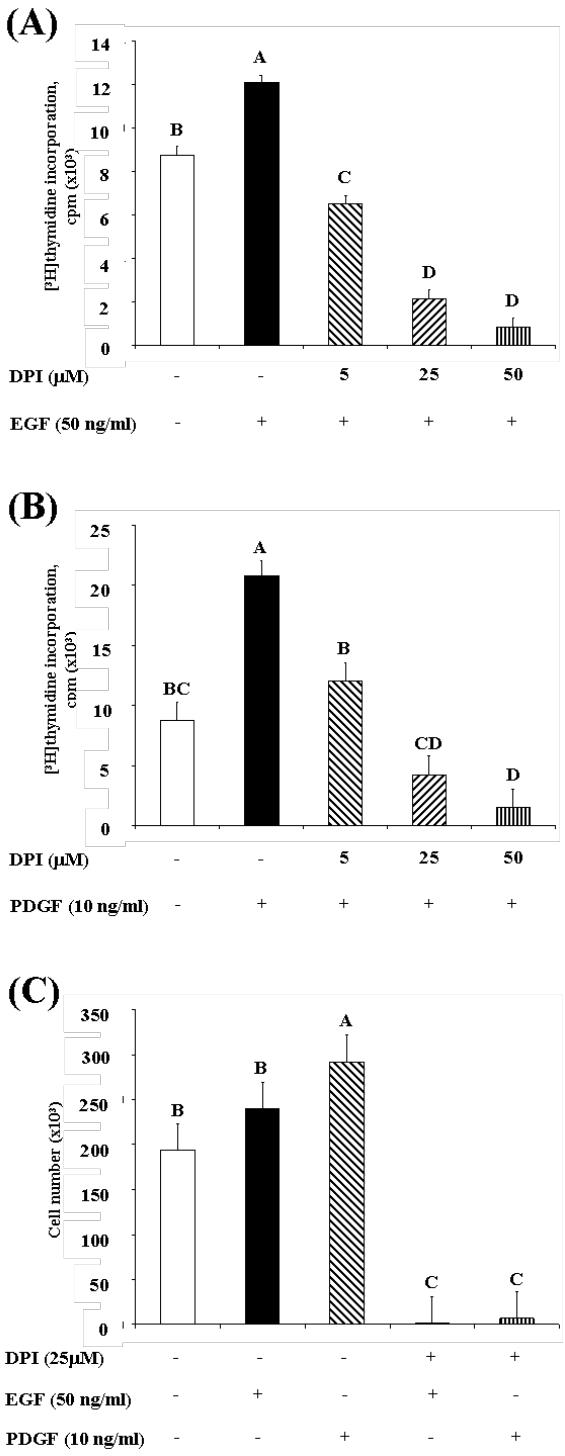


Figure 12. The NADPH oxidase inhibitor DPI blocks PDGF- and EGF-stimulated proliferation of LSMCs. (A) Effects of DPI on LSMC DNA synthesis in the presence of 50 ng/ml EGF; (B) Effects of DPI on LSMC DNA synthesis in the presence of 10 ng/ml PDGF. (C) Effects of DPI on LSMC numbers in response to EGF and PDGF. Cell numbers were determined by manual counting on a hemocytometer. (n=3. Bars represent LSmeans ± SEM. Different capital letters indicate statistical difference $p<0.05$).

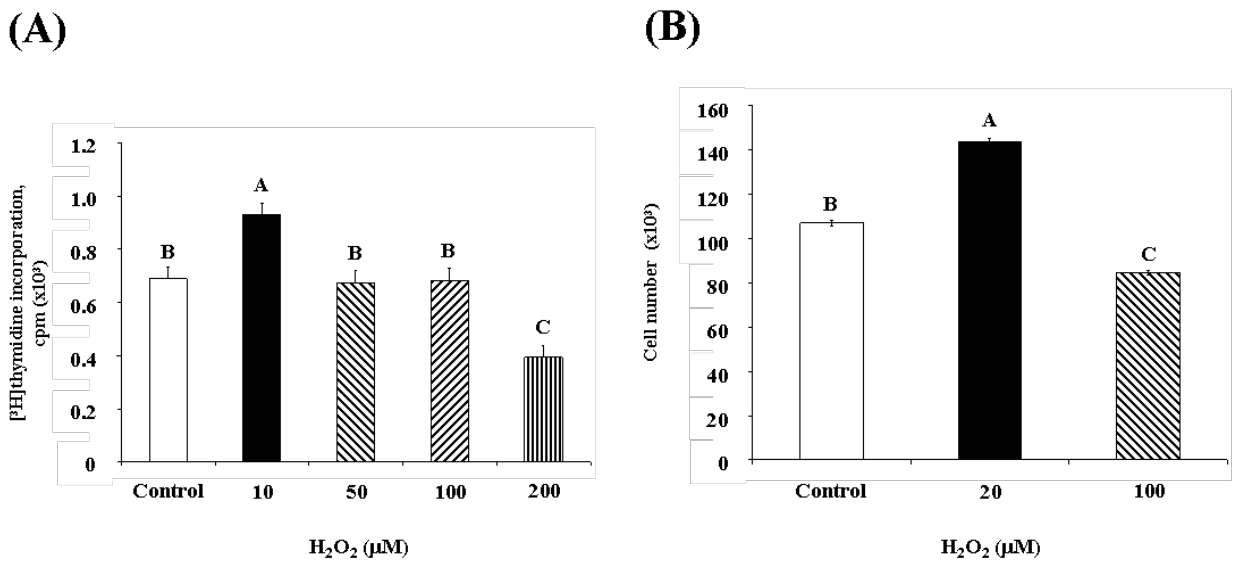


Figure 13. Exogenous $H_2O_2$ affects LSMC proliferation. (A) Effects of $H_2O_2$ pulses (10, 50, 100 and 200 μM) on DNA synthesis in LSMCs. (B) Effects of $H_2O_2$ pulses (20 and 100 μM) in LSMC number. Cell numbers were determined by manual counting using a hemocytometer. (n=3. Bars represent LSmeans ± SEM. Different capital letters indicate statistical difference $p<0.05$).

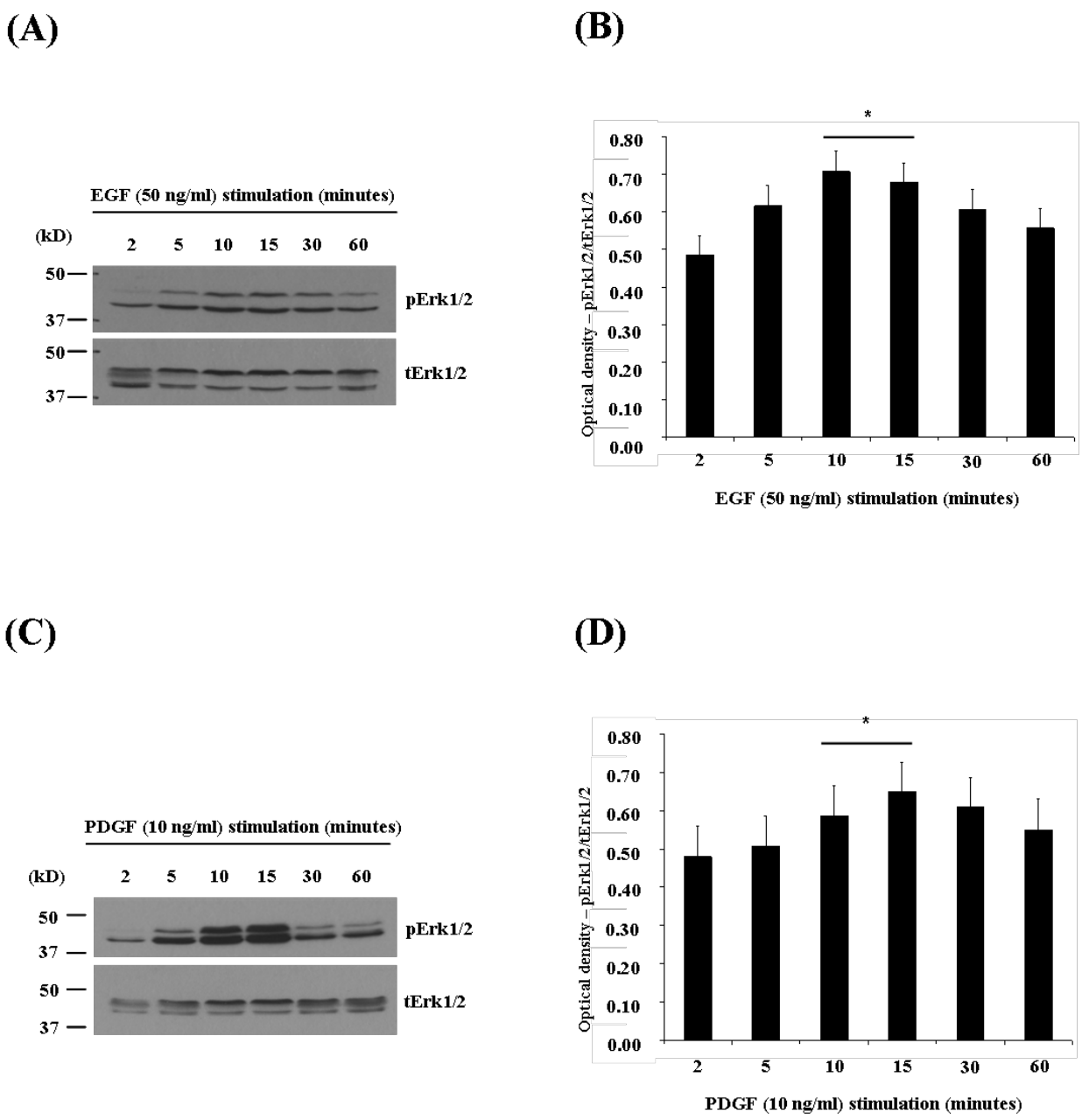


Figure 14. EGF and PDGF induce phosphorylation of ERK1/2 in LSMCs. (A) Immunoblot for time-course of ERK1/2 activation in response to EGF; (B) time-course of ERK1/2 activation in response to EGF; (C) Immunoblot for time-course of ERK1/2 activation in response to PDGF; anti-total ERK1/2 (tERK1/2) were used as loading control. Graphs represent the densitometric analysis of the immunoblots; (D) time-course of ERK1/2 activation in response to PDGF; (n=3. Bars represent LSmeans ± SEM. Line above 2 bars indicate both time-points were merged and compared to the other time-points. Asterisk above line indicates statistical difference in comparison to other time-points $p<0.05$).

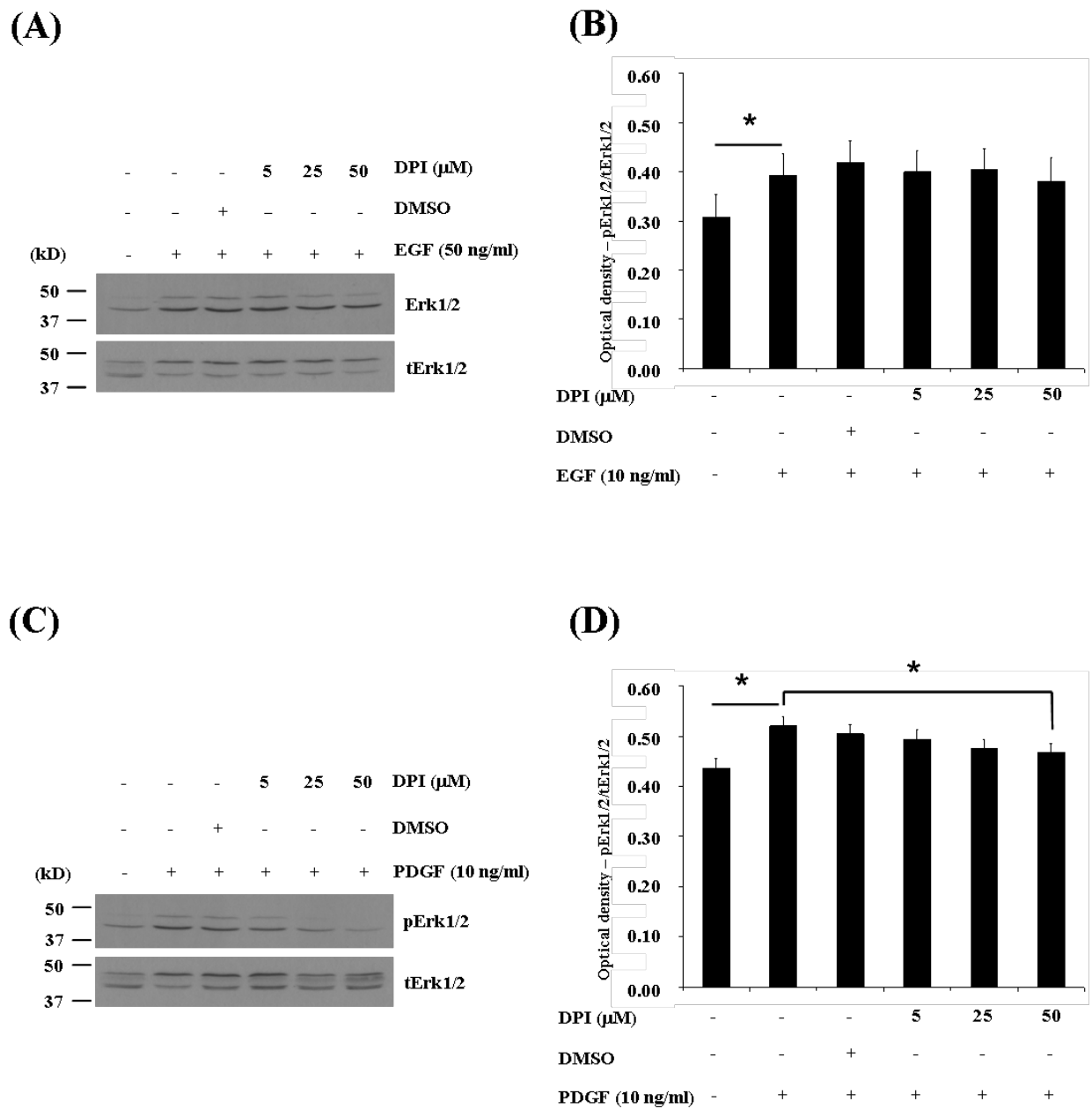


Figure 15. The NADPH oxidase inhibitor DPI blocks PDGF-stimulated ERK1/2phosphorylation in LSMCs. (A) Immunoblot for ERK1/2 activation in response to EGF in the presence or absence of DPI; (B) Effects of DPI on EGF-induced ERK1/2 activation; (C) Immunoblot for ERK1/2 activation in response to PDGF in the presence or absence of DPI; anti-total ERK1/2 (tERK1/2) were used as loading control. Graphs represent the densitometric analysis of the blots; (D) Effects of DPI on PDGF-induced ERK1/2 activation; (n=3. Bars represent LSmeans ± SEM. Asterisk above line connecting 2 treatment groups indicates statistical difference between the connected groups $p<0.05$).

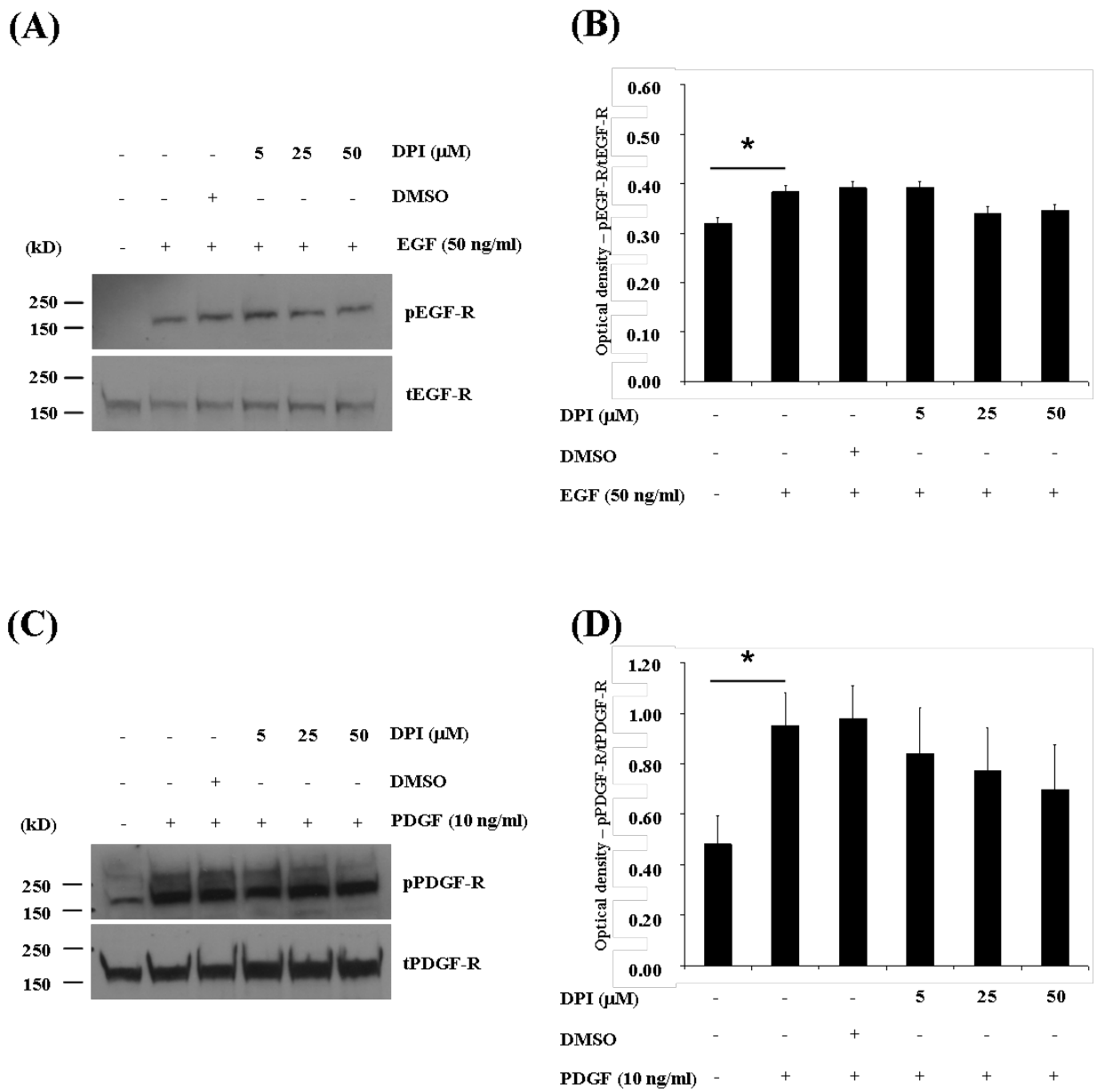


Figure 16. The NADPH oxidase inhibitor DPI does not affect EGF or PDGF receptor activation. (A) Immunoblot for EGF-R activation in response to EGF in the presence or absence of DPI; (B) Effects of DPI on EGF-R activation; (C) Immunoblot for PDGF-R activation in response to PDGF in the presence or absence of DPI; anti-total EGF-R (tEGF-R) and anti-total PDGF-R (tPDGF-R) were used as loading control. Graphs represent the densitometric analysis of the blots; (D) Effects of DPI on PDGF-R activation; (n=3. Bars represent LSmeans ± SEM. Asterisk above line connecting 2 treatment groups indicates statistical difference between the connected groups $p<0.05$).

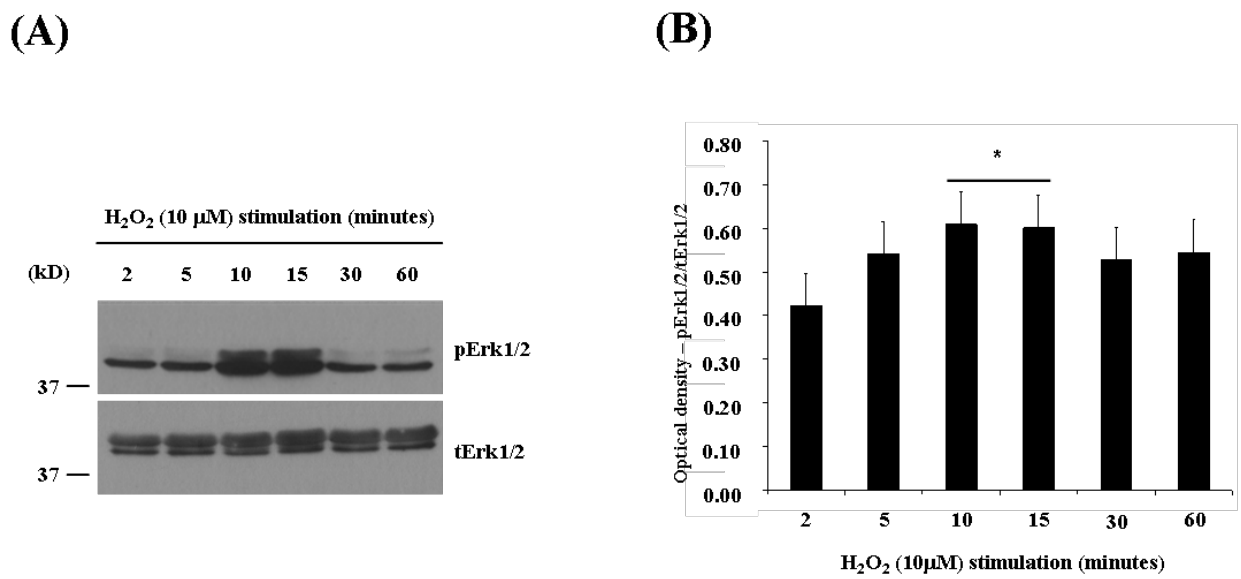


Figure 17. Exogenous $H_2O_2$ stimulates Erk1/2 phosphorylation in LSMCs. (A) Immunoblot for time-course of ERK1/2 activation in response to $H_2O_2$; anti-total ERK1/2 (tERK1/2) were used as loading control. Graphs represent the densitometric analysis of the blots showing the time-course of ERK1/2 activation in response to exogenous $H_2O_2$; (n=3. Bars represent LSmeans ± SEM. Line above 2 bars indicate both time-points were merged and compared to the other time-points. Asterisk above line indicates statistical difference in comparison to other time-points $p<0.05$).

# CHAPTER 4

# CHARACTERIZATION OF THE NADPH OXIDASE COMPLEX IN NORMAL MYOMETRIAL AND LEIOMYOMA SMOOTH MUSCLE CELLS

## 4.1 ABSTRACT

Uterine leiomyomas or fibroids are benign tumors that affect over 70% of women and are characterized by increased proliferation of smooth muscle cells (SMCs) as well as increased deposition of collagens type I and III. Reactive oxygen species (ROS) have been implicated as important players in the development of other fibrotic disorders with similar pathogenesis such as liver fibrosis and atherosclerosis. My goal was to determine the expression pattern of the components of the ROS-generating enzymatic complex, NADPH oxidase, in leiomyoma and myometrial SMCs as well as to study the mechanism of activation of the complex in these cell types. I used qRT-PCR to assess mRNA levels and immunohistochemistry to assess protein localization. The mechanism of activation was studied by focusing on the expression and phosphorylation of the cytosolic NADPH oxidase subunit, $p47^{phox}$, by immunofluorescence staining and immunoblotting after treatment with PDGF. Manipulations of PKC activity by the PKC inducer PMA and PKC inhibitors Bis and Go-6983 were used to determine the involvement of PKC in PDGF-induced ROS production and Erk activation. Results indicate that several genes encoding NADPH oxidase complex components are expressed in leiomyoma and myometrial tissues, and that $p47^{phox}$ protein is also found in both tissues. Messenger RNA data showed the existence of a subset of tumors with upregulation of the NADPH oxidase complex in comparison to their autologus normal myometrium. I also showed that PDGF and EGF treatment induced $p47^{phox}$ enrichment within lipid rafts. Moreover, stimulation of the PKC pathway with PMA led

to Erk phosphorylation and ROS production, whereas inhibition of PKC reduced PDGF-induced Erk phosphorylation and ROS production. The present study is the first to show the presence of the NADPH oxidase enzymatic complex in leiomyoma amd myometrial tissues. The upregulation of NADPH oxidase components commonly associated with increased ROS production may be involved in the development of a subset of leiomyoma tumors. Furthermore, activation of NADPH oxidase in leiomyoma and myometrial SMCs by PDGF involves activation of PKC.

## 4.2 INTRODUCTION

Uterine leiomyomas are non-cancerous tumors characterized by increased proliferation of uterine SMCs and extensive deposition of ECM, primarily collagens type I and III [2, 32]. It has been estimated that over 70% of women have leiomyoma tumors, although only approximately 25% of them are symptomatic [3]. This disorder has a significant economic impact due to the fact that it is the leading indication for hysterectomies with an estimated 240,000 leiomyoma-related hysterectomies carried out every year in the US [4]. Leiomyoma tumors are responsive to ovarian steroids and a large range of growth factors. In addition leiomyoma SMCs can produce their own supply of growth factors including PDGF. Leiomyoma SMCs produce and secrete PDGF and its expression is induced by estrogen but suppressed by GnRH agonists [60, 66].

PDGF stimulates proliferation of myometrial and leiomyoma SMCs. More recently PDGF has been shown to alter chromatin structure of around the promoter regions of SMC-specific genes in vascular SMCs and downregulate their expression in favor of growth-responsive genes implying a potential role for PDGF in the regulation of the phenotypic switch observed in VSMCs undergoing local injury [30, 75, 165]. PDGF can also trigger a receptor-

mediated activation of ROS production, which is known to be an important component of the PDGF signaling pathway in different cell types including leiomyoma cells [11, 17, 165].

Excessive production of ROS has been implicated with the development of numerous disorders such as liver and lung fibrosis [9, 126]. Higher expression of NADPH oxidase components has also been associated with excessive ROS production, however excessive stimulation of the complex could also be a reason for higher ROS levels. Activation of NADPH oxidase in phagocytes requires phosphorylation of cytosolic $p47^{phox}$ protein because this event leads to conformational changes that expose specific amino acids allowing for interaction with the membrane-bound components of the complex, specifically $p22^{phox}$ [129]. The mechanisms regulating the activation of NADPH oxidase in myometrial and leiomyoma SMCs are currently not known. However, in fibroblasts, Catarzi et al. (2005) determined that PKC and PI3K are involved in PDGF-induced ROS production [113].

ROS are short-lived molecules and once produced can be readily degraded by antioxidant enzymes, unless the levels of ROS production overcomes the rate of degradation leading to accumulation and intracellular damage. Efficient utilization of a controlled and transient increase in ROS production in a signaling pathway context can be reached by reorganization and relocation of molecules involving approximation of the ROS-producing NADPH oxidase complex and oxidation-sensitive targets. An interesting mechanism used by cells to bring signaling molecules in close proximity by creating a micro-intracellular environment involves cell membrane structures called lipid rafts. Lipid rafts are cholesterol and sphingolipid rich plasma membrane microdomains that serve as an intracellular compartment for signaling [166]. NADPH oxidase has been detected in lipid rafts and its compartmentalization and control of spatial distribution appears to be related to localization in lipid rafts [167]. The goal of my

studies was to determine the expression pattern of the components of the ROS-generating enzymatic complex, NADPH oxidase, in leiomyoma and myometrial SMCs as well as to study the mechanism of activation of the complex in these cell types.

## 4.3 MATERIAL AND METHODS

### *4.3.1 NADPH oxidase components mRNA expression*

Total RNA was isolated from 10-paired (collected from the same patient) myometrial and leiomyoma tissue specimens. NanoDrop spectrophotometer from Thermo Scientific (Wilmington, DE) was used to quantify RNA samples and these samples were submitted to Bionalyzer from Agilent Technologies (Santa Clara, CA) for determination of RNA quality. Cutoff for RNA integrity number (RIN) determined by the Bioanalyzer was 7.0. Reverse-transcription reactions were carried out for 1 ug of total RNA for each sample using the High Capacity kit from Applied Byosystems (Foster City, CA). Primer/probe sets for the following NADPH oxidase components were purchased from Applied Biosystems (Foster City, CA): CYBB/Nox2, Nox4, CYBA/$p22^{phox}$, NCF1/$p47^{phox}$, NCF2/$p67^{phox}$, NCF4/$p40^{phox}$, Rac1, Nox1, Nox5, NOXA1, and NOXO1. Ribosomal gene 18-S was used as an endogenous loading control. The relative standard curve method was used to determine relative gene expression differences between normal myometrium and leiomyoma tissues. Briefly, a pool of samples was established to set up the standard curve for all assays. Every tested gene, including the endogenous control, had a standard curve along with the unknown samples within the same plate. Expression values for the target genes were normalized for 18-S gene expression. Expression values adjusted for the endogenous control were normalized by the average of normal myometrial tissue expression.

This approach allowed us to establish the value for normal myometrium as the base level control, which was set as 1, as well as to calculate a measurement of error.

*4.3.2 Effects of PKC on Erk activation*

Leiomyoma and normal myometrial cells were cultured in 60mm dishes until they reached 90% confluence. Cells were then switched to DMEM containing 0.5% fetal bovine serum (FBS) for 1 hour prior to adding treatments. Cells were treated with either 0, 200 nM or 400 nM phorbol 12-myristate 13-acetate (PMA - P1585) from Sigma (St. Louis, MO) in DMEM containing 0.5% FBS for 15 minutes. To collect the cell lysates, warm Laemmli sample buffer was added directly to the cells, lysates were scraped off the dishes, and transferred to a 1.5 ml tubes. Lysates were heated at 95°C for 3 minutes and then frozen at -20°C. Lysates were later sonicated to shear genomic DNA and protein concentrations determined by BCA assay. Approximately 5 ug of protein for each sample were loaded onto SDS-PAGE gels and electrophoresis was performed. Protein transfers were performed overnight and successful transfer was checked by Ponceau staining. Membranes were blocked in 5% milk for 1 hour and primary rabbit anti-Erk1/2 (diluted at 1:1000) or mouse anti-phosphorylated Erk1/2 (diluted at 1:2000) antibodies from Cell Signaling (Danvers, MA) were incubated in 3% BSA or 5% milk respectively, overnight at 4°C. HRP-conjugated horse anti-mouse IgG and HRP-conjugated goat anti-rabbit IgG antibodies, purchased from from Cell Signaling (Danvers, MA), were diluted at 1:10000, and incubation was carried out at room temperature for 1 hour, followed by addition of chemiluminescence substrate to the membrane and X-ray film exposure and development.

Experiments assessing the effects of PKC inhibition on PDGF-induced Erk activation were performed following a similar methodology with adaptations according to the specific

treatment. Depletion of PKC was achieved by treating cells with the PKC inhibitor bisindolylmaleimide I (Bis - 203291) from EMD Chemiclas (Gibbstown, NJ) at 1 or 5 μM for 30 minutes, followed by addition of DMEM containing 0.5% fetal bovine serum with or without PDGF (10 ng/ml) for 15 minutes. The positive control consisted of cells treated with PDGF without preexposure to Bis.

*4.3.3 Effects of PKC stimulation on ROS production*

Leiomyoma and normal myometrial cells were plated in IbiTreat μ-dishes (80136) from Ibidi (Munich, Germany) at an initial density of 2,000 cells per dish in phenol red free DMEM containing 10% serum and cultured until reaching 50% confluence. At this stage cells were transferred to DMEM containing 10% serum and transferred to an incubator at the imaging facility. Cells were washed 3 times in Dulbecco's PBS and incubated with the oxidation sensitive dye carboxy-$H_2$DCFDA for 15 minutes. Cells were then washed 2 times with DPBS and incubated with or without PMA or PDGF in DPBS for 15 minutes. PKC inhibition experiments involved 15 minutes of pre-treatment with the PKC inhibitors Bis or Go-6983 followed by PDGF treatment for 15 minutes in the presence of Bis (5 μM) or Go-6983 (5 μM). Cells exposed to PMA, Go-6983 or Bis only, in the absence of carboxy-$H_2$DCFDA were used to control for each compound's auto-fluorescence. After addition of growth factor or PMA cells were transferred to the fluorescence microscope and were kept in a chamber under controlled temperature and $CO_2$ concentration while images were captured. A change in fluorescent signal was interpreted as a change in ROS production.

*4.3.4 Immunohistochemistry for p47$^{phox}$*

Normal myometrial and leiomyoma tissues embedded in paraffin were sectioned to 5 μm thick sections. Following deparaffinization and dehydration, antigen retrieval was performed by boiling slides in citrate buffer for 30 minutes at 50% power in the microwave. After cooling down the slides to room temperature the quenching of endogenous peroxidase activity was performed by incubating samples in a solution of 0.3% hydrogen peroxide in methanol for 15 minutes. Samples were then blocked in 1.5% goat serum (PBS/0.05% Tween-20) for 1 hour and primary antibody incubation with rabbit anti-human p47$^{phox}$ antibody (ab63361) from Abcam (Cambridge, MA) diluted at 1:400, was performed overnight at 4°C. The Vectastain Elite ABC Kit from Vector Laboratories (Burlingame, CA) was used for immunostaining detection. Following overnight incubation with the primary antibody samples were incubated with biotinylated anti-rabbit secondary antibody for 1 hour at room temperature. ABC reagent, containing avidin and biotinylated horseradish peroxidase H was then prepared and incubated with slides for 30 minutes. Samples were then exposed to DAB and the colorimetric reaction was stopped in tap water. Hematoxylin counterstaining was performed followed by dehydration, clearing and mounting of slides.

*4.3.5 Immunofluorescent detection of phosphorylated p47$^{phox}$ after treatment with PDGF*

Leiomyoma and normal myometrial cells were plated in ibiTreat μ-dishes (80136) from Ibidi (Munich, Germany) at 6,000 cells per well in phenol red free DMEM/10% serum. Cells were grown until 50% confluence and then cultured in DMEM containing 0.5% fetal bovine serum (FBS) for one hour. Stimulation with PDGF (10 ng/mL) was performed in DMEM containing 0.5% fetal bovine serum (FBS) for 15 or 30 minutes. After treatment cells were rinsed

3 times with Dulbecco's PBS, and fixed with 4% paraformaldehyde (15710) from Electron Microscopy Sciences (Hatfield, PA) for 25 minutes at room temperature. Following fixation cells were washed 3 times with DPBS and permeabilized in 0.2% Triton X-100 for 10 minutes. Blocking of non-specific binding was performed with Image-iT FX signal enhancer (I36933) from Invitrogen (Carlsbad, CA) for one hour. Primary antibody incubation with rabbit anti-phospho-$p47^{phox}$ (ab74095) from Abcam (Cambridge, MA) diluted at 1:400 was performed overnight at 4°C in DPBS containing 0.2% BSA and 0.05% Tween 20. Secondary antibody, Alexa Fluor 546 goat anti-rabbit IgG (A11035) from Invitrogen (Carlsbad, CA) was diluted at 1:100, and incubation was performed at room temperature for one hour using the same buffer as for primary antibody incubation. DAPI (D3571) from Invitrogen (Carlsbad, CA) was added to cells at 5μg/ml prior to mounting the slides and incubated for 10 minutes. Dishes were washed once with DPBS and ProLong Gold antifade reagent (P36930) from Invitrogen (Carlsbad, CA) was used to mount slides. Slides were then incubated overnight at room temperature and stored at 4°C for subsequent imaging. Refer to APPENDIX G for a more detailed immunofluorescence protocol and to APPENDIX H to a detailed step-by-step procedure on imaging immunofluorescent images.

### *4.3.6 Immunoblotting for detection of $p47^{phox}$ phosphorylation*

Cell culture conditions, serum starvation, cell lysate collection and western blotting procedure followed the steps described in item 4.3.2, with the exception of the amount of total protein loaded for $p47^{phox}$ immunodetection, which was around 30 μg. To determine the time-course of $p47^{phox}$ phosphorylation, leiomyoma and normal myometrial cells were exposed to either PDGF (10 ng/ml) or PMA (1 μM) for 5, 10 or 30 minutes and cell lysates were collected.

Next, experiments were performed to assess the effects of PKC inhibitors on PDGF and PMA-induced $p47^{phox}$ phosphorylation. Cells were pretreated with either 5 μM of Go-6983 (G1918) from Sigma (St. Louis, MO), 5 μM of Bis or DMEM only (0.5% FBS) for 15 minutes, then exposed to either PDGF (10 ng/ml) or PMA (1 μM) for 5 minutes in the presence or absence of the inhibitors. Cell lysates were collected at the end of the treatment periods. Immunodetection of the phosphorylated form of $p47^{phox}$ was achieved by incubating membranes with a rabbit anti-human phosphorylated-$p47^{phox}$ polyclonal antibody (ab74095) from Abcam (Cambridge, MA) diluted in 5% BSA/TBS-T for 90 minutes at room temperature. Membranes were then stripped at room temperature for 20 minutes and reprobed with a rabbit anti-human $p47^{phox}$ polyclonal antibody (BS1846) from Bioworld (Minneapolis, MN) at room temperature for 90 minutes.

*4.3.7 Sucrose gradient ultra-centrifugation for localization of $p47^{phox}$ in lipid rafts*

Leiomyoma cells were plated into 100 cm plastic dishes at approximately 600,000 cells/dish and grown to 90% confluence. After reaching 90% confluence cells were serum starved for 24 hours and then treated with PDGF (10ng/ml), EGF (50ng/ml) or DMEM/0.5% FBS (Control) for 3 minutes. Cells were washed with PBS/5 mM EDTA and placed on ice. Cell scrapers were used to remove cells from the dishes and cell suspensions collected into 50 ml conical tubes and later centrifuged at 1,000 RPM for 5 minutes at 4°C. Supernatants were removed and 500 μl ice-cold lysis buffer added to ressuspend cell pellets followed by incubation on ice for 15 minutes. Sucrose gradients were obtained by adding 500 μl of ice-cold 80% sucrose buffer to yield a solution of cell lysate in 40% sucrose buffer. This solution was transferred to ultracentrifuge tubes and 2.5 ml of 35% sucrose was layered on top of the 40% solution, followed by addition of 5% sucrose buffer (500 μl) on top of the 35% solution. Cell lysates on

sucrose gradients were centrifuged at 45,000 RPM for 12 hours at 4°C. TX-100 sucrose gradient fractions of 500 μl were collected for a total of 8 fractions. Warm 1X Laemmli sample buffer (LSB) was added to the insoluble pellet, fractions mixed to 4X LSB, and then heated to 95°C for 5 minutes prior to loading onto SDS-PAGE gels. Refer to APPENDIX I for a more detailed protocol. Densitometry analysis was performed to quantify the proportion of $p47^{phox}$ that was present in lipid raft fractions versus total $p47^{phox}$. The average proportion of $p47^{phox}$ present in lipid rafts was compared between LSMCs exposed to either EGF or PDGF and untreated cells. To determine whether the increase in $p47^{phox}$ in lipid rafts after growth factor treatment was statistically significant a paired one-tailed t-test was performed.

## 4.4 RESULTS

### *4.4.1 NADPH oxidase complex expression in leiomyoma and myometrial tissues*

Quantitative RT-PCR performed on RNA from matched pairs of leiomyoma and normal myometrial tissues detected the expression of the majority of the NADPH oxidase complex components. The average cycle threshold (Ct) values across all tested samples are indicators of how abundant the expression of a given gene is. The results presented in Table 1 show the average Ct values for all genes tested. As a preliminary assessment of the data one can compare average Ct values among isoforms and estimate which isoforms are more abundant and potentially more relevant in the cell types being studied. For example, of the Nox enzymes tested (Nox1, Nox2, Nox3, Nox4, and Nox5; DUOX1 and DUOX2 were not tested) Nox2 ($gp91^{phox}$) and Nox4 were the most abundant. NOXA1 and NOXO1 were almost undetectable in these tissues, suggesting that their homologues, $p67^{phox}$ and $p47^{phox}$, respectively, are more relevant biologically.

Analysis of relative gene expression between leiomyoma and normal myometrial tissues within matched pairs showed no differential expression for most of the subunits with the exception of two genes that showed overall reduced expression in leiomyoma tumors (Figure 18). However, further analysis involving examination of gene expression levels in a patient-specific manner revealed an interesting pattern that can be observed in Table 2. When analyzing the expression of the 7 NADPH subunits present in the tested tissues I observed that out of the 10 matched pairs, three of these pairs showed increased expression of at least 4 of the subunits in leiomyoma tissues. Findings of this study indicate significant tumor heterogeneity in regards to the pattern of expression of the NADPH oxidase subunits, suggesting that some NADPH oxidase subunits might be involved in the pathogenesis of a subgroup of leiomyoma tumors.

*4.4.2 Effects of PKC on ROS production*

Activation of the NADPH oxidase complex in some cell types is triggered by serine phosphorylation of the cytosolic component $p47^{phox}$. Phosphorylation of $p47^{phox}$ induces its conformational change that leads to unmasking of a protein domain that then interacts with membrane-bound $p22^{phox}$, targeting $p47^{phox}$ and the rest of the cytosolic complex to the cell membrane leading ultimately to ROS production. Based on previous studies in other cell types I hypothesize that PKC is the kinase responsible for phosphorylating $p47^{phox}$ and driving NADPH oxidase activation. To assess whether alterations in PKC activity would affect ROS production directly, I used the cell-permeant indicator for ROS, carboxy-$H_2$DCFDA. Treatment with PDGF was used as a positive control because I have used it previously as a potent trigger of ROS production. Whereas exposure of cells to DPBS alone resulted only in a basal fluorescence signal, treatment with PMA at 400 nM for 15 minutes induced a noticeable increase in

fluorescence, indicating increased ROS production (Figure 19). To test the involvement of PKC in PDGF or PMA-induced ROS production I used the PKC inhibitor Bis as a pre-treatment prior to exposing cells to PDGF. Surprisingly, after PDGF treatment in the presence of Bis there was a significant increase in the fluorescence signal (Figure 19). I determined that the increased signal was due to autofluorescence of the Bis compound (APPENDIX J). To overcome this technical difficulty I used a different compound also known to inhibit PKC activity called Go-6983. The second PKC inhibitor tested also showed background fluorescence above that of DPBS-only treated cells (APPENDIX J). However, the fluorescence background induced by Go-6983 was below the signal observed in PDGF and PMA-treated cells (APPENDIX J). Furthermore, the pattern of fluorescent signal observed in cells exposed to Go-6983 or Bis only, which consisted of highly fluorescent spots (APPENDIX J), was different than the smooth and evenly distributed signal observed in PDGF or PMA-treated cells, as shown in Figures 20 and 21. The increase in ROS production induced by either PDGF or PMA was not observed in the presence of the PKC inhibitor, Go-6983, indicating that PKC activity is necessary for the PDGF or PMA-induced increase in ROS production in leiomyoma and normal myometrial cells.

*4.4.3 Effects of PKC on Erk activation*

To continue testing the hypothesis that ROS are necessary for the Erk1/2 signaling pathway, the next goal was to determine whether manipulations of PKC activity, which I showed to regulate ROS production, would interfere the activation of the downstream effector Erk1/2. I therefore tested whether induction of PKC by the phorbol ester PMA would alter phosphorylation of Erk1/2, or whether inhibition of PKC would reduce Erk1/2 phosphorylation induced by PDGF. PMA treatment alone for 15 minutes was sufficient to induce Erk1/2

phosphorylation while pre-treatment with the PKC inhibitor Bis reduced PDGF-induced Erk1/2 activation (Figure 22).

### *4.4.4 Immunohistochemistry for p47$^{phox}$*

The results from the gene expression analysis confirmed the presence of the Nox2, p22$^{phox}$, p47$^{phox}$, p67$^{phox}$ and Rac1 subunits in leiomyoma tumors as well as in normal myometrium. I hypothesize that the activation of the NADPH oxidase complex is triggered upon phosphorylation of p47$^{phox}$, leading to targeting of this protein with the other cytosolic components, p67$^{phox}$, p40$^{phox}$ and Rac1, to the cell membrane. I decided to focus the subsequent analysis on p47$^{phox}$ because of the availability of an antibody to this subunit and the necessity of phosphorylation of this subunit for membrane targeting. Immunohistochemistry analysis of leiomyoma and normal myometrial tissues detected cytosolic p47$^{phox}$ protein expression in SMCs as well as in the endometrial epithelium and endothelial cells (Figure 23). Interestingly, the majority of the endometrial epithelial cells showed nuclear staining, whereas only a fraction of the leiomyoma and myometrial SMCs had nuclear p47$^{phox}$ expession. When comparing the intensity of cytoplasmic and nuclear staining between paired (from the same patient) leiomyoma and myometrial tissues, overall cytoplasmic staining did not appear to be different between leiomyoma and myometrial tissue, whereas nuclear staining was slightly more intense in leiomyoma than in myometrial tissue. The relevance of the nuclear localization as well as the more intense nuclear staining in leiomyoma tissue remains to be determined.

### *4.4.5 Immunofluorescent detection of p47$^{phox}$ phosphorylation*

An alternative way of testing the involvement of p47$^{phox}$ as a primary player in PDGF-induced ROS production was to assess the level of p47$^{phox}$ phosphorylation in response to PDGF. The approach used to test the above hypothesis involved immunofluorescence detection of the phosphorylated form of p47$^{phox}$ protein in cultured cells. Immunofluorescence results showed a modest increase in the signal for phosphorylated p47$^{phox}$ in both cell types, but this was more prevalent in leiomyoma SMCs (Figure 24). The pattern of imunostaining showed an accumulation of cytoplasmic phosphorylated p47$^{phox}$ in a punctate manner around the nucleus, as well as nuclear staining. Staining was more pronounced at 30 minutes after PDGF induction versus 15 minutes. There was also phosphorylated p47$^{phox}$ staining of cell projections that became enriched over-time. Interestingly, there was also some indication that leiomyoma cells showed a higher basal level of p47$^{phox}$ phosphorylation than normal myometrial cells.

### *4.4.6 Immunoblot detection of p47$^{phox}$ phosphorylation*

Immunodetection by immunoblotting was used to determine whether p47$^{phox}$ phosphorylation is a downstream event following the activation of leiomyoma and normal myometrial cells by PDGF, and whether p47$^{phox}$ phosphorylation is regulated by PKC. I observed that the basal phosphorylation levels of p47$^{phox}$ were high in cells that were exposed to DMEM containing 0.5% FBS only. There was no further increase above basal levels of p47$^{phox}$ phosphorylation after either PDGF or PMA stimulation for 5, 10 or 30 minutes (Figures 25 A and B). To test whether PKC inhibitors would alter p47$^{phox}$ phosphorylation levels, I pre-treated both leiomyoma and normal myometrial cells with the PKC inhibitors Go-6983 or Bis for 15 minutes and then exposed them to PDGF or PMA in the presence or absence of the inhibitors.

There was no difference in the phosphorylation levels of $p47^{phox}$ between cells exposed to PDGF or PMA in absence or presence of PKC inhibitors (Figures 26 A and B). No differential response was observed between leiomyoma and normal myometrial cells.

### *4.4.7 Localization of $p47^{phox}$ in lipid rafts*

Lipid rafts are specialized plasma membrane microdomains that can bring signaling molecules together or keep them apart. In many signaling pathways the proximity between molecules is sufficient to trigger their interaction leading to activation or inhibition of signaling activity. I hypothesized that during the activation of the NADPH oxidase complex in SMCs the complex may be targeted to lipid rafts where its transient and controlled ROS production would be in close proximity to potential target molecules facilitating the role of ROS as a signaling molecule. I used sucrose gradients and ultra-centrifugation to separate lipid raft fractions from leiomyoma SMC lysates isolated with TX-100 detergent. Caveolin-1 detection by immunoblot indicated that the technique was accurately separating the lipid raft fractions (Figure 27A). Results suggest that in response to both PDGF and EGF there was an enrichment of $p47^{phox}$ protein into the lipid raft fractions (Figure 27B) in comparison to untreated cells. However, densitometry analysis showed that PDGF treatment induces an increase in the proportion of total $p47^{phox}$ that is present in lipid rafts ($p=0.051$), whereas EGF did not show statistically significant changes. These data suggest that lipid rafts may play an important role in the mechanism of action of NADPH oxidase-derived ROS as a signaling molecule.

## 4.5 DISCUSSION

The goals of this study were to characterize the expression pattern of NADPH oxidase complex components in leiomyoma tumors in comparison to the normal myometrium expression pattern, determine the mechanism leading to the activation of this complex by PDGF, and assess the participation of PKC in this process. This manuscript is the first to report the expression of specific NADPH oxidase components in leiomyoma SMCs, and the first to suggest that $p47^{phox}$ may be one of the critical cytosolic subunits of NADPH oxidase in normal myometrial and leiomyoma SMCs. In addition, I have also demonstrated that translocation of $p47^{phox}$ into lipid rafts occurs in response to PDGF, and the involvement of PKC as a mediator of Erk activation by PDGF as well as an inducer of ROS production.

The NADPH oxidase complex and its components have been identified in a variety of tissues, cell types, and species. Ishikawa et al. (1984) reported the existence of a hydrogen peroxide-producing NADPH oxidase in the endometrial epithelium of rats [168]. Jain et al. (2000) demonstrated NADPH oxidase-dependent superoxide production in the mouse uterus, which increased at pro-estrus and during the pre-implantation period in pregnant mice [169]. Expression of the Nox proteins Nox1, Nox2, Nox4, Nox5, Duox1 and Duox2 has been reported in the human uterus [11, 137, 170]. Cui et al (2009) reported by non-quantitative RT-PCR the expression of $p22^{phox}$, $p47^{phox}$, $p67^{phox}$, $p40^{phox}$, Rac1 and Rac2 in the human uterus, and Nox1, Nox2, Nox4, Nox5, and Duox1 in an immortalized human myometrial SMC line [170]. Results obtained in the present study of gene expression are similar to those of Cui and coworkers and suggest that $p47^{phox}$ and $p67^{phox}$ are more relevant than their isoforms with negligible expression, NOXO1 and NOXA1, respectively. With respect to the Nox proteins results indicated that Nox4 also had high levels of expression similar to the data reported by Cui and coworkers. Nox2 was

less abundant than Nox1 in this study, whereas Cui et al. reported an opposite trend of expression between the two subunits. Some of the differences may be attributed to the different techniques used to assess gene expression, qRT-PCR in present work and non-quantitative RT-PCR by Cui et al (2009) [170].

Immunohistochemistry results showed that $p47^{phox}$ protein expression in smooth muscle cells of leiomyoma and myometrial tissues is cytoplasmic as did immunofluorescence staining of cultured leiomyoma and myometrial cells. In both cases, although cytosolic staining was detected in smooth muscle cells, strong nuclear staining was also observed in many SMCs as well as in all endometrial epithelial cells. Nuclear localization of $p47^{phox}$ has been reported by Mofarrahi et al (2008), who observed this pattern in 30% of human myoblast cells transfected with the fusion protein cyan-fluorescent protein-$p47^{phox}$ [171]. The multiple protein binding domains present in $p47^{phox}$ confirm its function as an adapter protein. Gu et al. (2003) also observed nuclear localization of $p47^{phox}$ as well as an interaction between $p47^{phox}$ and RelA, a member of the NFκB complex that has a nuclear localization sequence [172]. These authors went further to determine the specificity and functional importance of this interaction and demonstrated its effects on RelA phosphorylation and activation leading to NFκB activation [172]. Colocalization of NADPH oxidase subunits in lipid rafts reported by Jin et al. (2008) showed a pattern of expression consisting of punctate staining clustered around the nucleus of some cells [173]. Confocal images from Jin et al. (2008) clearly showed that although the signal was stronger close to nucleus it was not present within the nucleus. Although the images from the present study were not taken under a confocal microscope the pattern observed suggests cytoplasmic punctate staining as well as nuclear staining [173]. This unexpected nuclear localization of the cytosolic $p47^{phox}$ subunit in leiomyoma and myometrial SMCs suggests an

interaction with another protein or complex of proteins, as $p47^{phox}$ itself does not have a nuclear localization sequence. Mofarrahi et al (2008) also observed that $p47^{phox}$ protein expression declined over-time as myoblast cells differentiate into myotubes [171]. Taken together with the findings in the present work, which showed strong $p47^{phox}$ nuclear expression in endometrial epithelial cells and some SMCs as well as more intense nuclear staining in leiomyoma SMCs in comparison to myometrial SMCs, I speculate that $p47^{phox}$ nuclear localization may be related to the state of differentiation of cells, or whether cells are actively proliferating.

I know from my previous work that PDGF induces ROS production in leiomyoma and myometrial SMCs, and that this ROS production is derived from the NADPH oxidase complex [165]. My next goal was to determine more specifically how PDGF might be leading to the activation of NADPH oxidase. In human monocytes PKC δ was identified as the PKC isoform responsible for $p47^{phox}$ phosphorylation and translocation to the cell membrane [174]. Additionally, in human neutrophils PKCs α, βII, ζ, and δ were able to phosphorylate $p47^{phox}$ and induce its translocation [175]. Catarzi et al. (2005) showed that in NIH3T3 fibroblasts PDGF-induced ROS production is dependent on the NADPH oxidase complex, PKC and PI3K [113]. My working hypothesis was that PDGF would activate the NADPH oxidase complex by inducing phosphorylation of $p47^{phox}$, and that PKC was the kinase involved in activation of NADPH oxidase. The results of the immunofluorescence studies agree with previously reported results indicating that PDGF induces a subtle increase in $p47^{phox}$ phosphorylation which was more pronounced in leiomyoma than in myometrial SMCs. However, immunodetection of the phosphorylated form of $p47^{phox}$ by immunoblotting did not show an increase in the levels of phosphorylated $p47^{phox}$ in cells treated with PDGF or PMA. Furthermore, the PKC inhibitors Bis and Go-6983 had no effect on $p47^{phox}$ phosphorylation in PDGF or PMA-exposed SMCs.

Immunoblotting is a technique more likely to provide an accurate quantitation of changes in protein phosphorylation levels in comparison to immunofluorescence. Thus, the discrepancy between the results might be explained by the different techniques utilized. Furthermore, it is possible that the apparent increase in $p47^{phox}$ phosphorylation observed by immunofluorescence might in fact indicate a redistribution and accumulation of phosphorylated $p47^{phox}$ in subcellular compartments in response to PDGF, as observed by a distinctly higher fluorescent signal at the edges of cell projections in PDGF-treated cells. This observation is in agreement with the lipid raft data, which indicates that PDGF induces an enrichment of $p47^{phox}$ into lipid rafts.

The observation that phosphorylated $p47^{phox}$ is present in unstimulated cells suggests the existence of a preassembled NADPH complex, because $p47^{phox}$ must be phosphorylated in order to interact with the other subunits. Li et al. (2002) reported similar findings. These authors determined that the NADPH oxidase complex is found preassembled in the cytosol and that unstimulated endothelial cells have detectable basal intracellular ROS production [134]. Overall, it also appears that $p47^{phox}$ phosphorylation staining is higher in leiomyoma SMCs than in myometrial SMCs. Findings of this study go further and indicate that $p47^{phox}$ phosphorylation is not involved with PDGF or PMA-induced ROS production. Although PDGF and PMA induce ROS production, they fail to induce $p47^{phox}$ phosphorylation, suggesting that another NADPH oxidase subunit, regulated by PKC, may involved in the PDGF-induced NADPH oxidase activation. Other two potential candidates as targets of PKC and reglulators of ROS production in leiomyoma and myometrial SMCs are $p40^{phox}$ and $p67^{phox}$, which have been implicated in NADPH oxidase activation in neutrophils and endothelial cells in response to PDGF and PMA, respectively [176, 177]. In addition, I also showed that manipulation of PKC activity alters ROS production, a marker of NADPH oxidase activity, and Erk phosphorylation, a downstream

marker of the PDGF-induced proliferation. Erk activation by PDGF has been shown to be dependent on ROS production and ROS alone are sufficient to induce Erk activation in leiomyoma SMCs [165].

As part of the characterization of the NADPH oxidase complex and its mechanism of action in uterine SMCs, I further hypothesized that upon $p47^{phox}$ activation its translocation to the plasma membrane would involve localization in lipid rafts. The involvement of lipid rafts in the assembly of signaling platforms, specifically the ROS-generating NADPH oxidase has been reported. In macrophages and promyelocytic leukemia cells the membrane-bound components of the NADPH oxidase complex are present in lipid rafts as well as the cytosolic components $p47^{phox}$ and $p67^{phox}$ are present in lipid rafts which become more enriched upon stimulation of PKC by PMA [178]. Jin et al. (2008) reported that in bovine endothelial cells endostatin induces enrichment of Nox2 and $p47^{phox}$ into lipid rafts and leads to increased activity of the complex. In these studies I also observed an enrichment of $p47^{phox}$ protein in response to exposure to PDGF into lipid raft fractions as determined by TX-100 sucrose gradient centrifugation. In VEGF-stimulated migration of endothelial cells, targeting of the NADPH oxidase complex to lipid rafts leads to a series of localized events necessary for establishment of the focal complexes on the lamellipodial leading edge of migrating cells. Additionally, VEGF-R2 localization at the focal complexes, which is necessary for proper activation of VEGF-induced ROS-dependent angiogenic signaling, depends on phosphorylation of the lipid raft component caveolin-1 (reviewed by [166]). Interestingly, I observed a clear pattern of enrichment of phosphorylated $p47^{phox}$ staining at the edge of the cell membranes of SMCs showing long projections in the immunofluorescence experiments. Similarly, Gu et al. (2003) observed colocalization of $p47^{phox}$ and RelA on some of these projections, identified by the authors as focal protrusions [172]. In

the present experiments cells were fixed for immunostaining at approximately 50% confluence and it was evident that a large number of relatively small cells were emitting projections suggesting cell migration. Whether this observed pattern was due to localization of phosphorylated $p47^{phox}$ in lipid rafts and whether this mechanism is relevant for cell migration in uterine SMCs remains to be tested.

In summary, the NADPH oxidase complex is present in normal human myometrial and leiomyoma tissues and the in vitro data support the involvement of $p47^{phox}$ in the activation of the complex, potentially through its translocation into lipid rafts in response to PDGF as well as the involvement of PKC as a component of the ROS-generating system in these cells.

## 4.5 FIGURES AND TABLES

| Genes | *AVG Ct* |
|---|---|
| **Nox1** | ND |
| **Nox2** | 27.86 |
| **Nox3** | NT |
| **Nox4** | 29.87 |
| **Nox5** | LE |
| **p22phox** | 29.5 |
| **p47phox** | 29.83 |
| **NOXA1** | LE |
| **p67phox** | 30.07 |
| **NOXO1** | LE |
| **p40phox** | 30.59 |
| **Rac1** | 26.77 |

Table 1. Average cycle threshold (Ct) values of all tested (myometrium and leiomyoma tissue) samples for each tested member of the NADPH oxidase complex. Higher average Ct values are indicate higher abundance of subunits. Not detected (ND); Low expression (LE); Not tested (NT).

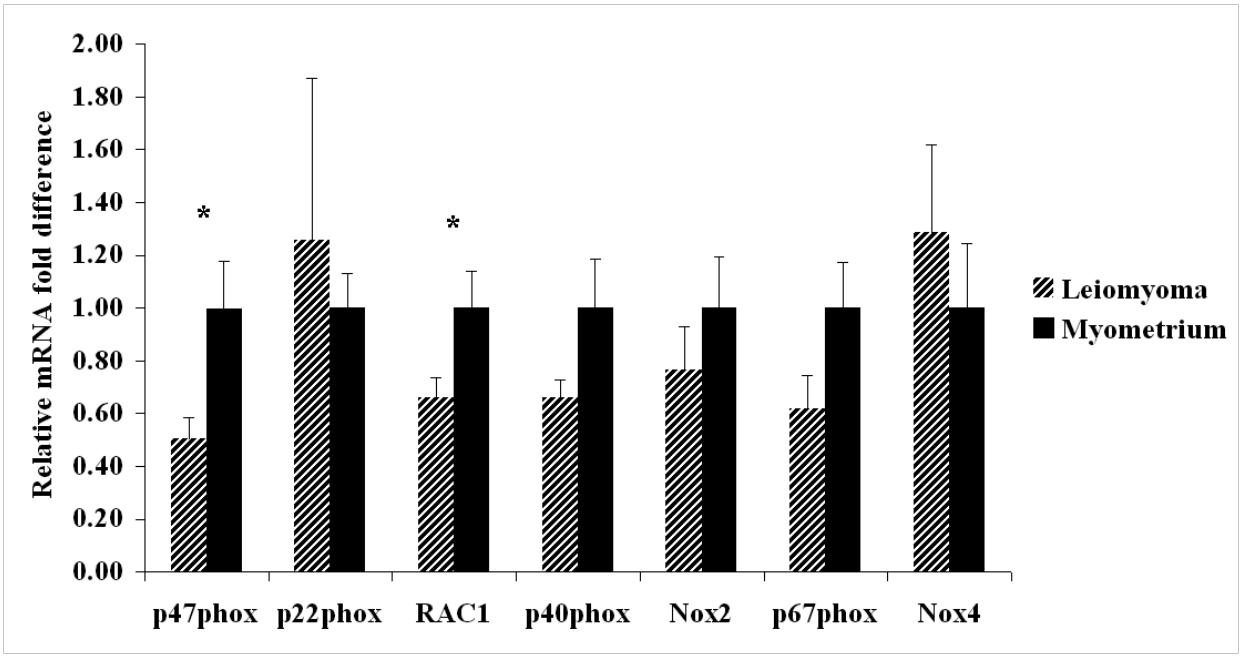


Figure 18. Relative fold difference in gene expression between normal myometrium and leiomyoma tissues measured by qRT-PCR. Asterisks indicate significant difference in gene expression between myometrium and leiomyoma. ($p<0.05$; $n=10$).

| | | | *Genes* | | | | |
|---|---|---|---|---|---|---|---|
| **Patients** | *p47phox* | *p22phox* | *Rac1* | *p40phox* | *Nox2* | *p67phox* | *Nox4* |
| **620** | 0.38 | 0.60 | 0.61 | 1.16 | 0.88 | 0.49 | 1.82 |
| **1378** | 0.39 | 0.65 | 0.48 | 0.46 | 0.40 | 0.42 | 0.96 |
| **2276** | 0.30 | 0.62 | 0.46 | 0.44 | 0.38 | 0.33 | 1.15 |
| **2699** | 1.93 | 1.04 | 0.90 | 1.94 | 6.35 | 1.68 | 3.78 |
| **3368** | 0.34 | 1.17 | 0.34 | 0.63 | 0.43 | 0.30 | 1.44 |
| **3644** | 0.34 | 0.66 | 0.67 | 0.59 | 0.44 | 0.47 | 0.92 |
| **5027** | 1.03 | 0.93 | 1.67 | 1.30 | 1.54 | 1.11 | 1.39 |
| **5339** | 0.27 | 0.29 | 0.61 | 0.32 | 0.22 | 0.25 | 0.88 |
| **8011** | 0.28 | 4.10 | 0.76 | 0.41 | 0.58 | 0.66 | 0.87 |
| **9912** | 1.71 | 0.93 | 0.95 | 1.60 | 2.96 | 2.02 | 1.47 |

Table 2. Relative fold difference of gene expression between normal myometrium and leiomyoma tissues within patient matched tissue pairs. Numbers under gene columns represent ratio of expression with myometrial gene expression as the normalizer. Patient numbers represent a pair of tissue specimens, normal myometrium and leiomyoma tumors.

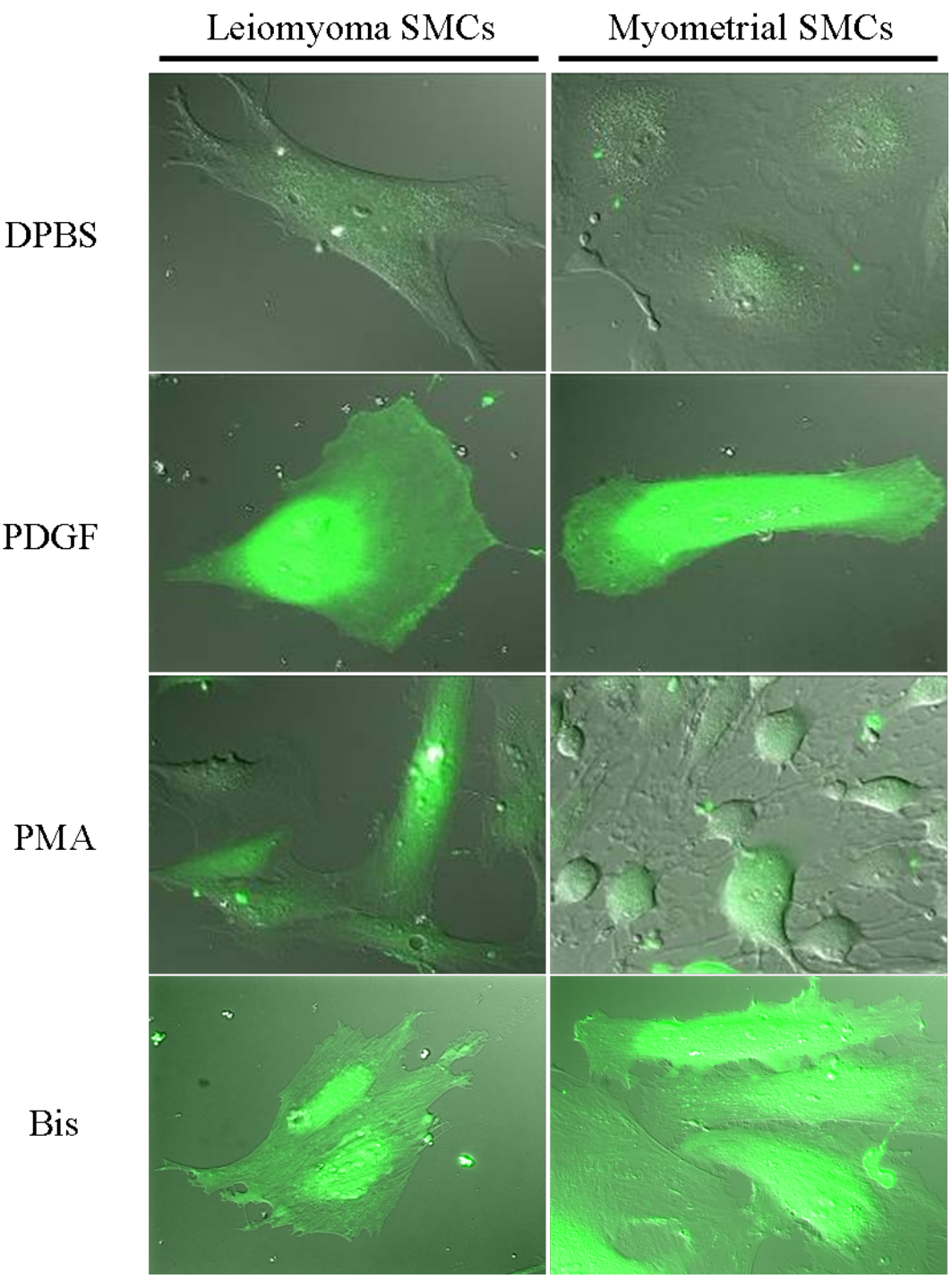


Figure 19. ROS production in response to PDGF, PMA and PDGF + Bis. Detection of ROS production by oxidation-sensitive dye carboxy-$H_2$DCFDA in leiomyoma and myometrial SMCs. Cell were treated with DPBS (negative control – top images) in the presence or absence of PMA (400 nM) or PDGF (10 ng/ml) for 15 minutes. Bottom images (Bis) refer to cells pre-treated with Bis (5 μM) for 15 minutes, followed by PDGF treatment in the presence of Bis for 15 minutes. Green signal indicates ROS production. Images were captured at 400X magnification.

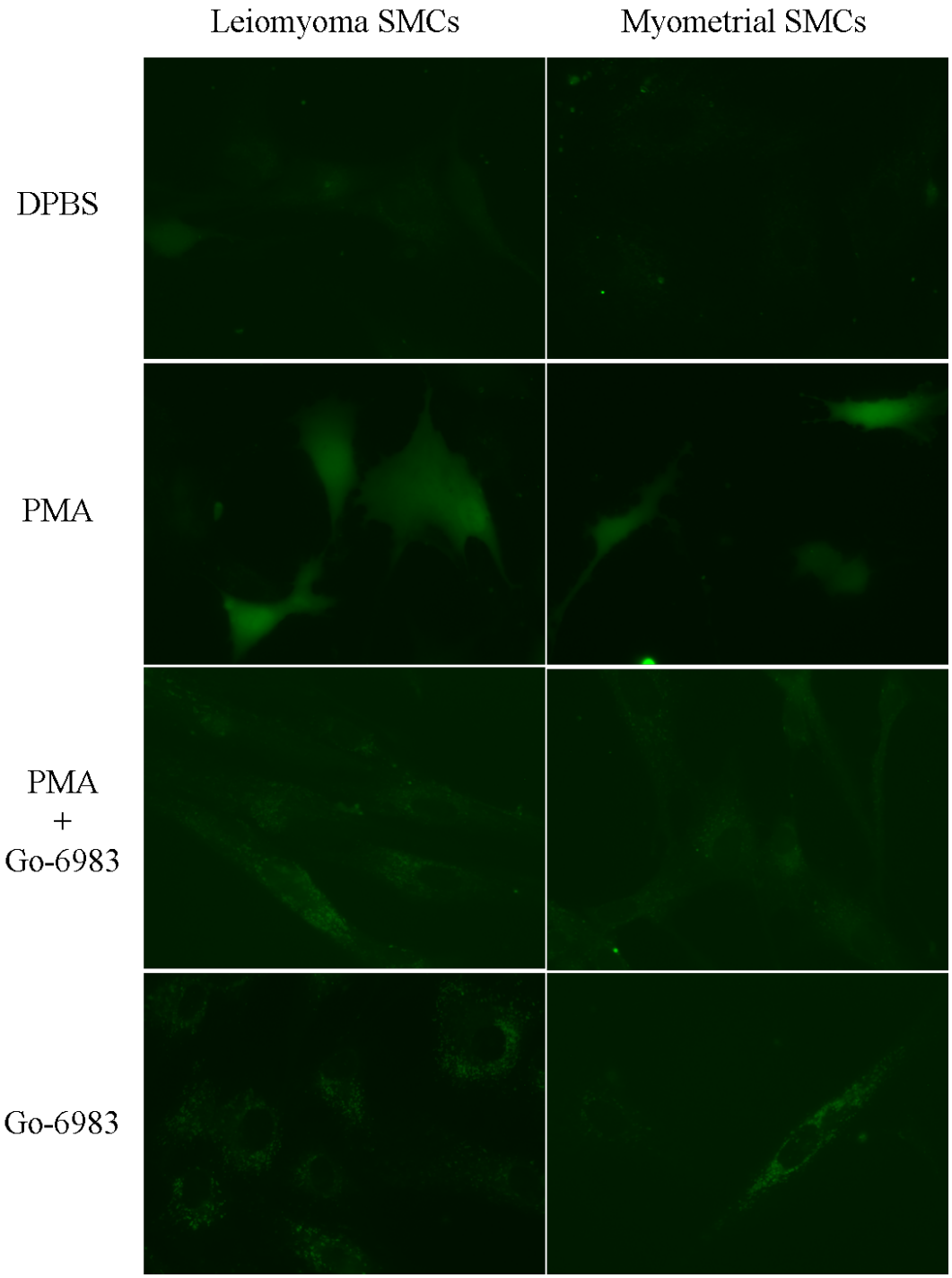


Figure 20. Effects of manipulations of PKC activity in ROS production. Detection of ROS production by oxidation-sensitive dye carboxy-$H_2$DCFDA in leiomyoma and myometrial SMCs. Cell were treated with DPBS (negative control) and PMA (1 μM) for 15 minutes. Inhibition of PKC was attained by pre-treating cells with Go-6983 (5 μM) for 15 minutes followed by PMA treatment in the presence of Go-6983. Green signal indicates ROS production. Images were captured at 400X magnification.

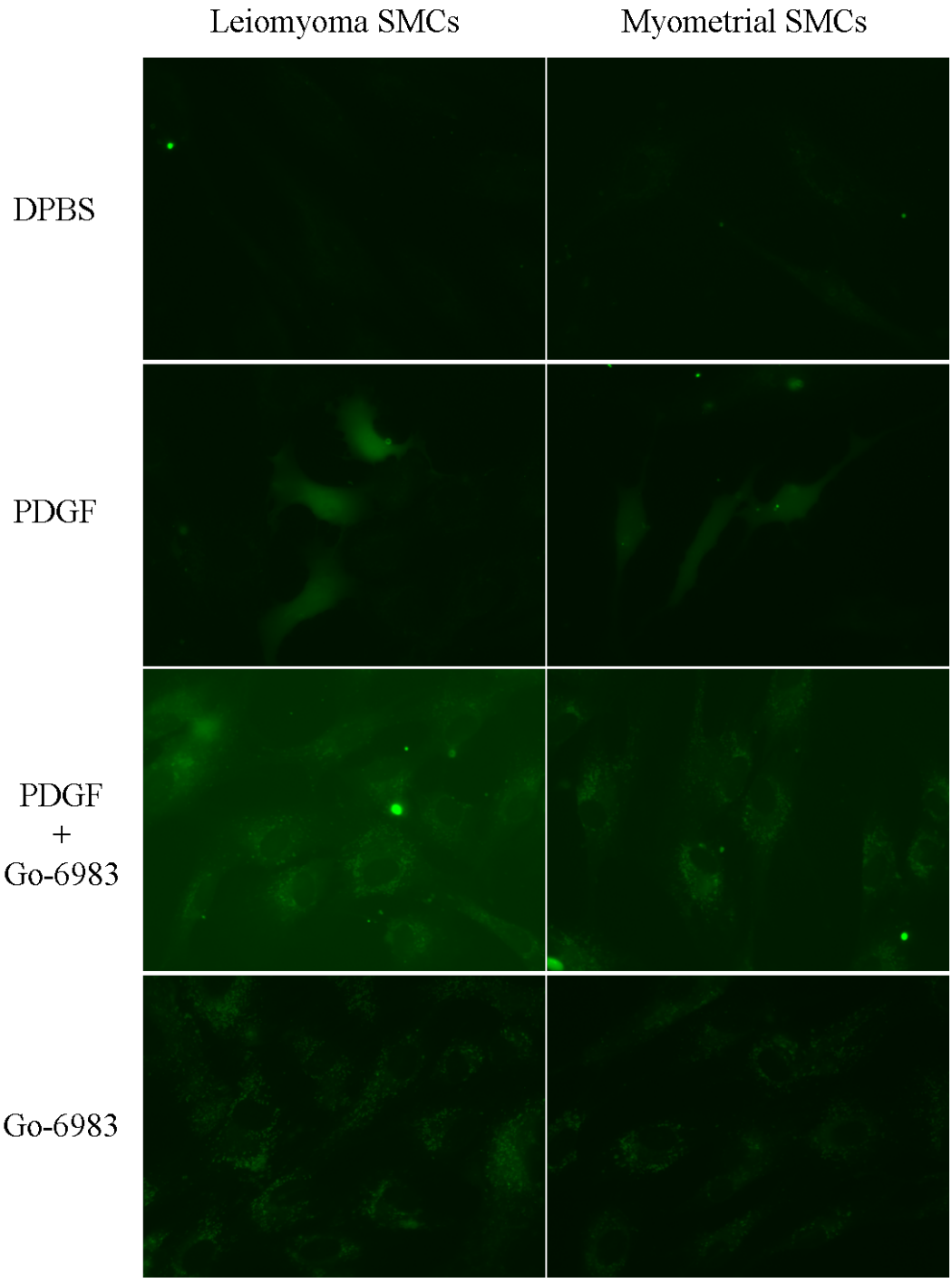


Figure 21. Involvement of PKC in PDGF-induced ROS production. Detection of ROS production by oxidation-sensitive dye carboxy-$H_2$DCFDA in leiomyoma and myometrial SMCs. Cell were treated with DPBS (negative control) and PDGF (10 ng/ml) for 15 minutes. Inhibition of PKC was attained by pre-treating cells with Go-6983 (5 μM) for 15 minutes followed by PDGF treatment in the presence of Go-6983. Green signal indicates ROS production. Images were captured at 400X magnification.

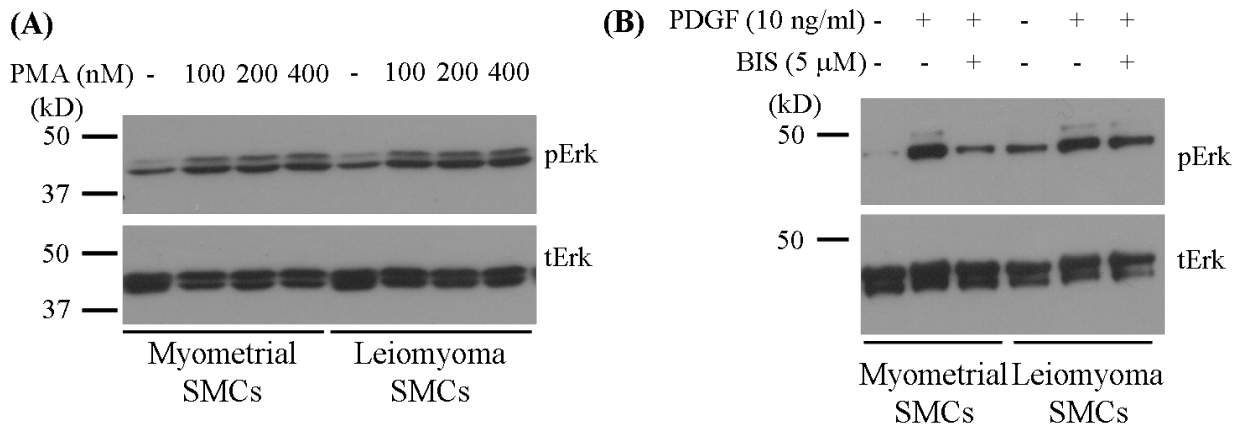


Figure 22. Involvement of PKC in Erk activation. Immunoblots for phosphorylated Erk (pErk) and total Erk protein (tErk-loading control) are shown. A) Cells were stimulated with or without PMA for 15 minutes. B) Cells were pre-treated with or without Bis for 30 minutes, followed by stimulation with or without PDGF for 15 minutes.

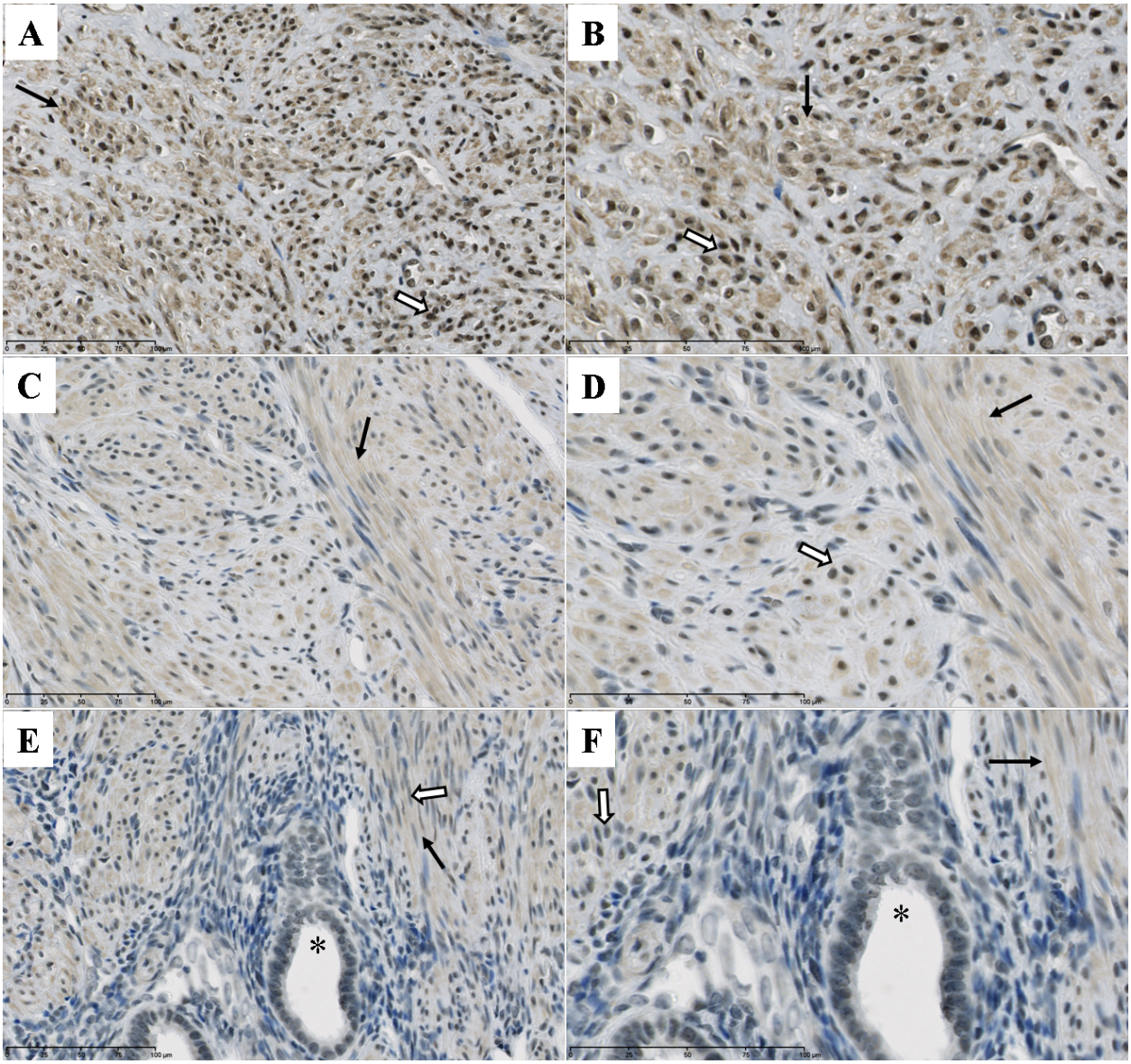


Figure 23. Immunohistochemistry for $p47^{phox}$. Representative cross sections of leiomyoma (A and B), myometrial (C and D) and myometrial+endometrial tissue (E and F). Images A, C and E are represent 400X magnification, and images B, D and F represent 630X magnification. Black arrows indicate bundles of smooth muscle cells with cytosolic staining. White arrows indicate smooth muscle cells nuclear staining. Asterisk indicates glandular epithelium with nuclear staining.

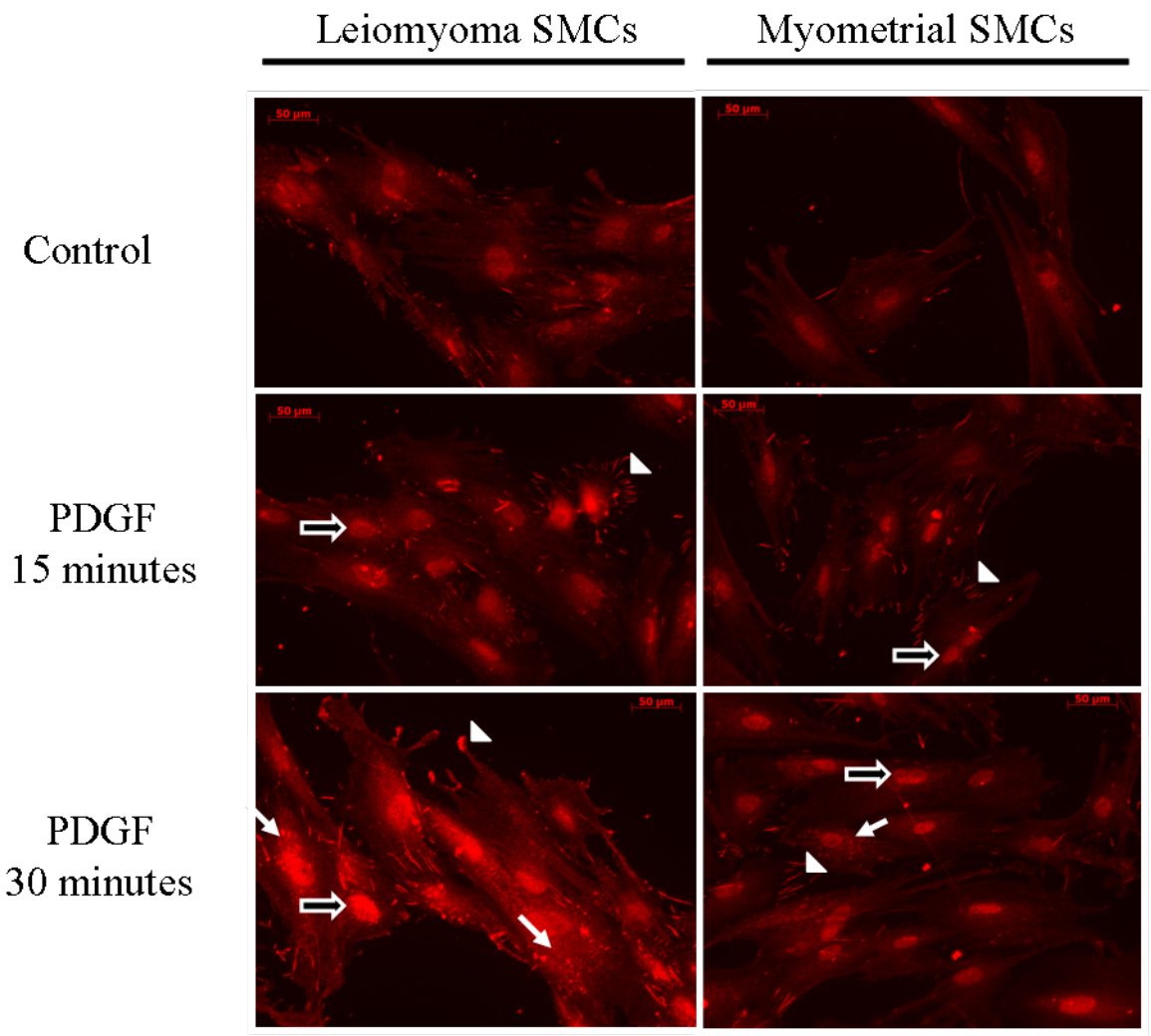


Figure 24. Immunofluorescence detection of phosphorylated $p47^{phox}$ in leiomyoma and myometrial SMCs. Immunodetection of the phosphorylated form of $p47^{phox}$ as a sign of NADPH oxidase activation in response to PDGF over time. White triangles indicate stronger staining at cell projections. White arrows indicate punctate staining around the nuclei. Dark arrows indicate nuclear staining.

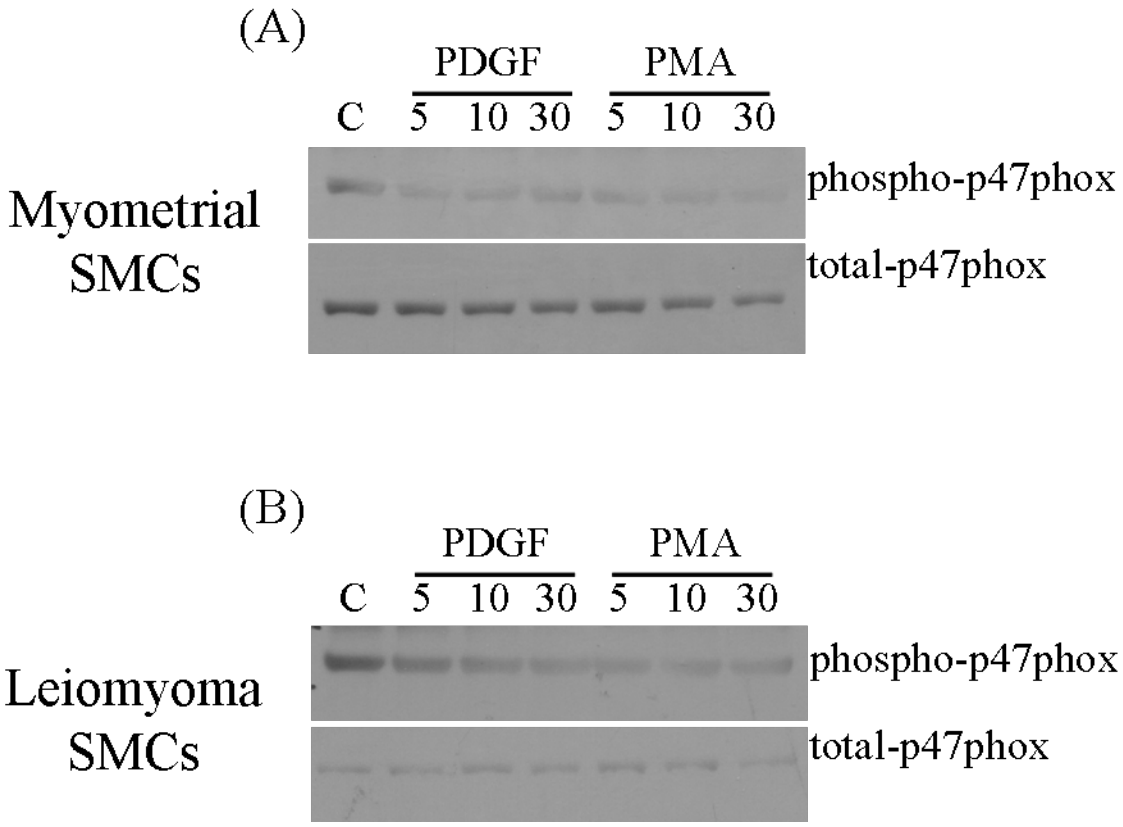


Figure 25. Immunoblotting detection of phosphorylated $p47^{phox}$ in leiomyoma and myometrial SMCs – Response to PDGF and PMA. Time-course of $p47^{phox}$ phosphorylation in response to PDGF (10 ng/ml) and PMA (1 μM) in (A) leiomyoma and (B) myometrial SMCs. Letter C indicates cells treated with DMEM/0.5% FBS at time-point zero, whereas other groups included cells treated with either PDGF or PMA for 5, 10 and 30 minutes.

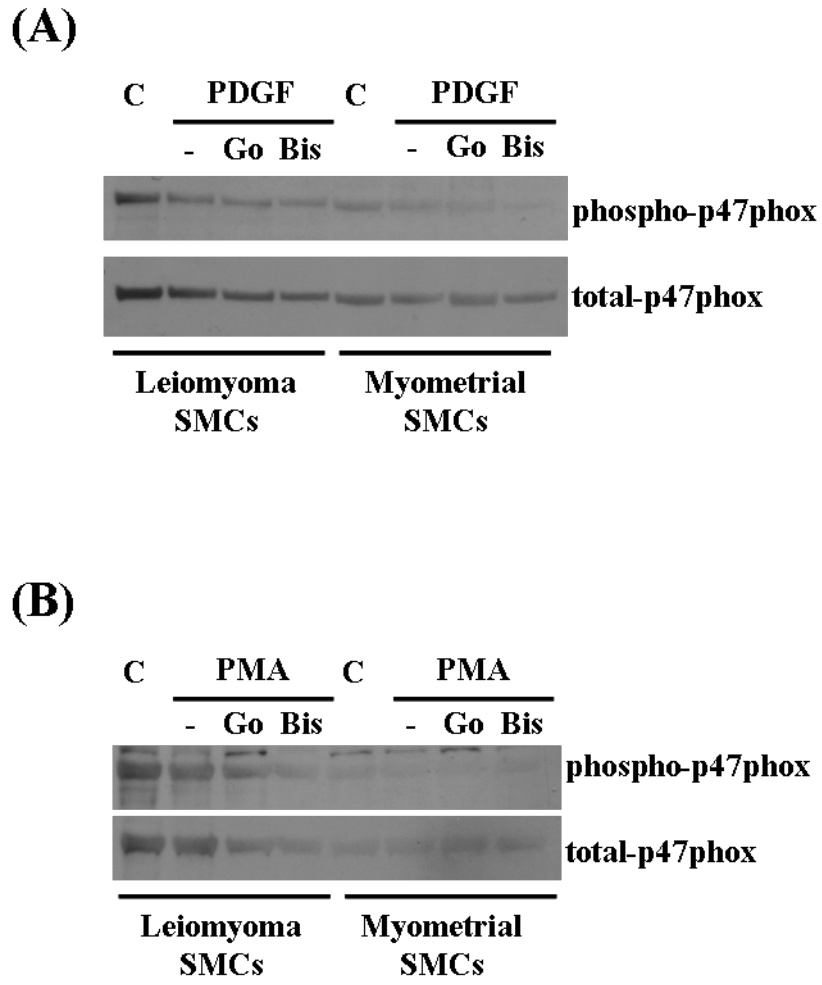


Figure 26. Immunoblotting detection of phosphorylated $p47^{phox}$ in leiomyoma and myometrial SMCs – Involvemente of PKC. $p47^{phox}$ phosphorylation in response to (A) PDGF (10 ng/ml) and (B) PMA (1 μM) in the absence or presence of 5 μM of Go-6983 (Go) or 5 μM of Bis. Letter C indicates cells treated with DMEM/0.5% FBS for 5 minutes, whereas other groups included cells treated with either PDGF or PMA for 5 minutes.

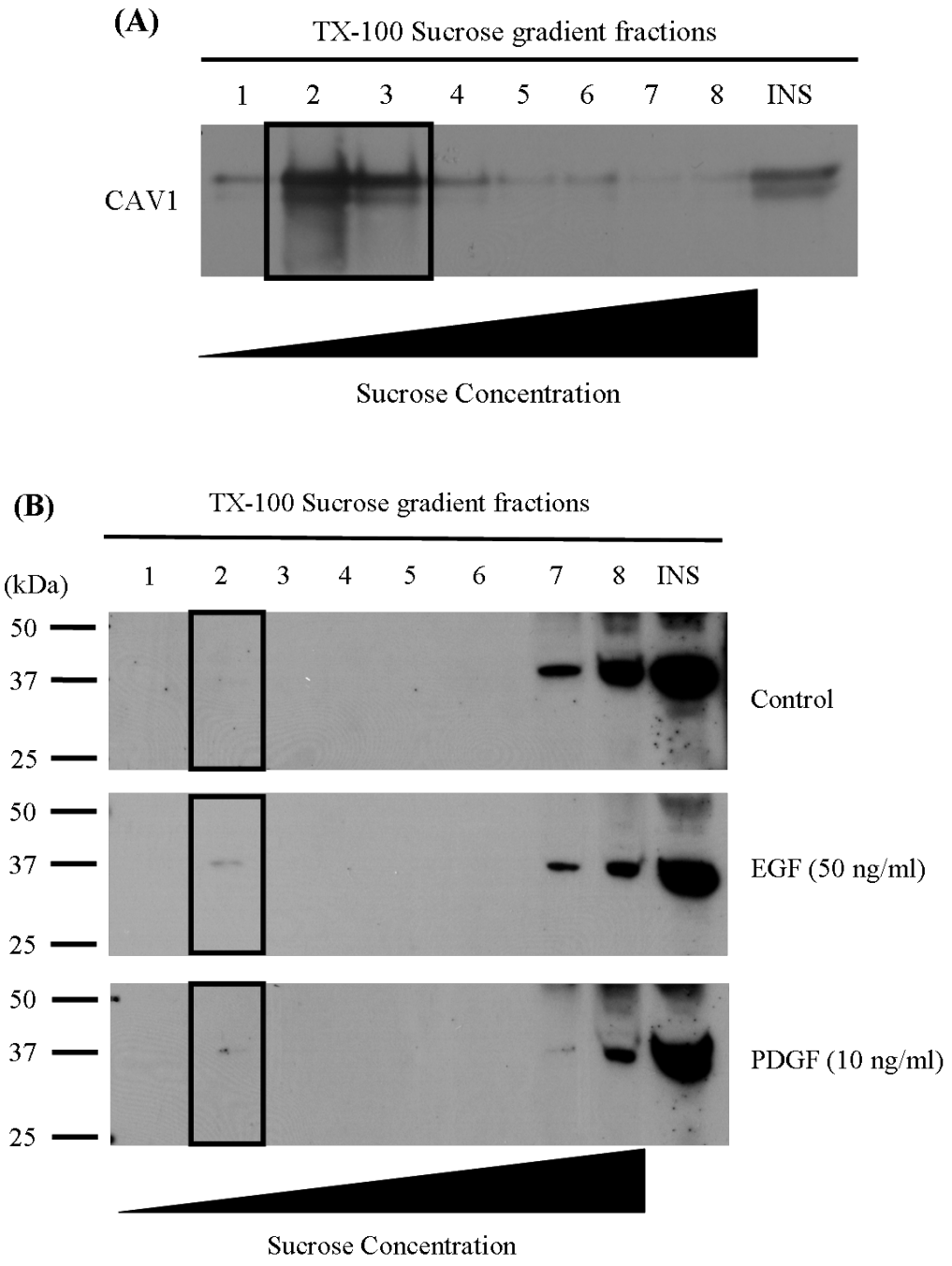


Figure 27. Immunodetection of p47$^{phox}$ in lipid raft fractions by sucrose gradient centrifugation. A) Immunoblot for caveolin-1 (CAV-1) as a marker for lipid rat fractions. Insoluble pellet (INS). B) Immunoblot for p47$^{phox}$ on TX-100 sucrose gradient fractions of leiomyoma cells treated with EGF or PDGF for 3 minutes and unstimulated. Boxes on each blot indicate lipid raft fractions.

# CHAPTER 5

# ROS-DEPENDENT ACTIVATION OF PROTEIN TYROSINE PHOSPHATASES AND THEIR INVOLVEMENT IN THE PROLIFERATIVE PATHWAY OF NORMAL MYOMETRIAL AND LEIOMYOMA SMOOTH MUSCLE CELLS

## 5.1 ABSTRACT

My previous work indicates that NADPH oxidase-derived reactive oxygen species (ROS) play an important role in the PDGF proliferative pathway in leiomyoma smooth muscle cells (SMCs). ROS can act as signaling molecules by modifying specific targets such as protein tyrosine phosphatases (PTPases). My aim in this study was to determine whether ROS could affect PTPase activity and whether changes in PTPase activity might regulate proliferation of myometrial and leiomyoma SMCs through the PDGF signaling pathway by altering PDGF receptor (PDGF-R) phosphorylation. I used primary cultures of normal myometrial and leiomyoma smooth muscle cells as the experimental model. PTPase activity in cell lysates of treated cells was measured using a colorimetric tyrosine phosphatase assay. The PTPase inhibitor sodium orthovanadate was used to assess the involvement of these enzymes in the cellular responses tested. Cell proliferation was measured by tritiated thymidine incorporation assays, and phosphorylation of PDGF-R was assessed by immunoblotting. My results show that an exogenous source of ROS, hydrogen peroxide, was sufficient to inhibit PTPase activity in leiomyoma SMCs, but not in myometrial cells. No effect of PDGF on PTPase activity was observed in either cell type. Inhibition of PTPase activity by low concentrations of sodium orthovanadate led to an induction of cell proliferation, with higher concentrations reducing proliferation. Interestingly, leiomyoma SMCs were sensitive to much lower concentrations of

sodium orthovanadate than myometrial SMCs. No effect of PTPase inhibition by sodium orthovanadate on basal PDGF-R phosphorylation was observed. In conclusion, PTPase activity is important for cell proliferation and is sensitive to regulation by hydrogen peroxide in leiomyoma SMCs.

## 5.2 INTRODUCTION

Leiomyoma tumors are benign neoplasms that arise from uterine smooth muscle cells that proliferate excessively and are characterized by a change in the composition and deposition of extracellular matrix proteins (i.e., overproduction of collagens type I and III) [2, 32, 33]. PDGF and PDGF receptors are also more highly expressed in leiomyoma tumors than in normal myometrium and their expression fluctuates throughout the menstrual cycle [179].

Estrogen stimulates PDGF production and secretion in leiomyoma cells [60]. Of interest to our laboratory is the fact that PDGF induces ROS production in a number of cell types, including leiomyoma SMCs, and that ROS are necessary for PDGF-induced DNA synthesis [17, 165]. In addition, ROS production is also necessary for PDGF-induced Erk phosphorylation in human leiomyoma SMCs and ELT-3 rat leiomyoma SMCs [165, 180].

ROS cannot alter the phosphorylation status of proteins to directly modulate the activation of downstream effectors, however numerous families of proteins have amino acid residues that are sensitive to oxidation. Protein tyrosine phosphatases are known targets of ROS due to a cysteine residue that is sensitive to oxidation rendering the enzyme inactive. The oxidized residue is stable however the reaction is reversible indicating that it can be regulated by post-translational modifications by ROS [15, 143]. It has been shown that Insulin or PDGF treatment leads to inactivation of PTPases, and more recently that NADPH oxidase-derived ROS

are responsible for inactivating PTPases [143-146]. Moreover, PTPase activation is associated with decreased activation of downstream effectors, and PTPase inactivation appears to be necessary to achieve proper tyrosine phosphorylation levels [18, 144, 145]. Further evidence for the importance of the oxidation mechanism for controlling PTPase activity comes from studies showing that suppression of hydrogen peroxide production by inhibition of superoxide desmutase 1 (SOD1) protects PTPases from inactivation and reduces growth factor-induced Erk phosphorylation [181]. In addition, enhanced glutaredoxin expression maintains activation of low molecular weight PTPase (LMW-PTP) and suppresses PDGF-induced cell proliferation by reducing phosphorylation of PDGF-Rβ [21].

One of the aims of my work was to determine more specifically some potential downstream targets of ROS action that could relate to the main hypothesis I are testing, which is that ROS are necessary components of the proliferative pathways controlled by PDGF. Based on results obtained by our group and other evidence from the literature I propose that PTPases are regulated by ROS and that modulation of PTPase activity alters cell proliferation in leiomyoma and myometrial SMCs.

## 5.3 MATERIAL AND METHODS

### *5.3.1 Effects of $H_2O_2$ and PDGF on PTPase activity*

Leiomyoma and normal myometrial cells were cultured in 60 mm dishes at 150,000 cells per dish until reaching 90% confluence. Cells were then cultured in DMEM containing 0.5% fetal bovine serum for 1 hour and treated with either PDGF (10 ng/ml) for either 15 or 30 minutes, or with $H_2O_2$ at 10 or 100 μM for 15 minutes. After treatment cells were washed in ice-cold PBS once, and ice-cold lysis buffer (50 mM Tris, pH 5.5, 100 μM EDTA, 100 μM EGTA,

0.5% TX-100) plus protease inhibitors was added. Cells were incubated for 10 minutes at 4°C in a belly dancer rocker and subsequently scraped off of the dish and transferred to a 1.5 ml tube. A tyrosine phosphatase assay system from Promega (Madison, WI) was used to determine tyrosine phosphatase activity in cell LSMCs and MSMCs lysates. Assays were performed according to the manufacturer's protocol. Briefly, cell lysates were cleared by ultra-centrifugation at 100,000 x g for 30 minutes at 4°C. To remove free phosphate from the cell lysates, samples were passed through a Sephadex G25 column and spun at 600 x g for 6 minutes. Protein concentrations were determined by BCA assay and 2.5 μg of protein were used for the tyrosine phosphatase assay. Cell lysates were first incubated with the substrate, a tyrosine phosphopeptide at 100 μM final concentration with the following sequence: END(pY)INASL, for 15 minutes in 96 well plates and an acidic dye solution was then added to stop the reaction as well as to react with free phosphate and allow quantitation of phosphatase activity. Dye incubation was carried out for 30 minutes at room temperature and plates were then read at 590 nm on a plate reader. Appropriate standards for the standard curve were prepared by diluting 1 mM phosphate standard in phosphate-free water, and added to 1X reaction buffer in a 50 μl final volume.

### *5.3.2 Effects of protein tyrosine phosphatase inhibitor, sodium orthovanadate, on cell proliferation*

Leiomyoma and normal myometrial cells were cultured in 96 well plates at 6,000 cells per well in DMEM containing 10% serum until reaching 90% confluence. Cells were then cultured in DMEM containing 0.5% FBS for 2 days and exposed to treatment. Tritiated thymidine was added during the last 24 hours of treatment. Treatments consisted of sodium

orthovanadate at 0.6, 1.25, 2.5, 5, 10, 20, 40, 80, and 160 nM for 48 hours followed by cell harvest and assessment of the DNA synthesis.

*5.3.3 Effects of protein tyrosine phosphatase inhibitor, sodium orthovanadate, on PDGF-R phosphorylation*

Leiomyoma and normal myometrial cells were cultured in 60mm dishes at 150,000 cells per dish in DMEM containing 10% serum until reaching 90% confluence. Cells were then cultured in DMEM containing 0.5% serum for 1 hour followed by treatment with DMEM containing 0.5% FBS or sodium orthovanadate at 1nM and 10 nM for 15 minutes. These concentrations were chosen based on the results obtained from the cell proliferation assays, in which 1 nM showed a trend to induce cell proliferation and 10 nM induced maximum stimulation, suggesting a range of active sodium orthovanadate concentrations. Cells were washed once with PBS and cell lysates were collected according to the protocol described earlier.

## 5.4 RESULTS

*5.4.1 Effects of $H_2O_2$ and PDGF on protein tyrosine phosphatase activity*

I hypothesized that ROS are regulating PDGF signaling by specifically oxidizing protein tyrosine phosphatases, thus modulating the phosphorylation levels of kinases and other important enzymes. To test our hypothesis I used a protein tyrosine phosphatase assay capable of measuring enzymatic activity in cell lysate. The specific question I asked was whether exogenous hydrogen peroxide alone or PDGF treatment were able to alter protein tyrosine phosphatase activity in leiomyoma and myometrial cells. There was no significant effect of

either hydrogen peroxide or PDGF on protein tyrosine phosphatase activity in normal myometrial cells (Figures 28A and 29A). However, in leiomyoma cells hydrogen peroxide induced a significant decrease in enzymatic activity, with no effect of PDGF (Figures 28B and 29B, respectively). Interestingly, when comparing the basal levels of protein tyrosine phosphatase activity in untreated leiomyoma cells versus untreated normal myometrial cells, leiomyoma cells appeared to have a higher basal level.

*5.4.2 Effects of protein tyrosine phosphatase inhibitor, sodium orthovanadate, on cell proliferation*

PTPases regulate signaling by dephosphorylating proteins and can therefore affect pathways that rely on protein phosphorylation to become activated. I know that the PDGF proliferative pathway, for instance, depends on auto-phosphorylation of PDGF-R to induce cell proliferation. I then hypothesized that inhibition of PTPase would alter the proliferation of leiomyoma or myometrial cells measured by [$^3$H]thymidine incorporation. Sodium orthovanadate, a broad-spectrum tyrosine phosphatase inhibitor, was used to target the enzymatic activity of this broad family of enzymes at a large range of concentrations. Orthovanadate had a biphasic effect in that at low concentrations it induced cell proliferation while higher doses had inhibitory effects (Figures 30A and B). Leiomyoma cells were more sensitive to the effects of orthovanadate than normal myometrial cells. Whereas leiomyoma cells showed increased proliferation at orthovanadate concentrations as low as 0.6 nM, myometrial cells were only induced to proliferate when treated with concentrations between 10 and 20 nM.

*5.4.3 Effects of protein tyrosine phosphatase inhibitor, sodium orthovanadate, on PDGF-R phosphorylation*

Protein tyrosine phosphatases counteract the actions of kinases thereby regulating activation or inhibition of different proteins by post-translational modifications. Based upon the results indicating that hydrogen peroxide regulates the activity of tyrosine phosphatases in leiomyoma cells as well as the evidence for regulation of cell proliferation by a tyrosine phosphatase inhibitor, I assume there is a significant biological link between ROS, tyrosine phosphatases and the proliferative pathway in leiomyoma cells. My initial hypothesis was that inhibition by tyrosine phosphatases could be occurring at the level of the PDGF-R. Although it is reasonable to hypothesize that inhibition of tyrosine phosphatases, which counteract the auto-phosphorylation of the PDGF-R, would allow the receptor to be more highly phosphorylated and/or remain phosphorylated longer, the experiments testing the effects of orthovanadate on basal PDGF-R phosphorylation did not show a significant effect on receptor phosphorylation (Figure 31).

## 5.5 DISCUSSION

The goal of my study was to identify potential downstream targets that may be regulated by ROS and also play a role in the proliferative pathways of leiomyoma and myometrial SMCs. The main findings of this study are that an exogenous source of ROS, hydrogen peroxide, inhibits the activity of PTPases in leiomyoma SMCs, and that the regulation of PTPase activity is important for myometrial and leiomyoma SMC proliferation. Treatment with an exogenous source of ROS, hydrogen peroxide, reduced PTPase activity in leiomyoma SMCs, but not in normal myometrial SMCs. However, treatment with PDGF had no effect on PTPase activity.

Regulation of PTPase by oxidation is well documented in the literature. A cysteine residue located at a unique position renders the enzyme susceptible to inactivation by oxidation, a process that is reversible [15]. Hydrogen peroxide is an oxidative molecule and has been implicated in several pathways as a regulator of PTPase activity [19, 143, 146]. Interestingly, only leiomyoma cells responded to hydrogen peroxide treatment with a decrease in PTPase activity in our studies. Overall the basal levels of PTPase activity were also higher in leiomyoma cells than in normal myometrial cells. It is possible that the levels of proteins that scavenge oxidative molecules are higher in myometrial cells so that the threshold of hydrogen peroxide levels necessary to show a significant effect on PTPase activity is higher than that of leiomyoma cells. According to Kappert et al. (2006) the use of antioxidants reduced hydrogen peroxide-induced inhibition of PTPases as well as hydrogen peroxide and PDGF-induced PDGF-R phosphorylation [19]. Additionally, higher expression of SOD1, which scavenges hydrogen peroxide, protects PTPase from inactivation [181]. Higher levels of ROS scavengers in myometrial SMCs may protect them from both oxidative stress-related alterations and over-activation of signaling pathways regulated by ROS.

To test whether manipulation of PTPase activity could in fact alter cell proliferation of leiomyoma and myometrial SMCs, I altered my approach and used a well-characterized and potent broad inhibitor of PTPases, sodium orthovanadate. This approach allowed us to be sure that PTPases would be inhibited equally well in all cell lines even though one cell line might potentially have higher levels of antioxidants/ROS scavengers than another. Inhibition of PTPases by sodium orthovanadate caused an increase in proliferation of both cell types. However, leiomyoma cells responded to very low concentrations of sodium orthovanadate, whereas myometrial cells only responded to sodium orthovanadate concentrations that were over

15-fold higher. Although basal levels of PTPase activity were higher in leiomyoma cells versus myometrial cells as discussed in the previous paragraph, it is possible that higher levels of intracellular antioxidants/ROS scavengers in myometrial cells protect PTPases from oxidative-regulated inhibition.

My speculations that inhibition of PTPases by sodium orthovanadate would increase basal levels of PDGF-R phosphorylation in unstimulated cells were not confirmed. Sodium orthovanadate has been shown to alter protein tyrosine phosphorylation levels of signaling molecules in response to several factors including EGF, FGF-2, IGF-1 and PDGF [181-183]. Sodium orthovanadate alone or in combination with hydrogen peroxide has insulinomimetic activity in a mechanism that involves inhibition of PTPases and increased protein tyrosine phosphorylation [184]. Heffetz et al. (1990) reported that vanadate inhibited activity of extracted PTPases in vitro, as well as PTPase activity of intact cells in combination with hydrogen peroxide, but not alone. Others reported a synergistic effect of vanadate in tyrosine phosphorylation of signaling molecules in response to growth factors [181, 183]. The concentrations of vanadate used in the PDGF-R phosphorylation experiments were chosen based on the [$^3$H]thymidine incorporation experiments according to concentrations that maximally stimulated cell proliferation. However, studies assessing the effects of vanadate on PTPase activity or tyrosine phosphorylation in intact cells have used concentrations that range from 2 μM to 1 mM [125, 181, 183, 184]. According to the literature, experiments assessing the effects of vanadate are normally carried out by incubating vanadate with cells for 15 or 30 minutes prior to stimulus or by adding vanadate simultaneously with the stimulus, which does not differ from the approach I used in my experiments. It is possible that assessing the effects of vanadate at other time-points may show different results, however I believe that the major difference

between the results present in this study and those form other studies is due to the fact that I assessed the effects of vanadate alone and not in the presence of PDGF stimulation. Chiarugi et al. (2002) have shown increased and long-lasting PDGF-induced PDGF-R phosphorylation in the presence of vanadate [183]. Others showed that vanadate increased Erk1/2 phosphorylation in response to different factors, with a small effect of vanadate alone [125, 181].

In conclusion, results are suggestive of dissimilarities between leiomyoma and myometrial SMCs with respect to PTPase activity and its regulation. It is likely that the difference between the two cell types is causing the differential response to hydrogen peroxide and sodium orthovanadate. The exact mechanism leading to the higher or lower PTPase sensitivity is yet to be studied, but it certainly suggests that leiomyoma cells could have a lower threshold for inhibition of PTPases providing a potential growth advantage to these cells over normal myometrial cells. Observations from cell count experiments that MSMCs did not respond to hydrogen peroxide as did LSMCs (Figure 13B and APPENDIX B) support the differential response os these two cell types to ROS. Further characterization of the observations made in this study is necessary to confirm the findings and more detailed assessment of PTPase activity and its regulation may lead to a novel therapeutical target in leiomyoma tumors.

## 5.6 FIGURES

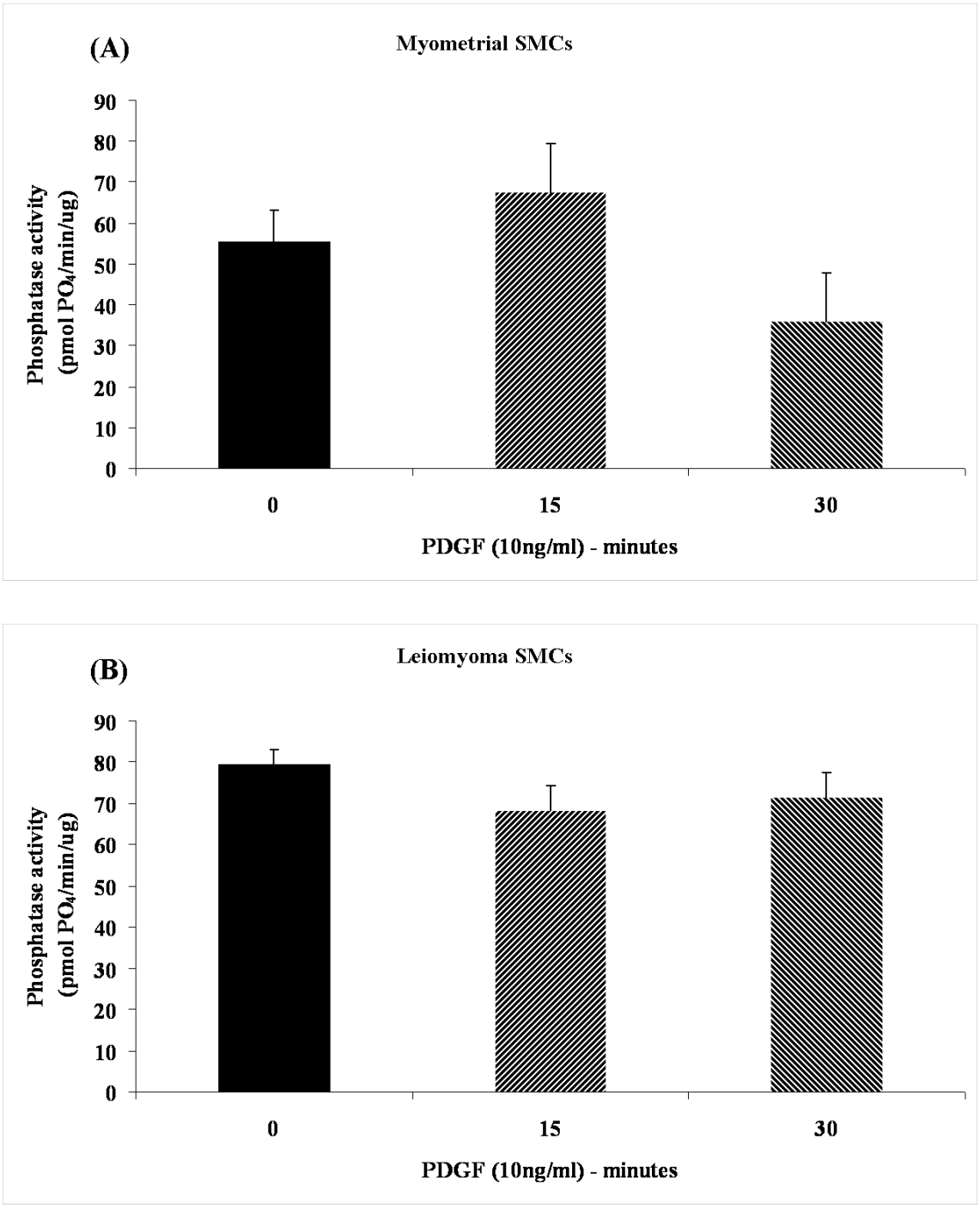


Figure 28. Regulation of protein tyrosine phosphatase activity in leiomyoma and myometrial SMCs. A) myometrial SMCs and B) leiomyoma SMCs were exposed to PDGF for 15 and 30 minutes and PTPase activity was measured on cell lysate.

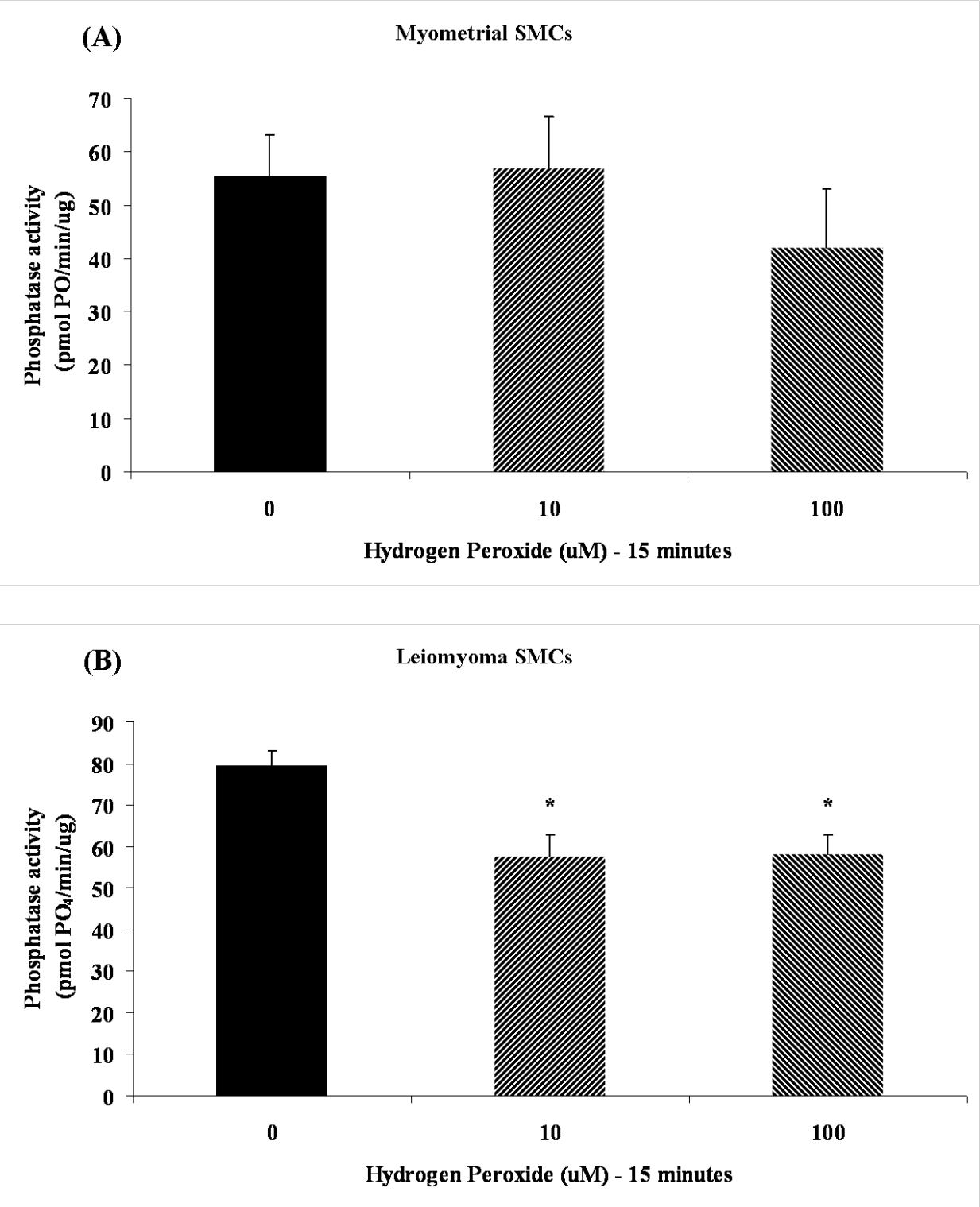


Figure 29. Regulation of protein tyrosine phosphatase activity in leiomyoma and myometrial SMCs. A) myometrial SMCs and B) leiomyoma SMCs were exposed to hydrogen peroxide at 10 and 100 μM for 15 minutes and PTPase activity was measured on cell lysate. Asterisk indicates that treatment is statistically different from untreated control ($p<0.05$).

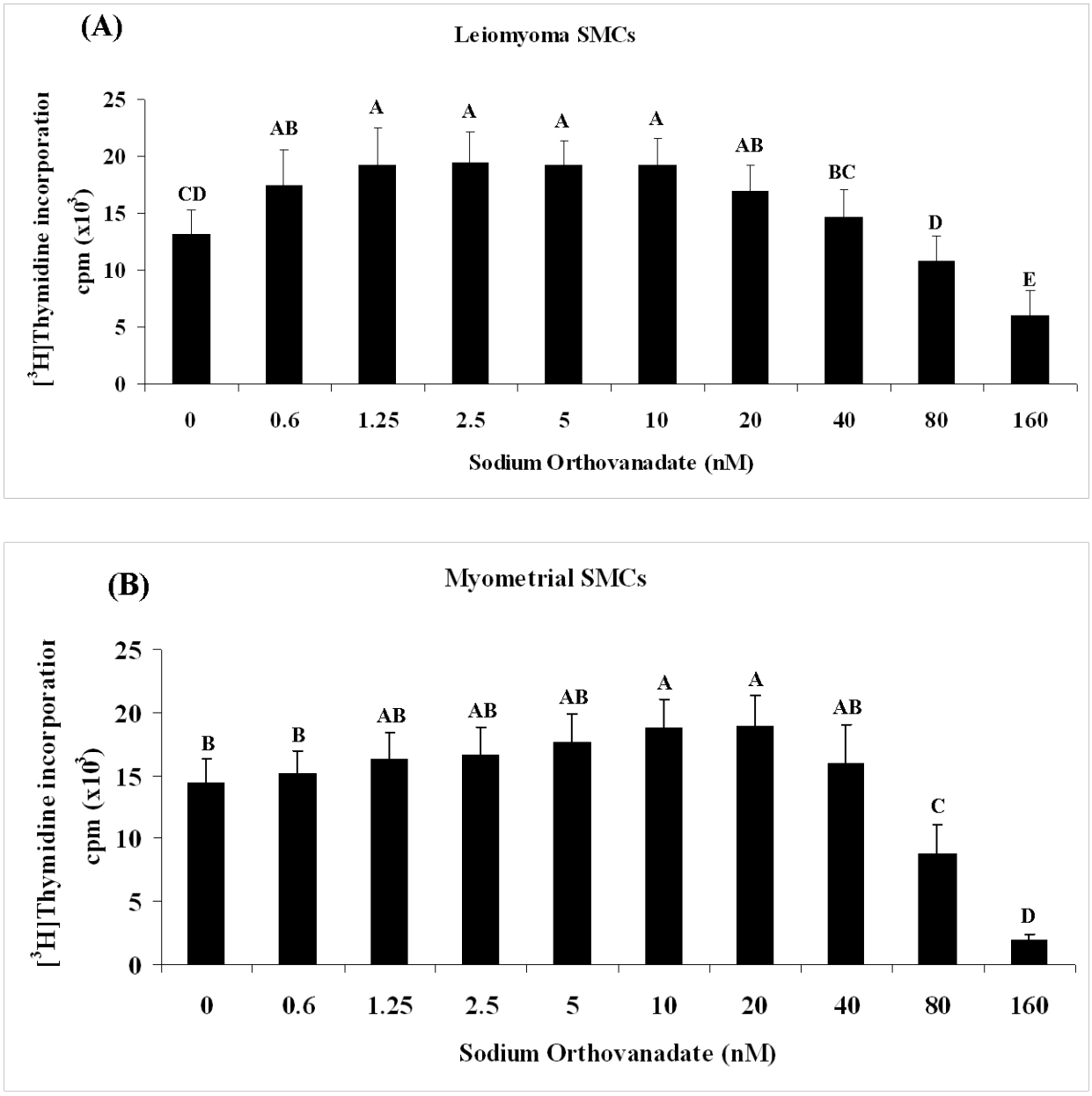


Figure 30. Effects of inhibition of protein tyrosine phosphatase on myometrial and leiomyoma SMCs. A) leiomyoma SMCs and B) myometrial SMCs were expose to different concentrations of sodium orthovanadate for 48 hours and rate of tritiated-thymidine incorporation was measured. Higher counts indicate higher cell proliferation. Different capital letters indicate statistical significance.

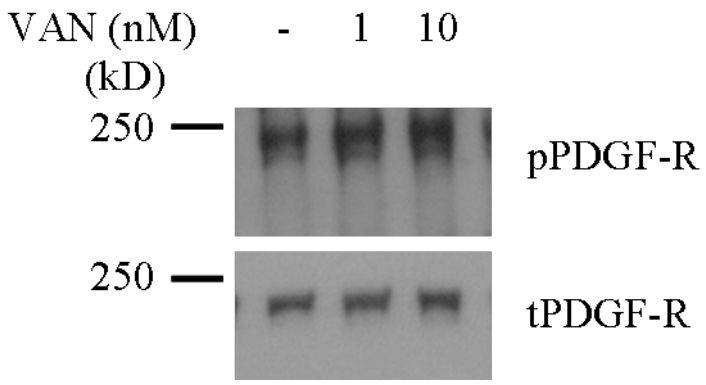


Figure 31. Effects of protein tyrosine phosphatase inhibition on PDGF-R phosphorylation. Immunoblots of phosphorylated PDGF-R (pPDGF-R) and total PDGF-R protein (tPDGF-R - loading control). LSMCs and MSMCs were exposed to 1 and 10 nM of sodium orthovanadate (VAN) for 15 minutes and cell lysate was collected for analysis. This is a representative image of the observed response for both cell types.

# CHAPTER 6

# CONCLUSIONS AND FUTURE DIRECTIONS

Reactive oxygen species (ROS) play a significant role in the development of a variety of chronic and fibrotic disorders such as human uterine leiomyomas. The overall goal of this work was to investigate the mechanisms involved in the production of ROS as well as the role of ROS as regulators of the proliferative pathways triggered by EGF and PDGF in myometrial and leiomyoma SMCs. The main findings of my studies are: 1) LSMCs and MSMCs produce ROS in response to EGF and PDGF; 2) ROS are necessary and sufficient to induce LSMCs and MSMCs proliferation; 3) ROS are necessary and sufficient to induce a significant portion of Erk activation in LSMCs and MSMCs; 4) NADPH oxidase components are expressed in leiomyoma and normal myometrial tissue; 5) PDGF induces translocation of $p47^{phox}$ into lipid rafts in LSMCs; 6) PKC mediates Erk activation by PDGF in MSMCs and LSMCs; 7) PKC alone is sufficient to induce ROS production in MSMCs and LSMCs; 8) hydrogen peroxide inhibits the activity of PTPases in LSMCs; and 9) regulation of PTPase activity is important for myometrial and leiomyoma SMC proliferation. Based on these findings I propose a revised model to illustrate my working hypothesis regarding the role of ROS in the proliferative pathway of PDGF and EGF in LSMCs and MSMCs (Figure 32). I showed that ROS mediate, at least partially, the downstream signaling events of the PDGF and EGF proliferative pathways. PDGF and EGF trigger ROS production by activating the NADPH oxidase complex. Inhibition of ROS reduces the ability of PDGF to induce Erk activation, but it does not influence Erk activation in response to EGF. I hypothesize that ROS are necessary for the EGF proliferative pathway as evidenced by the ability of EGF to induce ROS production, and the decrease in EGF-induced cell proliferation

upon ROS inhibition. However, since this work focused mainly on the involvement of ROS in the activation of the Erk pathway, other pathways triggered by EGF and potentially regulated by ROS in leiomyoma and normal myometrial cells remain to be tested.

Although there was no effect of PDGF treatment on the phosphorylation of the cytosolic NADPH oxidase subunit $p47^{phox}$, the relocation of the subunit into lipid rafts upon exposure to PDGF may well be a significant event in NADPH oxidase complex activation and potentially in the PDGF signaling pathway. My data also suggest that PKC may be the kinase involved in activation of the NADPH oxidase complex leading to ROS production. Additionally, ROS reduce the activity of PTPases in LSMCs, a mechanism that leads to increased proliferation of MSMCs and LSMCs.

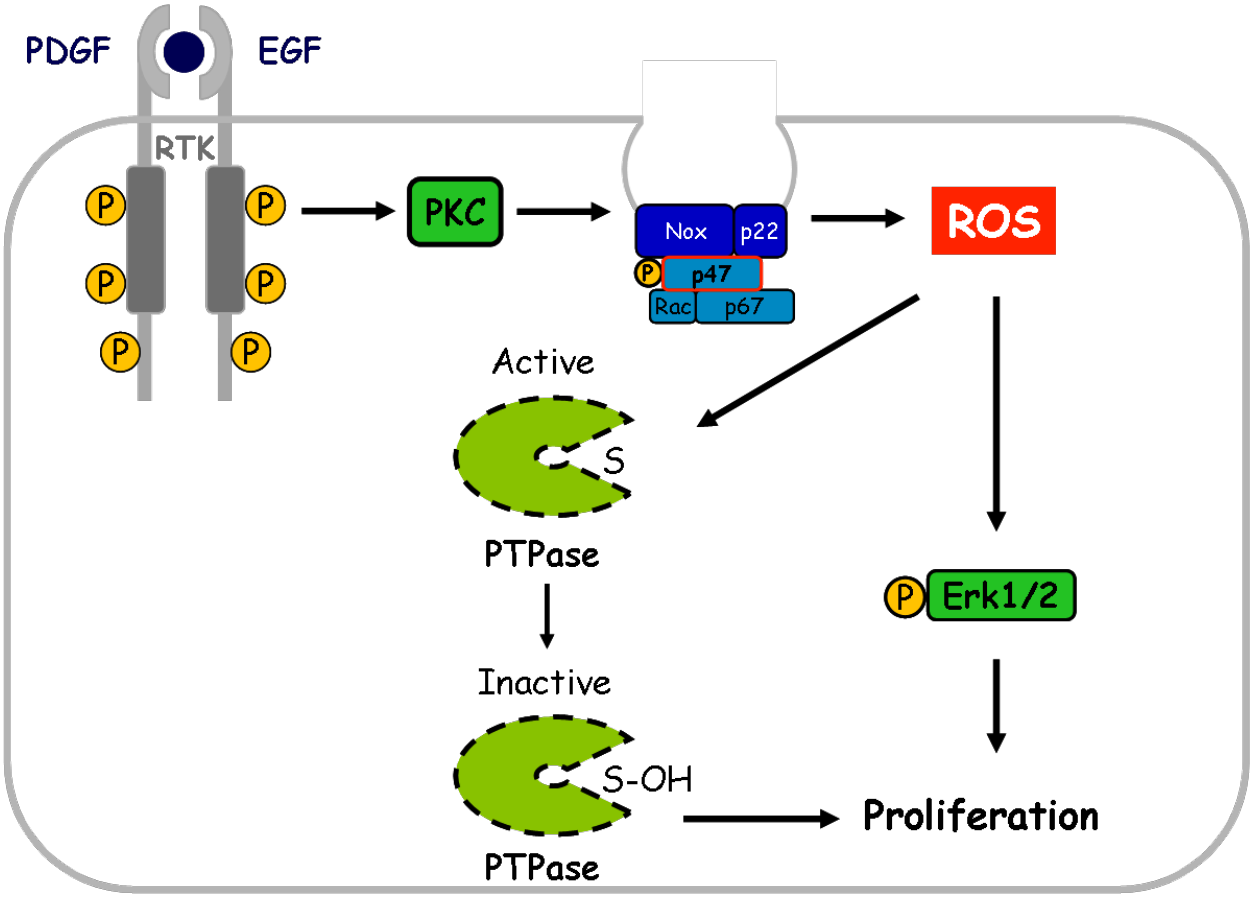


Figure 32 – Revised model illustrating my proposed working hypothesis of how ROS are involved in the proliferative pathway of PDGF in LSMCs and MSMCs.

The results of my studies have added to the increasingly growing body of literature that supports a role for ROS as signaling molecules that regulate proliferative pathways in a variety of cell types. While I focused on the second messenger role of controlled production of ROS, I cannot rule out the possibility that there may be excessive or uncontrolled production of ROS under certain conditions in the myometrium. Such high levels of ROS production may lead to oxidative stress and may potentially be responsible for the initial injury hypothesized to be important for the initiation of leiomyoma tumor development. This initial injury could originate from excessive ROS produced in response to the hypoxic conditions present in the uterus at menstruation. An alternative hypothesis proposes that the mechanism could also be similar to the

pathogenesis of atherosclerosis in which endothelial cells internalize low densisity lipoprotein (LDL) and, upon its accumulation, attract immune cells to phagocytize those cells, causing local release of large amounts of ROS. Increased local production of ROS can drive a phenotypic change in normally quiescent smooth muscle cells, making them myofibroblast-like cells, that are more proliferative and also produce large quantities of collagen. Epidemiological studies show an increased incidence of leiomyoms linked to obesity and hypertension that are associated with higher circulating levels of cholesterol.

Additional significant findings of my studies showed, for the first time, the existence of a fully active and biologically significant NADPH oxidase enzyme system in normal myometrial and leiomyoma SMCs. Second, results also indicated the existence of a subset of leiomyoma tumors, within a group of 10 patients I analyzed, in which several subunit components of the NADPH oxidase complex were upregulated. Third, in vitro experiments suggest that although higher basal levels of PTPase activity were present in LSMCs, these cells also showed a higher sensitivity to hydrogen peroxide and PTPase inhibition compared to MSMCs. Based upon evidence indicating the involvement of excessive ROS production with cell transformation, as well as the fact that numerous cancers are associated with excessive ROS production [146, 185], it is likely that a growth advantage may originate from higher expression of the NADPH oxidase complex. In vitro culture conditions have limitations in the sense that they obviously do not mimic the in vivo environment, thus myometrial and leiomyoma SMCs tend to behave similarly. This situation is a disadvantage because potentially important differences may become subtle, impairing their detection. Whether the basal levels of ROS production are higher in leiomyoma SMCs or in the precursor cells, or whether these cells will respond more robustly to factors such

as PDGF commonly found at higher levels of expression in leiomyoma tumors remains to be determined.

My work in characterizing the importance of NADPH oxidase-derived ROS in the pathogenesis of leiomyomas is certainly just beginning. The data presented in this dissertation suggested a number of new questions that I would like to propose for the continuity of this project:

- What are the mRNA and protein expression levels of proteins that counteract ROS, such as catalase, glutathione, superoxide dismutase 1, thioredoxin and glutaredoxin in normal myometrium versus leiomyoma tissues?
- Does induction of PKC by PMA induce $p47^{phox}$ phosphorylation and translocation into lipid rafts?
- Does disruption of lipid rafts by methyl-β-cyclodextrin, which enhances solubility of cholesterol thus extracting it from cells, affect the ability of leiomyoma or myometrial SMCs to produce ROS in response to PDGF?
- Does the PTPase inhibitor sodium orthovanadate affect the extent of PDGF-R phosphorylation in cells treated with PDGF?
- What specific PTPases are inhibited by ROS in myometrial and leiomyoma SMCs?
    - One potential target of these studies is PTP1B, a PTPase that has been identified as an important regulator of several receptor tyrosine kinase signaling pathways. It would be interesting to study the direct effects of ROS on PTP1B by immunoprecipitating the enzyme and checking its redox state by using an anti-oxidized-PTPase antibody. Another approach would be to knockdown PTPB1

gene expression and test the consequences of lower or absent PTPB1 expression on ROS-induced cellular responses.

- What other targets of ROS action are important for proliferative pathways in myometrial and leiomyoma SMCs?
    - Ras is a small G protein involved in signaling pathways of several receptor tyrosine kinases, and Ras mutations are involved in cell transformation. Ras-transformed cells have increased ROS levels, and furthermore, Ras has a cysteine residue that is regulated by oxidation triggering enhanced nucleotide exchange. One could immunoprecipitate Ras protein from cells exposed to ROS and perform a GTPase activity assay.
- How does an oxidized or reduced intracellular environment affect cell cycle status and global gene expression in myometrial and leiomyoma SMCs?
    - One could manipulate the intracellular environment by either targeting enzymes that scavenge ROS or counteract oxidation (e.g. catalase and thioredoxin), or directly target the NADPH oxidase enzymes. Gene expression knockdown of these enzymatic pathways, or the use of cell permeable enzymes such as catalase and superoxide dismutase could be tested. The latter can be achieved by using enzymes coupled with polyethylene glycol that allow cell permeability. Global gene expression can be measured by microarray analysis either through a whole genome screening or a targeted approach on smaller arrays focusing on specific pathways. Flow cytometry analysis of DNA content can be used to assess effects of the intracellular redox environemtnon cell cycle progression or arrest according to the intracellular redox environment.

In conclusion, leiomyoma and normal myometrial SMCs express a functional NADPH oxidase complex, which is the source of ROS produced in response to PDGF and EGF. NADPH oxidase-derived ROS are necessary for PDGF and EGF-regulated proliferation of both leiomyoma and myometrial SMCs. Although the Erk pathway is at least in part regulated by PDGF-induced ROS production, the EGF-induced ROS might regulate signaling molecules other than Erk involved in its proliferative pathway. Moreover, $p47^{phox}$ translocation into lipid rafts may be an important step in the PDGF signaling pathways, although $p47^{phox}$ phosphorylation is not necessary for PDGF-induced ROS production. I further conclude that PKC activity is necessary for ROS production in response to PDGF, and that ROS regulate protein tyrosine phosphatase activity, which in turn is a negative regulator of leiomyoma and normal myometrial SMCs proliferation. I demonstrated that ROS are necessary components of the PDGF and EGF signaling pathways, and showed to some extent how ROS production is triggered and how ROS act as second messengers to control cell proliferation. My overall findings suggest that a subset of tumors is composed of SMCs that overexpress NADPH oxidase components, and according to the current literature, overexpression of these components is correlated with increased ROS levels. The regulation of PTPases by ROS and the consequent effects on cell proliferation indicate a growth advantage of tumor cells that might explain partially the increased proliferation observed in leiomyoma tumors.

**REFERENCES**


1. Stewart EA, Friedman AJ, Peck K, Nowak RA. Relative overexpression of collagen type I and collagen type III messenger ribonucleic acids by uterine leiomyomas during the proliferative phase of the menstrual cycle. J Clin Endocrinol Metab 1994; 79: 900-906.

2. Walker CL, Stewart EA. Uterine fibroids: the elephant in the room. Science 2005; 308: 1589-1592.

3. Day Baird D, Dunson DB, Hill MC, Cousins D, Schectman JM. High cumulative incidence of uterine leiomyoma in black and white women: ultrasound evidence. Am J Obstet Gynecol 2003; 188: 100-107.

4. Merrill RM. Hysterectomy Surveillance in the United States, 1997 through 2005. Med Sci Monit 2008; 14: CR24-31.

5. Hirst SJ, Twort CH, Lee TH. Differential effects of extracellular matrix proteins on human airway smooth muscle cell proliferation and phenotype. Am J Respir Cell Mol Biol 2000; 23: 335-344.

6. Friedman SL. Molecular regulation of hepatic fibrosis, an integrated cellular response to tissue injury. J Biol Chem 2000; 275: 2247-2250.

7. Zeisberg M, Bonner G, Maeshima Y, Colorado P, Muller GA, Strutz F, Kalluri R. Renal fibrosis: collagen composition and assembly regulates epithelial-mesenchymal transdifferentiation. Am J Pathol 2001; 159: 1313-1321.

8. Gittenberger-de Groot AC, DeRuiter MC, Bergwerff M, Poelmann RE. Smooth muscle cell origin and its relation to heterogeneity in development and disease. Arterioscler Thromb Vasc Biol 1999; 19: 1589-1594.

9. Lambeth JD. Nox enzymes, ROS, and chronic disease: an example of antagonistic pleiotropy. Free Radic Biol Med 2007; 43: 332-347.

10. Arnold RS, Shi J, Murad E, Whalen AM, Sun CQ, Polavarapu R, Parthasarathy S, Petros JA, Lambeth JD. Hydrogen peroxide mediates the cell growth and transformation caused by the mitogenic oxidase Nox1. Proc Natl Acad Sci U S A 2001; 98: 5550-5555.

11. Suh YA, Arnold RS, Lassegue B, Shi J, Xu X, Sorescu D, Chung AB, Griendling KK, Lambeth JD. Cell transformation by the superoxide-generating oxidase Mox1. Nature 1999; 401: 79-82.

12. Deng X, Gao F, May WS, Jr. Bcl2 retards G1/S cell cycle transition by regulating intracellular ROS. Blood 2003; 102: 3179-3185.

13. Menon SG, Sarsour EH, Spitz DR, Higashikubo R, Sturm M, Zhang H, Goswami PC. Redox regulation of the G1 to S phase transition in the mouse embryo fibroblast cell cycle. Cancer Res 2003; 63: 2109-2117.

14. Rhee SG, Bae YS, Lee SR, Kwon J. Hydrogen peroxide: a key messenger that modulates protein phosphorylation through cysteine oxidation. Sci STKE 2000; 2000: pe1.

15. Tonks NK. Redox redux: revisiting PTPs and the control of cell signaling. Cell 2005; 121: 667-670.

16. Savitsky PA, Finkel T. Redox regulation of Cdc25C. J Biol Chem 2002; 277: 20535-20540.

17. Sundaresan M, Yu ZX, Ferrans VJ, Irani K, Finkel T. Requirement for generation of H2O2 for platelet-derived growth factor signal transduction. Science 1995; 270: 296-299.

18. Lee SR, Kwon KS, Kim SR, Rhee SG. Reversible inactivation of protein-tyrosine phosphatase 1B in A431 cells stimulated with epidermal growth factor. J Biol Chem 1998; 273: 15366-15372.

19. Kappert K, Sparwel J, Sandin A, Seiler A, Siebolts U, Leppanen O, Rosenkranz S, Ostman A. Antioxidants relieve phosphatase inhibition and reduce PDGF signaling in cultured VSMCs and in restenosis. Arterioscler Thromb Vasc Biol 2006; 26: 2644-2651.

20. Seo JH, Ahn Y, Lee SR, Yeol Yeo C, Chung Hur K. The major target of the endogenously generated reactive oxygen species in response to insulin stimulation is phosphatase and tensin homolog and not phosphoinositide-3 kinase (PI-3 kinase) in the PI-3 kinase/Akt pathway. Mol Biol Cell 2005; 16: 348-357.

21. Kanda M, Ihara Y, Murata H, Urata Y, Kono T, Yodoi J, Seto S, Yano K, Kondo T. Glutaredoxin modulates platelet-derived growth factor-dependent cell signaling by regulating the redox status of low molecular weight protein-tyrosine phosphatase. J Biol Chem 2006; 281: 28518-28528.

22. Chiarugi P, Fiaschi T, Taddei ML, Talini D, Giannoni E, Raugei G, Ramponi G. Two vicinal cysteines confer a peculiar redox regulation to low molecular weight protein tyrosine phosphatase in response to platelet-derived growth factor receptor stimulation. J Biol Chem 2001; 276: 33478-33487.

23. Noden DM. The control of avian cephalic neural crest cytodifferentiation. I. Skeletal and connective tissues. Dev Biol 1978; 67: 296-312.

24. Konishi I, Fujii S, Okamura H, Mori T. Development of smooth muscle in the human fetal uterus: an ultrastructural study. J Anat 1984; 139: 239-252.

25. Brody JR, Cunha GR. Histologic, morphometric, and immunocytochemical analysis of myometrial development in rats and mice: I. Normal development. Am J Anat 1989; 186: 1-20.

26. Cunha GR, Young P, Brody JR. Role of uterine epithelium in the development of myometrial smooth muscle cells. Biol Reprod 1989; 40: 861-871.

27. Ono M, Maruyama T, Masuda H, Kajitani T, Nagashima T, Arase T, Ito M, Ohta K, Uchida H, Asada H, Yoshimura Y, Okano H, Matsuzaki Y. Side population in human uterine myometrium displays phenotypic and functional characteristics of myometrial stem cells. Proc Natl Acad Sci U S A 2007; 104: 18700-18705.

28. Kumar MS, Owens GK. Combinatorial control of smooth muscle-specific gene expression. Arterioscler Thromb Vasc Biol 2003; 23: 737-747.

29. Wang D, Chang PS, Wang Z, Sutherland L, Richardson JA, Small E, Krieg PA, Olson EN. Activation of cardiac gene expression by myocardin, a transcriptional cofactor for serum response factor. Cell 2001; 105: 851-862.

30. McDonald OG, Owens GK. Programming smooth muscle plasticity with chromatin dynamics. Circ Res 2007; 100: 1428-1441.

31. Kawaguchi K, Fujii S, Konishi I, Nanbu Y, Nonogaki H, Mori T. Mitotic activity in uterine leiomyomas during the menstrual cycle. Am J Obstet Gynecol 1989; 160: 637-641.

32. Stewart EA. Uterine fibroids. Lancet 2001; 357: 293-298.

33. Leppert PC, Baginski T, Prupas C, Catherino WH, Pletcher S, Segars JH. Comparative ultrastructure of collagen fibrils in uterine leiomyomas and normal myometrium. Fertil Steril 2004; 82 Suppl 3: 1182-1187.

34. Benda JA. Pathology of smooth muscle tumors of the uterine corpus. Clin Obstet Gynecol 2001; 44: 350-363.

35. Lee DW, Gibson TB, Carls GS, Ozminkowski RJ, Wang S, Stewart EA. Uterine fibroid treatment patterns in a population of insured women. Fertil Steril 2009; 91: 566-574.

36. Hassan MH, Khatoon N, Curiel DT, Hamada FM, Arafa HM, Al-Hendy A. Toward gene therapy of uterine fibroids: targeting modified adenovirus to human leiomyoma cells. Hum Reprod 2008; 23: 514-524.

37. Hassan MH, Salama SA, Zhang D, Arafa HM, Hamada FM, Fouad H, Walker CC, Al-Hendy A. Gene therapy targeting leiomyoma: adenovirus-mediated delivery of dominant-negative estrogen receptor gene shrinks uterine tumors in Eker rat model. Fertil Steril 2009.

38. Faerstein E, Szklo M, Rosenshein N. Risk factors for uterine leiomyoma: a practice-based case-control study. I. African-American heritage, reproductive history, body size, and smoking. Am J Epidemiol 2001; 153: 1-10.

39. Huyck KL, Panhuysen CI, Cuenco KT, Zhang J, Goldhammer H, Jones ES, Somasundaram P, Lynch AM, Harlow BL, Lee H, Stewart EA, Morton CC. The impact of race as a risk factor for symptom severity and age at diagnosis of uterine leiomyomata among affected sisters. Am J Obstet Gynecol 2008; 198: 168 e161-169.

40. Faerstein E, Szklo M, Rosenshein NB. Risk factors for uterine leiomyoma: a practice-based case-control study. II. Atherogenic risk factors and potential sources of uterine irritation. Am J Epidemiol 2001; 153: 11-19.

41. Snieder H, MacGregor AJ, Spector TD. Genes control the cessation of a woman's reproductive life: a twin study of hysterectomy and age at menopause. J Clin Endocrinol Metab 1998; 83: 1875-1880.

42. Flake GP, Andersen J, Dixon D. Etiology and pathogenesis of uterine leiomyomas: a review. Environ Health Perspect 2003; 111: 1037-1054.

43. Townsend DE, Sparkes RS, Baluda MC, McClelland G. Unicellular histogenesis of uterine leiomyomas as determined by electrophoresis by glucose-6-phosphate dehydrogenase. Am J Obstet Gynecol 1970; 107: 1168-1173.

44. Hashimoto K, Azuma C, Kamiura S, Kimura T, Nobunaga T, Kanai T, Sawada M, Noguchi S, Saji F. Clonal determination of uterine leiomyomas by analyzing differential inactivation of the X-chromosome-linked phosphoglycerokinase gene. Gynecol Obstet Invest 1995; 40: 204-208.

45. Kiuru M, Launonen V, Hietala M, Aittomaki K, Vierimaa O, Salovaara R, Arola J, Pukkala E, Sistonen P, Herva R, Aaltonen LA. Familial cutaneous leiomyomatosis is a two-hit condition associated with renal cell cancer of characteristic histopathology. Am J Pathol 2001; 159: 825-829.

46. Reed WB, Walker R, Horowitz R. Cutaneous leiomyomata with uterine leiomyomata. Acta Derm Venereol 1973; 53: 409-416.

47. Hodge JC, K TC, Huyck KL, Somasundaram P, Panhuysen CI, Stewart EA, Morton CC. Uterine leiomyomata and decreased height: a common HMGA2 predisposition allele. Hum Genet 2009; 125: 257-263.

48. Rein MS, Friedman AJ, Barbieri RL, Pavelka K, Fletcher JA, Morton CC. Cytogenetic abnormalities in uterine leiomyomata. Obstet Gynecol 1991; 77: 923-926.

49. Mark J, Havel G, Grepp C, Dahlenfors R, Wedell B. Cytogenetical observations in human benign uterine leiomyomas. Anticancer Res 1988; 8: 621-626.

50. Meloni AM, Surti U, Contento AM, Davare J, Sandberg AA. Uterine leiomyomas: cytogenetic and histologic profile. Obstet Gynecol 1992; 80: 209-217.

51. Stewart EA, Morton CC. The genetics of uterine leiomyomata: what clinicians need to know. Obstet Gynecol 2006; 107: 917-921.

52. Al-Hendy A, Salama SA. Ethnic distribution of estrogen receptor-alpha polymorphism is associated with a higher prevalence of uterine leiomyomas in black Americans. Fertil Steril 2006; 86: 686-693.

53. Amant F, Dorfling CM, de Brabanter J, Vandewalle J, Vergote I, Lindeque BG, van Rensburg EJ. A possible role of the cytochrome P450c17alpha gene (CYP17) polymorphism in the pathobiology of uterine leiomyomas from black South African women: a pilot study. Acta Obstet Gynecol Scand 2004; 83: 234-239.

54. Maruo T, Matsuo H, Samoto T, Shimomura Y, Kurachi O, Gao Z, Wang Y, Spitz IM, Johansson E. Effects of progesterone on uterine leiomyoma growth and apoptosis. Steroids 2000; 65: 585-592.

55. Brandon DD, Bethea CL, Strawn EY, Novy MJ, Burry KA, Harrington MS, Erickson TE, Warner C, Keenan EJ, Clinton GM. Progesterone receptor messenger ribonucleic acid and protein are overexpressed in human uterine leiomyomas. Am J Obstet Gynecol 1993; 169: 78-85.

56. Benassayag C, Leroy MJ, Rigourd V, Robert B, Honore JC, Mignot TM, Vacher-Lavenu MC, Chapron C, Ferre F. Estrogen receptors (ERalpha/ERbeta) in normal and pathological growth of the human myometrium: pregnancy and leiomyoma. Am J Physiol 1999; 276: E1112-1118.

57. Kovacs KA, Oszter A, Gocze PM, Kornyei JL, Szabo I. Comparative analysis of cyclin D1 and oestrogen receptor (alpha and beta) levels in human leiomyoma and adjacent myometrium. Mol Hum Reprod 2001; 7: 1085-1091.

58. Viville B, Charnock-Jones DS, Sharkey AM, Wetzka B, Smith SK. Distribution of the A and B forms of the progesterone receptor messenger ribonucleic acid and protein in uterine leiomyomata and adjacent myometrium. Hum Reprod 1997; 12: 815-822.

59. Chegini N, Ma C, Tang XM, Williams RS. Effects of GnRH analogues, 'add-back' steroid therapy, antiestrogen and antiprogestins on leiomyoma and myometrial smooth muscle cell growth and transforming growth factor-beta expression. Mol Hum Reprod 2002; 8: 1071-1078.

60. Barbarisi A, Petillo O, Di Lieto A, Melone MA, Margarucci S, Cannas M, Peluso G. 17-beta estradiol elicits an autocrine leiomyoma cell proliferation: evidence for a stimulation of protein kinase-dependent pathway. J Cell Physiol 2001; 186: 414-424.

61. Sumitani H, Shozu M, Segawa T, Murakami K, Yang HJ, Shimada K, Inoue M. In situ estrogen synthesized by aromatase P450 in uterine leiomyoma cells promotes cell growth probably via an autocrine/intracrine mechanism. Endocrinology 2000; 141: 3852-3861.

62. Bulun SE, Simpson ER, Word RA. Expression of the CYP19 gene and its product aromatase cytochrome P450 in human uterine leiomyoma tissues and cells in culture. J Clin Endocrinol Metab 1994; 78: 736-743.

63. Mizutani T, Sugihara A, Nakamuro K, Terada N. Suppression of cell proliferation and induction of apoptosis in uterine leiomyoma by gonadotropin-releasing hormone agonist (leuprolide acetate). J Clin Endocrinol Metab 1998; 83: 1253-1255.

64. Felberbaum RE, Germer U, Ludwig M, Riethmuller-Winzen H, Heise S, Buttge I, Bauer O, Reissmann T, Engel J, Diedrich K. Treatment of uterine fibroids with a slow-release formulation of the gonadotrophin releasing hormone antagonist Cetrorelix. Hum Reprod 1998; 13: 1660-1668.

65. Hermon TL, Moore AB, Yu L, Kissling GE, Castora FJ, Dixon D. Estrogen receptor alpha (ERalpha) phospho-serine-118 is highly expressed in human uterine leiomyomas compared to matched myometrium. Virchows Arch 2008; 453: 557-569.

66. Di Lieto A, De Rosa G, De Falco M, Iannotti F, Staibano S, Pollio F, Scaramellino M, Salvatore G. Relationship between platelet-derived growth factor expression in leiomyomas and uterine volume changes after gonadotropin-releasing hormone agonist treatment. Hum Pathol 2002; 33: 220-224.

67. Swartz CD, Afshari CA, Yu L, Hall KE, Dixon D. Estrogen-induced changes in IGF-I, Myb family and MAP kinase pathway genes in human uterine leiomyoma and normal uterine smooth muscle cell lines. Mol Hum Reprod 2005; 11: 441-450.

68. Wang J, Ohara N, Takekida S, Xu Q, Maruo T. Comparative effects of heparin-binding epidermal growth factor-like growth factor on the growth of cultured human uterine leiomyoma cells and myometrial cells. Hum Reprod 2005; 20: 1456-1465.

69. Anania CA, Stewart EA, Quade BJ, Hill JA, Nowak RA. Expression of the fibroblast growth factor receptor in women with leiomyomas and abnormal uterine bleeding. Mol Hum Reprod 1997; 3: 685-691.

70. Mangrulkar RS, Ono M, Ishikawa M, Takashima S, Klagsbrun M, Nowak RA. Isolation and characterization of heparin-binding growth factors in human leiomyomas and normal myometrium. Biol Reprod 1995; 53: 636-646.

71. Di Lieto A, De Falco M, Mansueto G, De Rosa G, Pollio F, Staibano S. Preoperative administration of GnRH-a plus tibolone to premenopausal women with uterine fibroids: evaluation of the clinical response, the immunohistochemical expression of PDGF, bFGF and VEGF and the vascular pattern. Steroids 2005; 70: 95-102.

72. Maruo T, Ohara N, Wang J, Matsuo H. Sex steroidal regulation of uterine leiomyoma growth and apoptosis. Hum Reprod Update 2004; 10: 207-220.

73. Lumsden MA, West CP, Bramley T, Rumgay L, Baird DT. The binding of epidermal growth factor to the human uterus and leiomyomata in women rendered hypo-oestrogenic by continuous administration of an LHRH agonist. Br J Obstet Gynaecol 1988; 95: 1299-1304.

74. Rossi MJ, Chegini N, Masterson BJ. Presence of epidermal growth factor, platelet-derived growth factor, and their receptors in human myometrial tissue and smooth muscle cells: their action in smooth muscle cells in vitro. Endocrinology 1992; 130: 1716-1727.

75. Taniguchi Y, Morita I, Kubota T, Murota S, Aso T. Human uterine myometrial smooth muscle cell proliferation and vascular endothelial growth-factor production in response to platelet-derived growth factor. J Endocrinol 2001; 169: 79-86.

76. Sampath D, Zhu Y, Winneker RC, Zhang Z. Aberrant expression of Cyr61, a member of the CCN (CTGF/Cyr61/Cef10/NOVH) family, and dysregulation by 17 beta-estradiol and basic fibroblast growth factor in human uterine leiomyomas. J Clin Endocrinol Metab 2001; 86: 1707-1715.

77. Strawn EY, Jr., Novy MJ, Burry KA, Bethea CL. Insulin-like growth factor I promotes leiomyoma cell growth in vitro. Am J Obstet Gynecol 1995; 172: 1837-1843; discussion 1843-1834.

78. Gao Z, Matsuo H, Wang Y, Nakago S, Maruo T. Up-regulation by IGF-I of proliferating cell nuclear antigen and Bcl-2 protein expression in human uterine leiomyoma cells. J Clin Endocrinol Metab 2001; 86: 5593-5599.

79. Yu L, Saile K, Swartz CD, He H, Zheng X, Kissling GE, Di X, Lucas S, Robboy SJ, Dixon D. Differential expression of receptor tyrosine kinases (RTKs) and IGF-I pathway activation in human uterine leiomyomas. Mol Med 2008; 14: 264-275.

80. Chegini N, Tang XM, Ma C. Regulation of transforming growth factor-beta1 expression by granulocyte macrophage-colony-stimulating factor in leiomyoma and myometrial smooth muscle cells. J Clin Endocrinol Metab 1999; 84: 4138-4143.

81. Arici A, Sozen I. Expression, menstrual cycle-dependent activation, and bimodal mitogenic effect of transforming growth factor-beta1 in human myometrium and leiomyoma. Am J Obstet Gynecol 2003; 188: 76-83.

82. Lee BS, Nowak RA. Human leiomyoma smooth muscle cells show increased expression of transforming growth factor-beta 3 (TGF beta 3) and altered responses to the antiproliferative effects of TGF beta. J Clin Endocrinol Metab 2001; 86: 913-920.

83. Dou Q, Zhao Y, Tarnuzzer RW, Rong H, Williams RS, Schultz GS, Chegini N. Suppression of transforming growth factor-beta (TGF beta) and TGF beta receptor messenger ribonucleic acid and protein expression in leiomyomata in women receiving gonadotropin-releasing hormone agonist therapy. J Clin Endocrinol Metab 1996; 81: 3222-3230.

84. Arici A, Sozen I. Transforming growth factor-beta3 is expressed at high levels in leiomyoma where it stimulates fibronectin expression and cell proliferation. Fertil Steril 2000; 73: 1006-1011.

85. Dou Q, Tarnuzzer RW, Williams RS, Schultz GS, Chegini N. Differential expression of matrix metalloproteinases and their tissue inhibitors in leiomyomata: a mechanism for gonadotrophin releasing hormone agonist-induced tumour regression. Mol Hum Reprod 1997; 3: 1005-1014.

86. Wolanska M, Sobolewski K, Drozdzewicz M. [Glycosaminoglycans in uterine leiomyoma]. Ginekol Pol 1998; 69: 12-16.

87. Boynton-Jarrett R, Rich-Edwards J, Malspeis S, Missmer SA, Wright R. A prospective study of hypertension and risk of uterine leiomyomata. Am J Epidemiol 2005; 161: 628-638.

88. Baroni GS, D'Ambrosio L, Curto P, Casini A, Mancini R, Jezequel AM, Benedetti A. Interferon gamma decreases hepatic stellate cell activation and extracellular matrix deposition in rat liver fibrosis. Hepatology 1996; 23: 1189-1199.

89. Lu G, Greene EL, Nagai T, Egan BM. Reactive oxygen species are critical in the oleic acid-mediated mitogenic signaling pathway in vascular smooth muscle cells. Hypertension 1998; 32: 1003-1010.

90. Lu G, Meier KE, Jaffa AA, Rosenzweig SA, Egan BM. Oleic acid and angiotensin II induce a synergistic mitogenic response in vascular smooth muscle cells. Hypertension 1998; 31: 978-985.

91. Weber DS, Taniyama Y, Rocic P, Seshiah PN, Dechert MA, Gerthoffer WT, Griendling KK. Phosphoinositide-dependent kinase 1 and p21-activated protein kinase mediate reactive oxygen species-dependent regulation of platelet-derived growth factor-induced smooth muscle cell migration. Circ Res 2004; 94: 1219-1226.

92. Greene EL, Lu G, Zhang D, Egan BM. Signaling events mediating the additive effects of oleic acid and angiotensin II on vascular smooth muscle cell migration. Hypertension 2001; 37: 308-312.

93. Grewal JS, Mukhin YV, Garnovskaya MN, Raymond JR, Greene EL. Serotonin 5-HT2A receptor induces TGF-beta1 expression in mesangial cells via ERK: proliferative and fibrotic signals. Am J Physiol 1999; 276: F922-930.

94. Ushio-Fukai M, Alexander RW, Akers M, Griendling KK. p38 Mitogen-activated protein kinase is a critical component of the redox-sensitive signaling pathways activated by angiotensin II. Role in vascular smooth muscle cell hypertrophy. J Biol Chem 1998; 273: 15022-15029.

95. Isobe A, Takeda T, Sakata M, Miyake A, Yamamoto T, Minekawa R, Nishimoto F, Oskamoto Y, Walker CL, Kimura T. Dual repressive effect of angiotensin II-type 1 receptor blocker telmisartan on angiotensin II-induced and estradiol-induced uterine leiomyoma cell proliferation. Hum Reprod 2008; 23: 440-446.

96. Pan Q, Chegini N. MicroRNA signature and regulatory functions in the endometrium during normal and disease states. Semin Reprod Med 2008; 26: 479-493.

97. Collins R, Winkleby MA. African American women and men at high and low risk for hypertension: a signal detection analysis of NHANES III, 1988-1994. Prev Med 2002; 35: 303-312.

98. Takahashi T, Taniguchi T, Okuda M, Takahashi A, Kawasaki S, Domoto K, Taguchi M, Ishikawa Y, Yokoyama M. Participation of reactive oxygen intermediates in the angiotensin II-activated signaling pathways in vascular smooth muscle cells. Ann N Y Acad Sci 2000; 902: 283-287.

99. Lee SL, Wang WW, Finlay GA, Fanburg BL. Serotonin stimulates mitogen-activated protein kinase activity through the formation of superoxide anion. Am J Physiol 1999; 277: L282-291.

100. Rajagopalan S, Kurz S, Munzel T, Tarpey M, Freeman BA, Griendling KK, Harrison DG. Angiotensin II-mediated hypertension in the rat increases vascular superoxide production via membrane NADH/NADPH oxidase activation. Contribution to alterations of vasomotor tone. J Clin Invest 1996; 97: 1916-1923.

101. Ross R. Cell biology of atherosclerosis. Annu Rev Physiol 1995; 57: 791-804.

102. Shanahan CM, Weissberg PL. Smooth muscle cell heterogeneity: patterns of gene expression in vascular smooth muscle cells in vitro and in vivo. Arterioscler Thromb Vasc Biol 1998; 18: 333-338.

103. Morla AO, Mogford JE. Control of smooth muscle cell proliferation and phenotype by integrin signaling through focal adhesion kinase. Biochem Biophys Res Commun 2000; 272: 298-302.

104. Blindt R, Krott N, Hanrath P, vom Dahl J, van Eys G, Bosserhoff AK. Expression patterns of integrins on quiescent and invasive smooth muscle cells and impact on cell locomotion. J Mol Cell Cardiol 2002; 34: 1633-1644.

105. Patterson C, Ruef J, Madamanchi NR, Barry-Lane P, Hu Z, Horaist C, Ballinger CA, Brasier AR, Bode C, Runge MS. Stimulation of a vascular smooth muscle cell NAD(P)H oxidase by thrombin. Evidence that p47(phox) may participate in forming this oxidase in vitro and in vivo. J Biol Chem 1999; 274: 19814-19822.

106. Ushio-Fukai M, Tang Y, Fukai T, Dikalov SI, Ma Y, Fujimoto M, Quinn MT, Pagano PJ, Johnson C, Alexander RW. Novel role of gp91(phox)-containing NAD(P)H oxidase in vascular endothelial growth factor-induced signaling and angiogenesis. Circ Res 2002; 91: 1160-1167.

107. Greene EL, Houghton O, Collinsworth G, Garnovskaya MN, Nagai T, Sajjad T, Bheemanathini V, Grewal JS, Paul RV, Raymond JR. 5-HT(2A) receptors stimulate mitogen-activated protein kinase via H(2)O(2) generation in rat renal mesangial cells. Am J Physiol Renal Physiol 2000; 278: F650-658.

108. Greene EL, Velarde V, Jaffa AA. Role of reactive oxygen species in bradykinin-induced mitogen-activated protein kinase and c-fos induction in vascular cells. Hypertension 2000; 35: 942-947.

109. Touyz RM, Chen X, Tabet F, Yao G, He G, Quinn MT, Pagano PJ, Schiffrin EL. Expression of a functionally active gp91phox-containing neutrophil-type NAD(P)H oxidase in smooth muscle cells from human resistance arteries: regulation by angiotensin II. Circ Res 2002; 90: 1205-1213.

110. Touyz RM, Cruzado M, Tabet F, Yao G, Salomon S, Schiffrin EL. Redox-dependent MAP kinase signaling by Ang II in vascular smooth muscle cells: role of receptor tyrosine kinase transactivation. Can J Physiol Pharmacol 2003; 81: 159-167.

111. Touyz RM, Tabet F, Schiffrin EL. Redox-dependent signalling by angiotensin II and vascular remodelling in hypertension. Clin Exp Pharmacol Physiol 2003; 30: 860-866.

112. Svegliati S, Cancello R, Sambo P, Luchetti M, Paroncini P, Orlandini G, Discepoli G, Paterno R, Santillo M, Cuozzo C, Cassano S, Avvedimento EV, Gabrielli A. Platelet-derived growth factor and reactive oxygen species (ROS) regulate Ras protein levels in primary human fibroblasts via ERK1/2. Amplification of ROS and Ras in systemic sclerosis fibroblasts. J Biol Chem 2005; 280: 36474-36482.

113. Catarzi S, Biagioni C, Giannoni E, Favilli F, Marcucci T, Iantomasi T, Vincenzini MT. Redox regulation of platelet-derived-growth-factor-receptor: role of NADPH-oxidase and c-Src tyrosine kinase. Biochim Biophys Acta 2005; 1745: 166-175.

114. Zhang J, Jin N, Liu Y, Rhoades RA. Hydrogen peroxide stimulates extracellular signal-regulated protein kinases in pulmonary arterial smooth muscle cells. Am J Respir Cell Mol Biol 1998; 19: 324-332.

115. Bae YS, Kang SW, Seo MS, Baines IC, Tekle E, Chock PB, Rhee SG. Epidermal growth factor (EGF)-induced generation of hydrogen peroxide. Role in EGF receptor-mediated tyrosine phosphorylation. J Biol Chem 1997; 272: 217-221.

116. Lo YY, Wong JM, Cruz TF. Reactive oxygen species mediate cytokine activation of c-Jun NH2-terminal kinases. J Biol Chem 1996; 271: 15703-15707.

117. Fan J, Frey RS, Rahman A, Malik AB. Role of neutrophil NADPH oxidase in the mechanism of tumor necrosis factor-alpha -induced NF-kappa B activation and intercellular adhesion molecule-1 expression in endothelial cells. J Biol Chem 2002; 277: 3404-3411.

118. Seshiah PN, Weber DS, Rocic P, Valppu L, Taniyama Y, Griendling KK. Angiotensin II stimulation of NAD(P)H oxidase activity: upstream mediators. Circ Res 2002; 91: 406-413.

119. Colavitti R, Pani G, Bedogni B, Anzevino R, Borrello S, Waltenberger J, Galeotti T. Reactive oxygen species as downstream mediators of angiogenic signaling by vascular endothelial growth factor receptor-2/KDR. J Biol Chem 2002; 277: 3101-3108.

120. Baroni SS, Santillo M, Bevilacqua F, Luchetti M, Spadoni T, Mancini M, Fraticelli P, Sambo P, Funaro A, Kazlauskas A, Avvedimento EV, Gabrielli A. Stimulatory autoantibodies to the PDGF receptor in systemic sclerosis. N Engl J Med 2006; 354: 2667-2676.

121. Mitsushita J, Lambeth JD, Kamata T. The superoxide-generating oxidase Nox1 is functionally required for Ras oncogene transformation. Cancer Res 2004; 64: 3580-3585.

122. Lassegue B, Sorescu D, Szocs K, Yin Q, Akers M, Zhang Y, Grant SL, Lambeth JD, Griendling KK. Novel gp91(phox) homologues in vascular smooth muscle cells : nox1 mediates angiotensin II-induced superoxide formation and redox-sensitive signaling pathways. Circ Res 2001; 88: 888-894.

123. Fan C, Katsuyama M, Nishinaka T, Yabe-Nishimura C. Transactivation of the EGF receptor and a PI3 kinase-ATF-1 pathway is involved in the upregulation of NOX1, a catalytic subunit of NADPH oxidase. FEBS Lett 2005; 579: 1301-1305.

124. Wendt MC, Daiber A, Kleschyov AL, Mulsch A, Sydow K, Schulz E, Chen K, Keaney JF, Jr., Lassegue B, Walter U, Griendling KK, Munzel T. Differential effects of diabetes on the expression of the gp91phox homologues nox1 and nox4. Free Radic Biol Med 2005; 39: 381-391.

125. Torres M, Forman HJ. Vanadate inhibition of protein tyrosine phosphatases mimics hydrogen peroxide in the activation of the ERK pathway in alveolar macrophages. Ann N Y Acad Sci 2002; 973: 345-348.

126. Lambeth JD, Krause KH, Clark RA. NOX enzymes as novel targets for drug development. Semin Immunopathol 2008; 30: 339-363.

127. Chanock SJ, el Benna J, Smith RM, Babior BM. The respiratory burst oxidase. J Biol Chem 1994; 269: 24519-24522.

128. Matute JD, Arias AA, Dinauer MC, Patino PJ. p40phox: the last NADPH oxidase subunit. Blood Cells Mol Dis 2005; 35: 291-302.

129. Ago T, Nunoi H, Ito T, Sumimoto H. Mechanism for phosphorylation-induced activation of the phagocyte NADPH oxidase protein p47(phox). Triple replacement of serines 303, 304, and 328 with aspartates disrupts the SH3 domain-mediated intramolecular interaction in p47(phox), thereby activating the oxidase. J Biol Chem 1999; 274: 33644-33653.

130. Bokoch GM, Diebold BA. Current molecular models for NADPH oxidase regulation by Rac GTPase. Blood 2002; 100: 2692-2696.

131. Frey RS, Rahman A, Kefer JC, Minshall RD, Malik AB. PKCzeta regulates TNF-alpha-induced activation of NADPH oxidase in endothelial cells. Circ Res 2002; 90: 1012-1019.

132. Quinn MT, Evans T, Loetterle LR, Jesaitis AJ, Bokoch GM. Translocation of Rac correlates with NADPH oxidase activation. Evidence for equimolar translocation of oxidase components. J Biol Chem 1993; 268: 20983-20987.

133. Ozaki M, Deshpande SS, Angkeow P, Bellan J, Lowenstein CJ, Dinauer MC, Goldschmidt-Clermont PJ, Irani K. Inhibition of the Rac1 GTPase protects against nonlethal ischemia/reperfusion-induced necrosis and apoptosis in vivo. Faseb J 2000; 14: 418-429.

134. Li JM, Shah AM. Intracellular localization and preassembly of the NADPH oxidase complex in cultured endothelial cells. J Biol Chem 2002; 277: 19952-19960.

135. Cheng G, Lambeth JD. Alternative mRNA splice forms of NOXO1: differential tissue expression and regulation of Nox1 and Nox3. Gene 2005; 356: 118-126.

136. Lambeth JD. Nox/Duox family of nicotinamide adenine dinucleotide (phosphate) oxidases. Curr Opin Hematol 2002; 9: 11-17.

137. Cheng G, Cao Z, Xu X, van Meir EG, Lambeth JD. Homologs of gp91phox: cloning and tissue expression of Nox3, Nox4, and Nox5. Gene 2001; 269: 131-140.

138. De Deken X, Wang D, Many MC, Costagliola S, Libert F, Vassart G, Dumont JE, Miot F. Cloning of two human thyroid cDNAs encoding new members of the NADPH oxidase family. J Biol Chem 2000; 275: 23227-23233.

139. Dupuy C, Ohayon R, Valent A, Noel-Hudson MS, Deme D, Virion A. Purification of a novel flavoprotein involved in the thyroid NADPH oxidase. Cloning of the porcine and human cdnas. J Biol Chem 1999; 274: 37265-37269.

140. Geiszt M, Kopp JB, Varnai P, Leto TL. Identification of renox, an NAD(P)H oxidase in kidney. Proc Natl Acad Sci U S A 2000; 97: 8010-8014.

141. Geiszt M, Lekstrom K, Witta J, Leto TL. Proteins homologous to p47phox and p67phox support superoxide production by NAD(P)H oxidase 1 in colon epithelial cells. J Biol Chem 2003; 278: 20006-20012.

142. Takeya R, Ueno N, Kami K, Taura M, Kohjima M, Izaki T, Nunoi H, Sumimoto H. Novel human homologues of p47phox and p67phox participate in activation of superoxide-producing NADPH oxidases. J Biol Chem 2003; 278: 25234-25246.

143. Denu JM, Tanner KG. Specific and reversible inactivation of protein tyrosine phosphatases by hydrogen peroxide: evidence for a sulfenic acid intermediate and implications for redox regulation. Biochemistry 1998; 37: 5633-5642.

144. Meng TC, Buckley DA, Galic S, Tiganis T, Tonks NK. Regulation of insulin signaling through reversible oxidation of the protein-tyrosine phosphatases TC45 and PTP1B. J Biol Chem 2004; 279: 37716-37725.

145. Meng TC, Fukada T, Tonks NK. Reversible oxidation and inactivation of protein tyrosine phosphatases in vivo. Mol Cell 2002; 9: 387-399.

146. Kamata T. Roles of Nox1 and other Nox isoforms in cancer development. Cancer Sci 2009; 100: 1382-1388.

147. Mitsumata M, Gamou S, Shimizu N, Yoshida Y. Response of atherosclerotic intimal smooth muscle cells to epidermal growth factor in vitro. Arterioscler Thromb 1994; 14: 1364-1371.

148. Ross R, Raines EW, Bowen-Pope DF. The biology of platelet-derived growth factor. Cell 1986; 46: 155-169.

149. Griendling KK, Minieri CA, Ollerenshaw JD, Alexander RW. Angiotensin II stimulates NADH and NADPH oxidase activity in cultured vascular smooth muscle cells. Circ Res 1994; 74: 1141-1148.

150. Adachi T, Togashi H, Suzuki A, Kasai S, Ito J, Sugahara K, Kawata S. NAD(P)H oxidase plays a crucial role in PDGF-induced proliferation of hepatic stellate cells. Hepatology 2005; 41: 1272-1281.

151. Masamune A, Watanabe T, Kikuta K, Satoh K, Shimosegawa T. NADPH oxidase plays a crucial role in the activation of pancreatic stellate cells. Am J Physiol Gastrointest Liver Physiol 2008; 294: G99-G108.

152. Baumer AT, Ten Freyhaus H, Sauer H, Wartenberg M, Kappert K, Schnabel P, Konkol C, Hescheler J, Vantler M, Rosenkranz S. Phosphatidylinositol 3-kinase-dependent membrane recruitment of Rac-1 and p47phox is critical for alpha-platelet-derived growth factor receptor-induced production of reactive oxygen species. J Biol Chem 2008; 283: 7864-7876.

153. Matsubara T, Ziff M. Increased superoxide anion release from human endothelial cells in response to cytokines. J Immunol 1986; 137: 3295-3298.

154. Irani K, Xia Y, Zweier JL, Sollott SJ, Der CJ, Fearon ER, Sundaresan M, Finkel T, Goldschmidt-Clermont PJ. Mitogenic signaling mediated by oxidants in Ras-transformed fibroblasts. Science 1997; 275: 1649-1652.

155. Mukherjee SP, Lane RH, Lynn WS. Endogenous hydrogen peroxide and peroxidative metabolism in adipocytes in response to insulin and sulfhydryl reagents. Biochem Pharmacol 1978; 27: 2589-2594.

156. Rao GN, Berk BC. Active oxygen species stimulate vascular smooth muscle cell growth and proto-oncogene expression. Circ Res 1992; 70: 593-599.

157. Bhunia AK, Han H, Snowden A, Chatterjee S. Redox-regulated signaling by lactosylceramide in the proliferation of human aortic smooth muscle cells. J Biol Chem 1997; 272: 15642-15649.

158. Bleeke T, Zhang H, Madamanchi N, Patterson C, Faber JE. Catecholamine-induced vascular wall growth is dependent on generation of reactive oxygen species. Circ Res 2004; 94: 37-45.

159. O'Donnell BV, Tew DG, Jones OT, England PJ. Studies on the inhibitory mechanism of iodonium compounds with special reference to neutrophil NADPH oxidase. Biochem J 1993; 290 ( Pt 1): 41-49.

160. Ushio-Fukai M, Hilenski L, Santanam N, Becker PL, Ma Y, Griendling KK, Alexander RW. Cholesterol depletion inhibits epidermal growth factor receptor transactivation by angiotensin II in vascular smooth muscle cells: role of cholesterol-rich microdomains and focal adhesions in angiotensin II signaling. J Biol Chem 2001; 276: 48269-48275.

161. Biswas S, Gupta MK, Chattopadhyay D, Mukhopadhyay CK. Insulin-induced activation of hypoxia-inducible factor-1 requires generation of reactive oxygen species by NADPH oxidase. Am J Physiol Heart Circ Physiol 2007; 292: H758-766.

162. Li Q, Engelhardt JF. Interleukin-1beta induction of NFkappaB is partially regulated by H2O2-mediated activation of NFkappaB-inducing kinase. J Biol Chem 2006; 281: 1495-1505.

163. Ohba M, Shibanuma M, Kuroki T, Nose K. Production of hydrogen peroxide by transforming growth factor-beta 1 and its involvement in induction of egr-1 in mouse osteoblastic cells. J Cell Biol 1994; 126: 1079-1088.

164. Takahashi Y, Morales FC, Kreimann EL, Georgescu MM. PTEN tumor suppressor associates with NHERF proteins to attenuate PDGF receptor signaling. Embo J 2006; 25: 910-920.

165. Mesquita FS, Dyer SN, Heinrich DA, Bulun SE, Marsh EE, Nowak RA. Reactive Oxygen Species Mediate Mitogenic Growth Factor Signaling Pathways in Human Leiomyoma Smooth Muscle Cells. Biol Reprod 2009.

166. Ushio-Fukai M. VEGF signaling through NADPH oxidase-derived ROS. Antioxid Redox Signal 2007; 9: 731-739.

167. Ushio-Fukai M. Localizing NADPH oxidase-derived ROS. Sci STKE 2006; 2006: re8.

168. Ishikawa Y, Hirai K, Ogawa K. Cytochemical localization of hydrogen peroxide production in the rat uterus. J Histochem Cytochem 1984; 32: 674-676.

169. Jain S, Saxena D, Kumar GP, Laloraya M. NADPH dependent superoxide generation in the ovary and uterus of mice during estrous cycle and early pregnancy. Life Sci 2000; 66: 1139-1146.

170. Cui X, Chang B, Myatt L. Expression and Distribution of NADPH Oxidase Isoforms in Human Myometrium - Role in Angiotensin II-induced Hypertrophy. Biol Reprod 2009.

171. Mofarrahi M, Brandes RP, Gorlach A, Hanze J, Terada LS, Quinn MT, Mayaki D, Petrof B, Hussain SN. Regulation of proliferation of skeletal muscle precursor cells by NADPH oxidase. Antioxid Redox Signal 2008; 10: 559-574.

172. Gu Y, Xu YC, Wu RF, Nwariaku FE, Souza RF, Flores SC, Terada LS. p47phox participates in activation of RelA in endothelial cells. J Biol Chem 2003; 278: 17210-17217.

173. Jin S, Zhang Y, Yi F, Li PL. Critical role of lipid raft redox signaling platforms in endostatin-induced coronary endothelial dysfunction. Arterioscler Thromb Vasc Biol 2008; 28: 485-490.

174. Bey EA, Xu B, Bhattacharjee A, Oldfield CM, Zhao X, Li Q, Subbulakshmi V, Feldman GM, Wientjes FB, Cathcart MK. Protein kinase C delta is required for p47phox phosphorylation and translocation in activated human monocytes. J Immunol 2004; 173: 5730-5738.

175. Fontayne A, Dang PM, Gougerot-Pocidalo MA, El-Benna J. Phosphorylation of p47phox sites by PKC alpha, beta II, delta, and zeta: effect on binding to p22phox and on NADPH oxidase activation. Biochemistry 2002; 41: 7743-7750.

176. McLaughlin NJ, Banerjee A, Khan SY, Lieber JL, Kelher MR, Gamboni-Robertson F, Sheppard FR, Moore EE, Mierau GW, Elzi DJ, Silliman CC. Platelet-activating factor-mediated endosome formation causes membrane translocation of p67phox and p40phox that requires recruitment and activation of p38 MAPK, Rab5a, and phosphatidylinositol 3-kinase in human neutrophils. J Immunol 2008; 180: 8192-8203.

177. Fan LM, Teng L, Li JM. Knockout of p47 phox uncovers a critical role of p40 phox in reactive oxygen species production in microvascular endothelial cells. Arterioscler Thromb Vasc Biol 2009; 29: 1651-1656.

178. Vilhardt F, van Deurs B. The phagocyte NADPH oxidase depends on cholesterol-enriched membrane microdomains for assembly. Embo J 2004; 23: 739-748.

179. Liang M, Wang H, Zhang Y, Lu S, Wang Z. Expression and functional analysis of platelet-derived growth factor in uterine leiomyomata. Cancer Biol Ther 2006; 5: 28-33.

180. Finlay GA, Thannickal VJ, Fanburg BL, Kwiatkowski DJ. Platelet-derived growth factor-induced p42/44 mitogen-activated protein kinase activation and cellular growth is mediated by reactive oxygen species in the absence of TSC2/tuberin. Cancer Res 2005; 65: 10881-10890.

181. Juarez JC, Manuia M, Burnett ME, Betancourt O, Boivin B, Shaw DE, Tonks NK, Mazar AP, Donate F. Superoxide dismutase 1 (SOD1) is essential for H2O2-mediated oxidation and inactivation of phosphatases in growth factor signaling. Proc Natl Acad Sci U S A 2008; 105: 7147-7152.

182. Davidai G, Lee A, Schvartz I, Hazum E. PDGF induces tyrosine phosphorylation in osteoblast-like cells: relevance to mitogenesis. Am J Physiol 1992; 263: E205-209.

183. Chiarugi P, Cirri P, Taddei ML, Talini D, Doria L, Fiaschi T, Buricchi F, Giannoni E, Camici G, Raugei G, Ramponi G. New perspectives in PDGF receptor downregulation: the main role of phosphotyrosine phosphatases. J Cell Sci 2002; 115: 2219-2232.

184. Heffetz D, Bushkin I, Dror R, Zick Y. The insulinomimetic agents H2O2 and vanadate stimulate protein tyrosine phosphorylation in intact cells. J Biol Chem 1990; 265: 2896-2902.

185. Groeger G, Quiney C, Cotter TG. Hydrogen peroxide as a cell-survival signaling molecule. Antioxid Redox Signal 2009; 11: 2655-2671.

APPENDIX A: LIST OF ABBREVIATIONS

β-ME: beta mercaptoethanol

ABC: Avidin:Biotynilated enzyme complex

ACP1: acid phosphatase 1

ANOVA: analysis of variance

BCA: bicinchoninic acid

BCS: bovine calf serum

bFGF: basic fibroblast growth factor

Bis: bisindolylmaleimide, PKC inhibitor

BMI: body mass index

BSA: bovine serum albumin

CAV-1: caveolin 1

CBP: CREB binding protein

CDC25C: cell division cycle 25 homolog c

CPM: counts per minute

DAB: 3,3-Diaminobenzidine, liquid chromogen substrate kit

DCFDA: dichlorodihydrofluorescein diacetate, oxidation sensitive dye

DHE: dihydroethidium

DIC-Nomarski: differential interference contrast

DMEM: dulbecco's modified eagle medium

DMSO: dimethylsulphoxide

DPBS: dulbecco's PBS

DPI: diphenyleneiodonium

DTT: dithiothreitol, reducing agent

DUOX: dual oxidase NADPH oxidase

ECM: extracellular matrix

EGF: epidermal growth factor

EGF-R: EGF receptor

Eker rat: animal model for leiomyoma tumors

ELT-3: leiomyom smooth muscle cell line from Eker rat

ER: estrogen receptor

ERK: extracellular signal regulated kinase

FBS: fetal bovine serum

FGF: fibroblast growth factor

GAGs: glycosaminoglycans

GDP: guanosine diphosphate

GnRH: gonadotropin releasing hormone

GTPase: GTP exchange enzyme

H2O2: hydrogen peroxide

HB-EGF: heparin binding epidermal growth factor

HER-1: HB-EGF receptor

HGF-R: hepatocyte growth factor receptor

HRP: horseradish peroxidase

IGF-I: insulin-like growth factor-I

IL-1: interleukin 1

JNK: c-jun N-terminal kinase

LSB: laemmli sample buffer

LSMCS: leiomyoma SMCs

MAPK: mitogen-activated protein kinase

MAPK1/3: Erk1/2

M-CSF-R: macrophage colony-stimulating factor

MMP: matrix metalloproteinase

MSP-R:

NAC: n-acetyl-cysteine

Nox: **N**ADPH **ox**idase sub-unit

Noxa1: Nox activator 1

Noxo1: Nox organizer 1

PBS: phosphate buffer saline

PCNA: proliferating cell nuclear antigen

PDGF: platelet-derived growth factor

PDGF-R: PDGF receptor

pEGF-R: phosphorylated EGF receptor protein

PGF2$\alpha$: prostaglandin F2 alpha

Phox: **ph**agocyte **ox**idase subunit

PI3K: phosphatidyl inositol 3 phosphate

PKC: protein kinase C

PLC: phospholipase C

PMA: phorbol 12-myristate 13-acetate

PO4: phosphate

pPDGF-R: phosphorylated PDGF receptor protein

PR: progesterone receptor

PRF-DMEM: phenol red free DMEM

PTEN: phosphatase and tensin homolog

PTPase: protein tyrosine phosphatase

PTPN1: protein tyrosine phosphatase, non receptor type 1

qRT-PCR: real-time quantitative reverse transcription PCR

ROS: reactive oxygen species

RU-486: progesterone receptor antagonist

SCF-R: stem cell factor

SEM: standard error of the mean

SMC: smooth muscle cells

SM-MHC: smooth muscle-myosin heavy chain

SRF: serum response factor

TBS/T: tris buffer saline

tEGF-R: total EGF receptor protein

TGFβ1: transforming growth factor beta 1

TIMP: tissue inhibitor of metalloproteinase

TNFα: tumor necrosis factoa alpha

tPDGF-R: total PDGF receptor protein

UtSMCs: uterine SMCs (leiomyoma and myometrial SMCs)

VEGF: vascular endothelial growth factor

VSMCs: vascular SMCs

APPENDIX B: REGULATION OF CELL PROLIFERATION BY HYDROGEN PEROXIDE AND DPI IN MYOMETRIAL SMCS

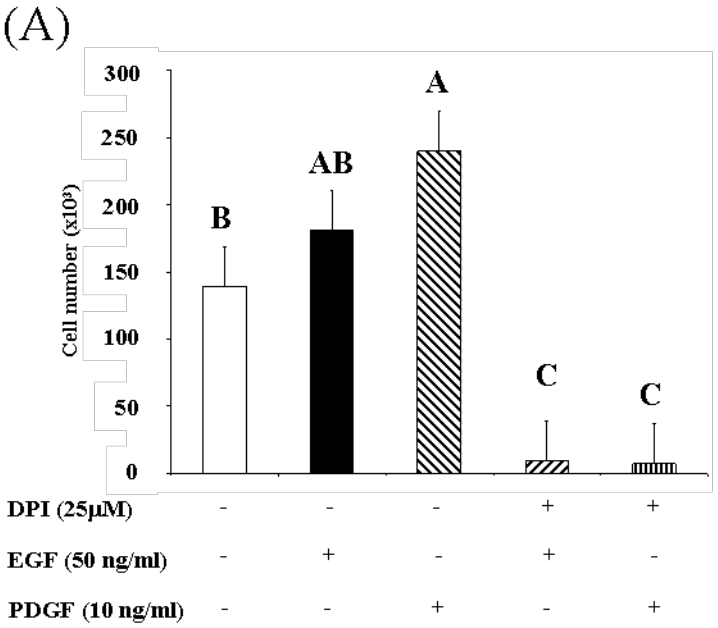


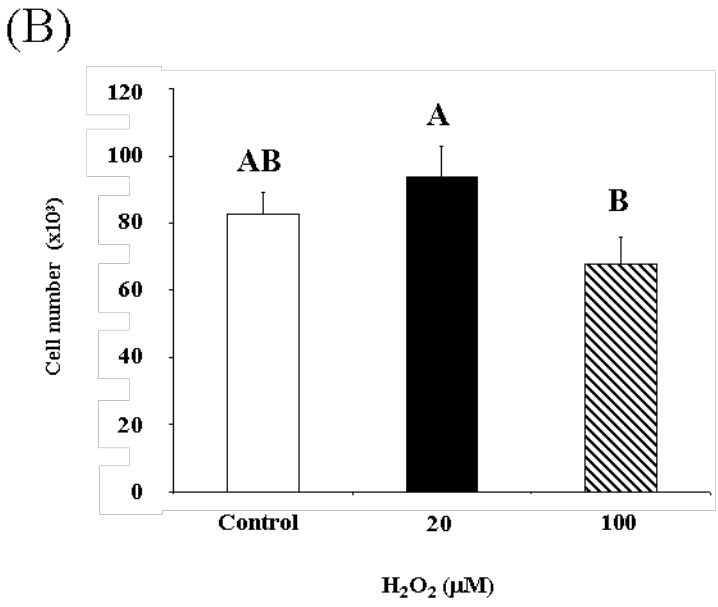

APPENDIX C: TIME-COURSE OF ERK1/2 PHOSPHORYLATION IN RESPONSE TO EGF AND PDGF IN MYOMETRIAL SMCS

(A)

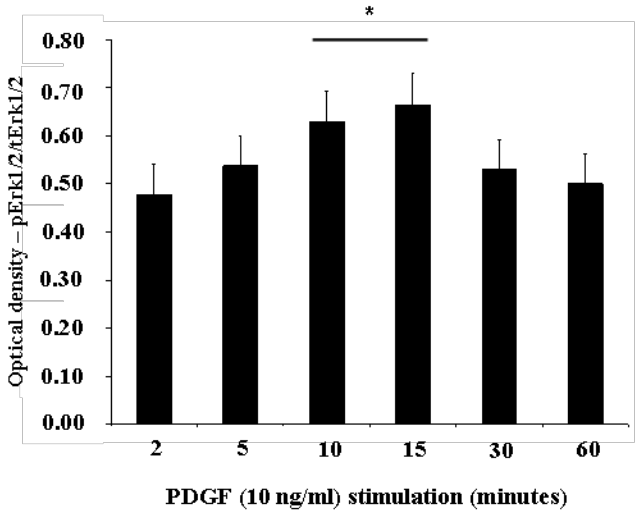


(B)

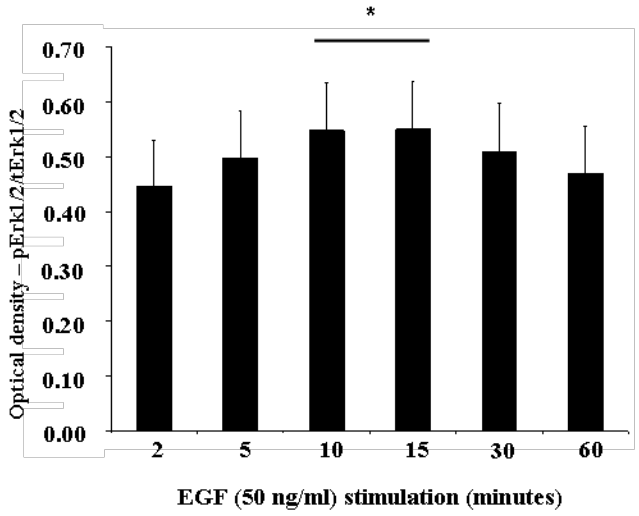

APPENDIX D: REGULATION OF EGF- AND PDGF-INDUCED ERK1/2 PHOSPHORYLATION BY DPI IN MYOMETRIAL SMCS

(A)

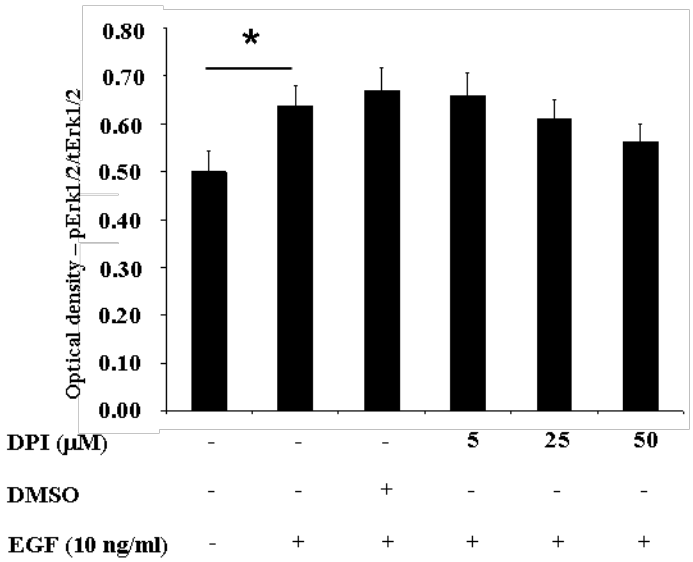


(B)

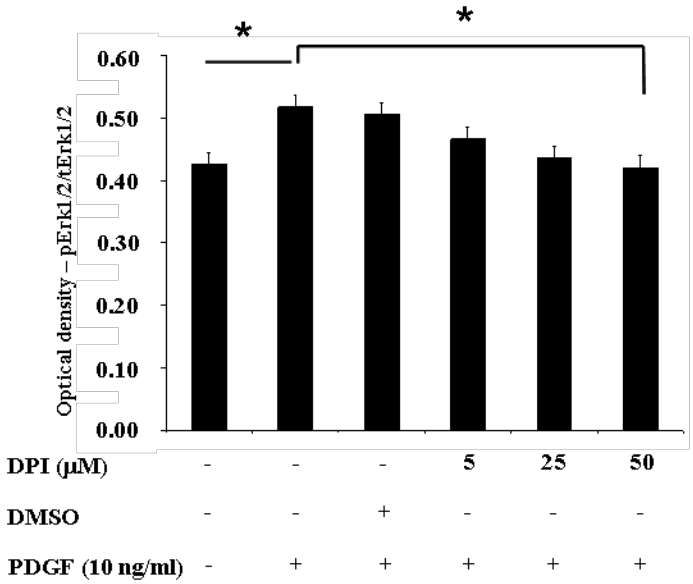

APPENDIX E: REGULATION OF EGF-R AND PDGF-R PHOSPHORYLATION BY DPI IN MYOMETRIAL SMCS

(A)

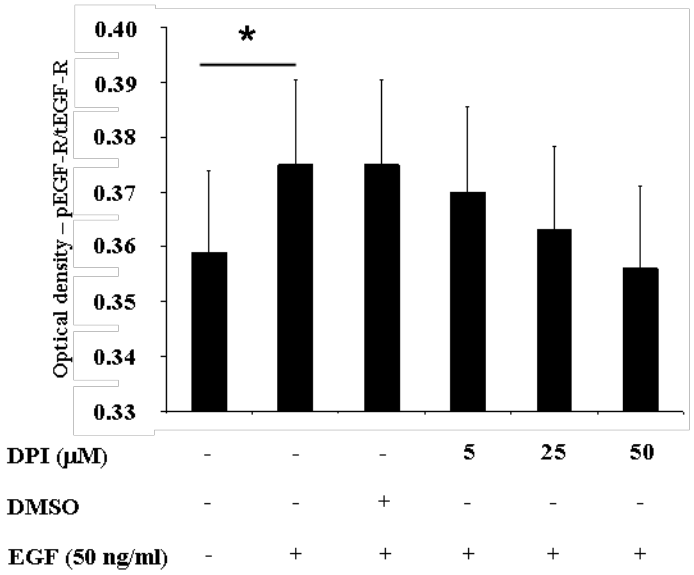


(B)

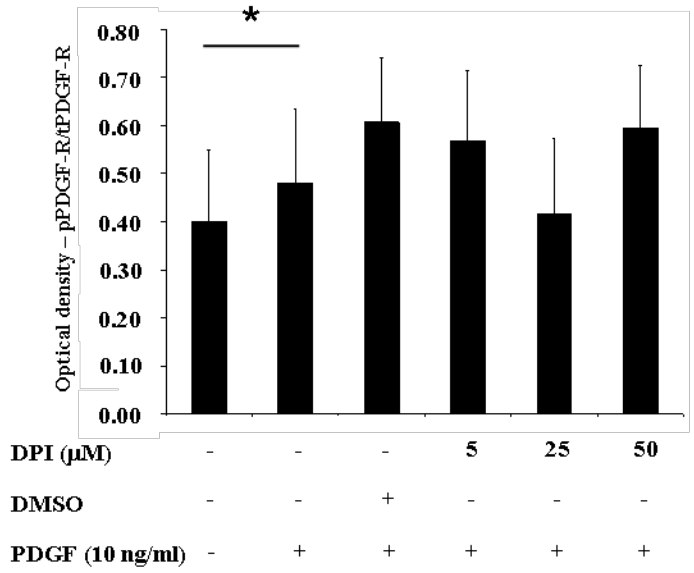

APPENDIX F: TIME-COURSE OF ERK1/2 PHOSPHORYLATION IN RESPONSE TO HYDROGEN PEROXIDE IN MYOMETRIAL SMCS

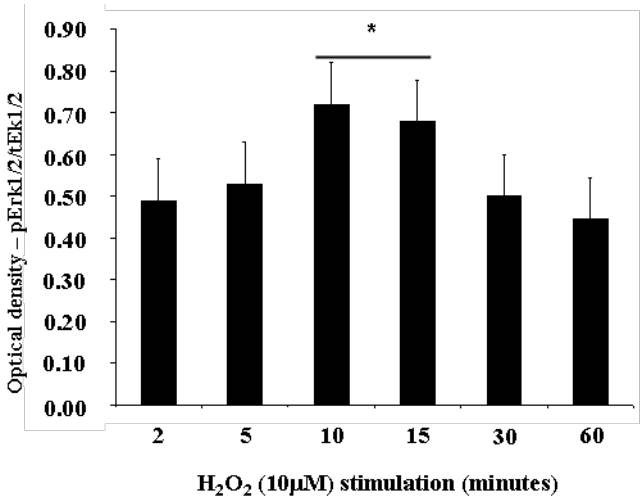

APPENDIX G: IMMUNOFLUORESCENCE STAINING PROTOCOL

Cell Culture:

1. Plate in 10% DMEM, no phenol red (Cells should be grown in plastic bottles (up to 90% confluence) in phenol red free medium washed in PR red free medium twice and trypsinized in PR free trypsin and transferred to wells). I feel the 4000 cell count is bit too much for that well size, so make it smaller but let it grow longer so that you will have new/fresh cells not just the cells trypsinized).
2. Let cells grow up to around 50% confluence.

*Normal:*
*PFA → rinse → Block → rinse → primary → rinse → secondary → rinse → DAPI → rinse → Prolong Gold*

3. Begin Fixation Procedure.

Fixation: All steps at Room Temperature;

- DO NOT LET SAMPLE DRY OUT!!!
- PROCESS ONE WELL AT A TIME!!!
    - Remove medium and replace it immediately

1. Wash cells in DPBS (RT) 3x with fresh DPBS each time (to remove debris and serum)
2. Fix all cells in Paraformaldehyde (4%) in DPBS (1x) for 25 minutes at room temperature.
    a. Add 200 µl/well
    b. Make 4% PFA with 1 ml of 16% PFA and 3 ml of 1xDPBS
    c. Kept 16% PFA aliquots at 4°C.
        i. Undiluted PFA should be used within a maximum of two weeks after opening the vial.
3. Wash wells 3x (5 min each) in DPBS.
4. Permeabilize cells
    a. Incubate slides in 0.2% Triton X 100 in DPBS for 10 min
    b. Wash once in DPBS
5. Blocking:
    a. Add signal FX to wells (be generous to cover the entire surface-250-300 microliters) and incubate for 60 minutes
6. Wash wells with 1x DPBS.
7. Dilute PRIMARY Ab in DPBS/10% Signal FX or DPBS containing 0.2% BSA and 0.05% Tween-20
8. Centrifuge it for 5 minutes at 12,000 RPM
    a. Add supernatant to wells
    b. KEEP wells that will receive secondary antibody only in blocking buffer until it is time to incubate with secondary antibodies

9. Incubate with primary antibodies separately (one at a time on same well) at appropriate concentrations for 2 hours at room temperature or overnight at 4°C.
10. Wash wells 3x (5 min each) in DPBS.

*(All steps from here on, keep the cell dish covered with a small box on the desk so that they are in the dark)*

11. Dilute secondary antibody in DPBS/10% FX or DPBS containing 0.2% BSA and 0.05% Tween-20 and centrifuge it for 5 minutes at 12,000 RPM
    a. Keep other wells on PRIMARY antibody until it is time to add secondary antibody;
    b. Secondary antibody used at 1:200 dilution and incubated for 1 hour;
12. Wash all wells/dishes 3x (5 minutes each) with 1x DPBS.
13. Incubate all wells/dishes in DAPI (5 μg/mL in 1x DPBS) for 15 minutes.
14. Rinse all wells/dishes briefly in 1x DPBS.
    a. Make Prolong gold 10ml into 20 aliquots of 500 μl each. Store 9 of them in -20 and leave 1 in the refrigerator.
15. Bring Prolong Gold (in the refrigerator) to room temperature first. Then mount in Prolong Gold (PG). Before that make sure you drain the final DPBS as much as possible. One may use a kimwipe around the well area, and then add PG without trapping bubbles. Add to cover all cells as solution in wells will form a depression in the center of wells;
16. Keep the dish in dark with lid loosely on top at room temp for 24 hours for prolong gold to cure;
17. Store in dark at 4°C with lids closed or sealed with parafilm until analysis.

APPENDIX H: IMAGING IMMUNOFLUORESCENCE STAINED CELLS OR LIVE CELL DETECTION OF ROS PRODUCTION

→ Turn fluorescent light ON
    - Wait 30 minutes before turning it OFF or back ON
        - Fixed cells: knob all the way up
        - Live cells: one notch up from the bottom
→ Turn microscope ON: right side, GREEN button
→ Turn Uniblitz (black box) ON
→ Lambda 10-3 power button
→ MCU28 – power button on back left side
→ Turn computer ON
    - After logging in, type "IU" for independent use
    - Camera: MRm or MR-3 Axio (Monochrome 1388x1048 resolution)
    - Before place sample on microscope: rotate course focus towards myself until sound indicating objective cannot go any further is heard to bring objective down
→ Before load the sample:
    - Polarizer has to be OUT
    - Apotome has to be OUT
    - Filter turret (DAPI-FITC-Rhodamine) has to be ON
    - For ROS production imaging, checl for the presence of the DIC cube
→ Configuration – MTB-2004
o Right click on IGB
    - Set active configuration – APPLY – OK
→ Axiovision release 4.6
→ Controls used to capture images
    - Microscope control
        - Microscope icon
    - Camera control
        - Activate camera
            - Acquisition – Select camera – MR-3
        - Acquisition – Camera – MR-3
    - Channel control
        - 6D – Acquisition
    - Live window – Live icon
    - Experiment window – File – Export
→ **To use high magnification**
→ Find focus on 5X on specific channel (DAPI for immunofluorescence, FITC for ROS production)
→ Record position
    - Mark/find icon
    - Position tab
    - Blue icon to mark position once focused
→ Move stage to the left, exposing 63X objective
→ Add oil (small drop)
→ Move to the recorded position

→ Change objective
    - Always on software
→ Every 2 wells, go back to 5X and repeat procedure above to add new oil
    - Before adding new oil, wipe bottom of the slide with liquid, but dry lens papers for objectives
    - If imaging ROS production adding oil once for each dish is usually enough
→ **Load experiment**
→ Under multidimensional acquisition click on LOAD, do not use drop down menu
→ Choose Fernando for fixed cells, and Fernando Live for ROS
→ On experiment tab, type image name on image name field
→ Click on "C" tab
→ Right click on channel to disable or enable it
→ **To use DAPI**
→ Go on Hardware settings and click on GO to activate channel
→ To turn it OFF, click on GO (off) to avoid photobleaching
→ Go on microscope control
→ Always start by bringing focus down, then click on 5X
→ Before taking the shot change light path to camera SIDE PORT LEFT
→ Now it is time to put slide ON
→ To make sure stage is snapped in place, press down on 4 corners
→ Bring the whole slide holder to the center, with equal space to the left and right side
→ Use joystick to bring first well above objective
→ Turn DAPI channel ON – GO
→ Adjust focus and turn light OFF by clicking first top button on right side of microscope
→ Record position
→ Move stage to the left side to expose 63X objective
→ Add drop of oil on objective, but not directly to lens
    - Not too much oil
→ Click on orange button (X) on Mark/Find
→ Then click on 63X
    - Normally needs to move objective up a little bit to adjust focus – Use fine focus
→ Change light path to camera only
→ Use joystick to move to different fields
→ Check on DAPI channel to adjust focus on Live image on computer
→ Go to camera control
→ On Live image – select OVER EXPOSE and LINEAR
→ Go to Frame tab and make sure resolution is maximum (1130x1088), and size is maximum
→ Click on center
→ Go to Adjust tab
→ Click on DAPI
→ Adjust exposure until a few RED dots show up, so that the whole dynamic range is covered
→ Change adjusted exposure on DAPI channel
    - Enter value under Time
        - If 1.81s = 1810ms
→ Click start to take shot on all channels
→ To save picture

    - Save as
    - My computer
    - Storage E
    - Users
    - Fernando
    - Create folder with the day's date as the name
    - Save as ZVI format (raw data)

→ On gallery mode, click on create image
→ Make sure color is ON (left bottom corner)
→ Save as
→ Change to TIFF format
→ Go to EXPORT window
→ Save image
→ Go to Fernando's folder and select correct day's folder
→ Click Start
→ Open live window again
→ Before leaving, make sure objective 5X is in use and focus is all the way down
→ Always change objective on software

## APPENDIX I: LIPID RAFT ISOLATION BY SUCROSE GRADIENT ULTRA-CENTRIFUGATION

- Cells were plated into 10 cm plastic dishes and grown up to confluence;
- Upon reaching confluence, cells were serum-starved in DMEM-serum free for 24 hours;
- After serum starvation, cells were treated with PDGF (10 ng/ml), EGF (50 ng/ml) or DMEM-serum free (Control) for 3 minutes, then cells were lysed according to the following procedure:
    - Taking 10 dishes at a time, remove medium of each dish and add 5 ml of ice-cold PBS/5mM EDTA, and place dish on ice;
    - After adding PBS/EDTA to the last dish, start scrapping cells off of the dish and collect cell suspension into a 50 ml conical tube; BE CAREFUL TO SCRAPE CELLS OFF OF THE EDGE OF THE DISHES;
    - Once cells are harvested from all dishes, centrifuge tube containing cells in PBS/EDTA at 1,000 RPM for 5 minutes (4°C);
    - Remove supernatant and add 500 μl of ice-cold lysis buffer to resuspend the cell pellet; Let cells incubate on ice for 10-15 minutes;
        - Lysis buffer
            - 0.5% TX-100
            - 25 mM Tris pH 7.4
            - 150 mM NaCl
            - 1 mM EDTA
            - 1 mM PMSF
            - 1 mM Na3VO4
            - 1 mM NaF
            - Protease inhibitor tablet
    - Add equal volume (500 μl) of ice-cold 80% Sucrose buffer to make a 40% Sucrose buffer + cell lysate;
        - Sucrose buffer
            - Sucrose (80%, 35%, 5%)
            - 25 mM Tris pH 7.4

        - 150 mM NaCl
    - Keep samples on ice;
    - Take the ultracentrifuge metal parts, which will hold the plastic tubes, from the cold room and keep them on ice as well as the plastic tubes;
    - Insert the plastic tubes into the metal holders, always on ice;
    - Transfer a maximum of 1 ml of the 40% Sucrose/cell lysate into a ultracentrifuge 5 ml plastic tube;
    - Very carefully and slowly load 2.5 ml of 35% Sucrose buffer; Keep the tip of the pipette touching the meniscus and pull the tip up as the buffer is added; Be extra cautious to prevent 40% and 35% buffers from mixing up;
    - Proceed similarly to add 0.5 ml of the 5% Sucrose buffer on top of the 35% layer;
    - Weight the whole set (metal holder, plastic tube with sample and metal lid) individually and add extra 5% Sucrose buffer to the lighter sets of samples up to the weight of the heaviest set so that the rotor stays balanced;
    - Remember to pre-cool ultracentrifuge to 3°C;
    - Centrifuge samples at 45,000 RPM for 12 hours at 3°C in a SW55Ti rotor, acceleration = max, deceleration = no brakes
    - Next day, collect fractions from top down;
    - Volume per fraction may be adjusted according to the total number of fractions one wants to collect; I collected 500 μl fractions for a total of 8 fractions; Leave the insoluble fraction in the tube;
    - Add warm (95°C) 1X LSB to the pellet and try to dissolve it by pipetting up and down many times; Keep warming the pellets up for 1-2 minutes and repeat the pipetting until the pellet is dissolved;
    - 300 μl of each fraction was combined with 100 μl of 4X LSB and denatured at 95°C for 5 minutes;
    - Load 50 μl of each fraction into a polyacrylamide gel and freeze the left over lysate;
        - Gel concentration will be determined by molecular weight of target protein(s)
        - I used precast gel which support 50 μl of sample per well

        - Precast gels from BioRad or PIERCE
    - I use 4-20% gradient gels because I am working with proteins that range from 22kDa to 190kDa
    - 6 gels were run;
- Precast gels
    - Remove comb carefully by adding water to wells and pulling it out gently
    - Use razor blade to cut and remove plastic membrane at the bottom of gel (demarking line) which will allow electric flow from negative to positive
- Proceed electrophoresis and transfer as usual;
    - When setting up the transfer make sure that the bottom of the gel (approximately 2 mm from the bottom), which is slightly thicker than the rest of the gel, is removed; Otherwise, it may impair proper contact with the membrane;
- After transfer, the top part of the gel including the wells will be very sticky and hard to remove from the membrane; Use a swab to remove gel pieces completely from the gel;

APPENDIX J: AUTOFLUORESCENCE OF PKC INHIBITOR COMPOUNDS